U.PORTO

FMUP FACULDADE DE MEDICINA UNIVERSIDADE DO PORTO

BRAIN MECHANISMS OF OSTEOARTHRITIS PAIN

JOANA DE BRITO BARROSO MONTEIRO

TESE DE DOUTORAMENTO EM NEUROCIÊNCIAS

APRESENTADA À FACULDADE DE MEDICINA DA UNIVERSIDADE DO PORTO

Porto, 2021

DISSERTAÇÃO DE CANDIDATURA AO GRAU DOUTOR APRESENTADA À FACULDADE DE MEDICINA DA UNIVERSIDADE DO PORTO, NO ÂMBITO DO PROGRAMA DOUTORAL EM NEUROCIÊNCIAS

ORIENTADOR:

Professor Doutor Vasco Galhardo
Professor Associado com Agregação da Faculdade de Medicina da Universidade do Porto

CO-ORIENTADOR:

Professor Doutor Apkar Vania Apkarian
Full Professor, Feinberg School of Medicine
Northwestern University

A candidata realizou o presente trabalho com o apoio de uma bolsa de doutoramento, concedida pelo Programa Operacional Regional do Norte, NORTE 2020, com a referência NORTE-08-5369-FSE-000026, Bolsa OARSI – *collaborative scholarship 2018*, Bolsa Grunenthal – *Jovem Investigador em Dor 2017* e Bolsa FLAD R@D scholarship 2018.

Artigo 48º, parágrafo 3:

“A Faculdade não responde pelas doutrinas expendidas na dissertação.”
(Regulamento da Faculdade de Medicina da Universidade do Porto – Decreto-Lei no 19337 de 29 de janeiro de 1931

Constituição do Júri

Presidente:

Doutor Rui Manuel Bento de Almeida Coelho

Professor Catedrático da Faculdade de Medicina da Universidade do Porto

Vogais:

Doctor Paul Geha

Assistant Professor, University of Rochester Medical Center, New York, USA

Doctor Ulrike Bingel

Professor, University Hospital Essen, Germany

Doctor Apkar Vania Apkarian

Professor, Feinberg School of Medicine Northwestern University, Illinois, USA

Doutor João José Carreiro Páscoa Pinheiro

Professor Associado, Faculdade de Medicina da Universidade de Coimbra

Doutora Isaura Ferreira Tavares

Professora Associada com Agregação, Faculdade de Medicina da Universidade do Porto

Doutor Fernando José Pereira Alves Abelha

Professor Catedrático, Faculdade de Medicina da Universidade do Porto

Corpo Catedrático da Faculdade de Medicina da Universidade do Porto

Professores Catedráticos

MARIA AMELIA DUARTE FERREIRA

PATRÍCIO MANUEL VIEIRA ARAÚJO SOARES SILVA

ALBERTO MANUEL BARROS DA SILVA

JOSE HENRIQUE DIAS PINTO DE BARROS

MARIA FÁTIMA MACHADO HENRIQUES CARNEIRO

MARIA DULCE CORDEIRO MADEIRA

ALTAMIRO MANUEL RODRIGUES COSTA PEREIRA

MANUEL JESUS FALCAO PESTANA VASCONCELOS

JOÃO FRANCISCO MONTENEGRO ANDRADE LIMA BERNARDES

MARIA LEONOR MARTINS SOARES DAVID

RUI MANUEL LOPES NUNES

JOSE MANUEL PEREIRA DIAS DE CASTRO LOPES ANTÓNIO

ALBINO COELHO MARQUES ABRANTES TEIXEIRAJOAQUIM

ADELINO CORREIA FERREIRA LEITE MOREIRA RAQUEL

ÂNGELA SILVA SOARES LINO

RUI MANUEL BENTO DE ALMEIDA COELHO

Professores Jubilados/Aposentados

ALEXANDRE ALBERTO GUERRA SOUSA PINTO

ÁLVARO JERONIMO LEAL MACHADO DE AGUIAR

ANTONIO AUGUSTO LOPES VAZ

ANTÓNIO CARLOS DE FREITAS RIBEIRO SARAIVA

ANTÓNIO CARVALHO ALMEIDA COIMBRA

ANTÓNIO FERNANDES OLIVEIRA BARBOSA RIBEIRO BRAGA

ANTÓNIO JOSÉ PACHECO PALHA

ANTÓNIO MANUEL SAMPAIO DE ARAÚJO TEIXEIRA

BELMIRO DOS SANTOS PATRICIO

CÂNDIDO ALVES HIPÓLITO REIS

CARLOS RODRIGO MAGALHÃES RAMALHÃO

CASSIANO PENA DE ABREU E LIMA

DEOLINDA MARIA VALENTE ALVES LIMA TEIXEIRA

EDUARDO JORGE CUNHA RODRIGUES PEREIRA

FERNANDO TAVARELA VELOSO

FRANCISCO FERNANDO ROCHA GONÇALVES HENRIQUE

JOSÉ FERREIRA GONÇALVES LECOUR DEMENEZES

ISABEL MARIA AMORIM PEREIRA RAMOS

JORGE MANUEL MERGULHAO CASTRO TAVARES

JOSÉ AGOSTINHO MARQUES LOPES

JOSE CARLOS NEVES DA CUNHA AREIAS

JOSÉ CARVALHO DE OLIVEIRA

JOSÉ EDUARDO TORRES ECKENROTH GUIMARÃES

JOSÉ FERNANDO BARROS CASTRO CORREIA

JOSÉ LUÍS MEDINA VIEIRA

JOSÉ MANUEL COSTA MESQUITA GUIMARÃES

LEVI EUGÉNIO RIBEIRO GUERRA

LUÍS ALBERTO MARTINS GOMES DE ALMEIDA

MANUEL ALBERTO COIMBRA SOBRINHO SIMÕES

MANUEL ANTÓNIO CALDEIRA PAIS CLEMENTE

MANUEL AUGUSTO CARDOSO DE OLIVEIRA

MANUEL MACHADO RODRIGUES GOMES MANUEL

MARIA PAULA BARBOSA

MARIA DA CONCEIÇÃO FERNANDES MARQUES MAGALHÃES

MARIA ISABEL AMORIM DE AZEVEDO

RUI MANUEL ALMEIDA MOTA CARDOSO

SERAFIM CORREIA PINTO GUIMARÃES

VALDEMAR MIGUEL BOTELHO DOS SANTOS CARDOSO

WALTER FRIEDRICH ALFRED OSSWALD

Às quatro da madrugada, o passarinho cantou.

Ao Bobô e ao Alex

To Professor Apkar Vania Apkarian,

Professor Thomas J. Schnitzer,

and Professor Vasco Galhardo

Ao Nuno, João Miguel, Berta e João

Ao abrigo do nº2 do artigo 8º do Decreto-Lei 338/70, fazem parte desta dissertação as seguintes publicações:

1. Barroso J, Wakaizumi K, Reckziegel D, Pinto-Ramos J, Schnitzer T, Galhardo V, Apkarian AV. *Prognostics for pain in osteoarthritis: Do clinical measures predict pain after total joint replacement?* PLoS One. 2020 Jan 8;15(1): e0222370. doi: 10.1371/journal.pone.0222370. PMID: 31914126; PMCID: PMC6948829.

2. Barroso J, Vigotsky AD, Branco P, Reis AM, Schnitzer TJ, Galhardo V, Apkarian AV. *Brain gray matter abnormalities in osteoarthritis pain: a cross-sectional evaluation*. Pain. 2020 Sep 1;161(9):2167-2178. doi: 10.1097/j.pain.0000000000001904. PMID: 32379222; PMCID: PMC7745790.

3. Barroso J, Wakaizumi K, Reis AM, Baliki M, Schnitzer TJ, Galhardo V, Apkarian AV. *Reorganization of functional brain network architecture in chronic osteoarthritis pain*. Hum Brain Mapp. 2021 Mar;42(4):1206-1222. doi: 10.1002/hbm.25287. PMID: 33210801; PMCID: PMC7856636.

4. Barroso J, Branco P, Baliki M, Reis AM, Schnitzer TJ, Galhardo V, Apkarian AV. *Limbic brain structural and functional properties predict pain after joint replacement surgery in knee osteoarthritis*. (Manuscript in preparation).

Table of contents

List of abbreviations

ACC, anterior cingulate cortex

ADAMSTS, a disintegrin and metalloproteinase with thrombospondin motif

ATF-3, activating transcription factor 3

CPM, conditioned pain modulation

CBP, chronic back pain

CGRP, calcitonin gene related peptide

DRG, dorsal root ganglia

DLPFC, dorsolateral prefrontal cortex

FGF-1, fibroblast growth factor 1

fMRI, functional magnetic resonance imaging

mPFC, medial prefrontal cortex

NAc, nucleus accumbens

NGF, nerve growth factor

NPY, neuropeptide Y

NRS, numeric rating scale

MIA, monoiodoacetate-induced arthritis

MMP, Matrix metalloproteinases

MRI, magnetic resonance imaging

OA, osteoarthritis

OAp, osteoarthritis pain persisting

OAr, osteoarthritis pain recovering

PET, positron emission scan

RVM, rostroventral medula

TJR, total joint replacement

TGF, transforming growth factor

VIP, vasoactive intestinal peptide

Abstract

Osteoarthritis (OA) is one of the most prevalent sources of chronic musculoskeletal pain, and a leading cause of disability worldwide. Pain is the hallmark symptom of the disease, contributing to reduced mobility, psychological stress and general low quality of life. Mechanisms of OA pain are not entirely understood. Though traditionally seen as the prototype of *nociceptive pain*, it is now widely accepted that the disorder is associated with nervous system reorganization. Neural changes in OA have mostly been studied from the perspective of peripheral sensitization of nociceptors, spinal cord mechanisms and dysfunction of descending modulator pathways; the role of the brain in OA pain remains mostly unknow. At the same time, brain corticolimbic structural and functional properties have been related to chronic low back pain, proving to be both adapting and imparting risk for pain chronification. In the present thesis we test these concepts in OA pain. We purpose to cross-sectionally evaluate brain structural and functional properties of ongoing OA pain, and longitudinally study clinical, psychological and brain biomarkers of pain persistence after total joint replacement (TJR) surgery, thus searching for brain biomarkers of the disease.

We conducted four studies with different aims. In the first publication we sought to study the relationship between OA pain indices and clinical, psychological and sociodemographic variables. We showed that different pain scales related to distinct dimensions of the pain experience; clinical variables were not robust predictors of pain persistence after TJR in OA, however these characteristics change/reorganize with surgery. In our second and third publications we evaluate brains anatomic and functional

reorganization is OA pain patients. Structural grey matter properties and the disruption of information sharing in the brain have been proposed as brain diagnostic biomarkers of chronic pain – reflecting the ongoing clinical condition. We show the brain is reorganizing, both anatomically and functionally, this reorganization is pervasive across neocortex and relates to clinical characteristics of OA. Moreover, we unveil specific localized patterns of functional reorganization, and propose specific mechanisms of adaptive/maldaptive plasticity in OA pain. Finally, in our last publication, we test the concept that the brain is not only reorganizing with pain, imparts risk for pain maintenance. We evaluate limbic brain properties as possible predictors of pain persistence after TJR surgery and show anatomic and functional properties of the bilateral amygdala, hippocampus and thalamus are reliable predictors of the surgical outcome.

Altogether, the present thesis provides original data on brain anatomical and functional changes underlying OA pain, suggests brain diagnostic biomarkers of the disease and proposes brain limbic circuit as potential biomarker of OA pain persistence after surgery. Our research opens new avenues in the understanding of pain mechanisms in OA, challenges the extent of dependence of OA pain on nociceptive encoding and highlights emotional-learning brain circuitry as a key factor for pain chronification.

Resumo

A osteoartrose (OA) é uma das causas mais prevalentes de dor crónica músculo-esquelética e incapacidade a nível mundial. A dor é o sintoma-chave da doença contribuindo para menor mobilidade e atividade física, dano psicológico e decréscimo de qualidade de vida. Os mecanismos de dor na OA não são completamente compreendidos. Apesar de tradicionalmente ser entendida como o protótipo da *dor nociceptiva*, é atualmente aceite que a dor na OA está associada à reorganização do sistema nervoso. Esta reorganização tem sido estudada essencialmente sob o ponto de vista do sistema nervoso periférico – sensibilização de terminações livres na articulação, e centralmente através do estudo de mecanismos espinhais e disfunção de vias de modulação descendente. O papel do cérebro na dor da OA continua largamente incompreendido. Paralelamente, alterações cerebrais estruturais e funcionais foram descritas na dor lombar crónica. Estes parâmetros parecem não só traduzir uma adaptação neural ao processo doloroso, como também aparentam constituir fatores de risco para a cronificação da dor. Na presente tese testamos estes conceitos na dor da OA. Propusemo-nos estudar alterações cerebrais estruturais e funcionais em doentes com OA de forma transversal, e realizamos estudos longitudinais, com o objetivo de avaliar fatores clínicos, psicológicos e marcadores cerebrais de persistência de dor.

Realizamos quatro estudos com objetivos distintos. Na primeira publicação desta tese propusemo-nos a estudar a relação entre diferentes escalas de dor e fatores clínicos, psicológicos e sociodemográficos; verificamos que diferentes escalas de dor se relacionam com facetas distintas da experiência dolorosa. As variáveis clínicas testadas não demonstraram ser preditores robustos da persistência de dor na OA, no entanto

estes índices sofreram alteração/reorganização após a cirurgia, relacionada com o alívio álgico. Na segunda e terceira publicações desta tese avaliamos marcadores cerebrais de reorganização estrutural e funcional. Propriedades anatómicas da matéria cinzenta neocortical e subcortical e a disrupção da conectividade funcional cerebral foram recentemente propostas como biomarcadores diagnósticos de dor crónica – refletindo o custo da doença no sistema nervoso central. As nossas publicações demonstram que há um padrão de reorganização estrutural e funcional que é difuso a nível neocortical e esta reorganização traduz propriedades clínicas (intensidade de dor; padrão neuropático). Revelamos ainda que paralelamente às alterações de larga escala, há padrões localizados de reorganização cerebral e propomos mecanismos específicos de plasticidade adaptativa/mal-adaptativa na dor da OA. Por último, testamos o conceito de que o cérebro não só se reorganiza na dor, mas também pode ser responsável pela sua manutenção após resolução da patologia periférica. Desta forma, avaliamos as propriedades do sistema límbico como possíveis preditores de persistência de dor na OA após artroplastia e demonstramos que propriedades anatómicas e funcionais da amígdala, tálamo e hipocampo são indicativas da persistência de dor pós-cirurgica.

Em suma, apresentamos dados originais acerca das alterações estruturais e funcionais que decorrem na dor da OA, sugerimos biomarcadores cerebrais diagnósticos, e propomos o sistema límbico como potencial biomarcador de persistência de dor na OA após cirurgia. A nossa linha de investigação abre novas oportunidades para a compreensão da dor na OA, desafia a dependência da dor em mecanismos nociceptivos e aponta o cérebro emocional-motivacional como fator chave na persistência da dor.

1. Introduction

1.1 Osteoarthritis

Osteoarthritis is a chronic arthropathy characterized by abnormal structural changes in the joint and peri-articular tissue. Often described as a degenerative joint disease, it is known that inflammation plays a key role in its initiation and progression, driving the characteristic pathological changes: degradation of the articular cartilage, synovial inflammation, osteophyte formation, and hypertrophy of the joint capsule. The entire joint structure is affected leading to deformation, loss of function and pain[1].

It is one of the most prevalent musculoskeletal disorders worldwide, affecting 7% of the global population (>500 million people). In 2019 it was the 15th cause of years lived with disability worldwide, and a leading cause of disability among older adults. The number of people affected is likely to increase over the next decades, given the ageing population and the obesity epidemic [2]. The increase in prevalence of an already common disease suggests a future larger impact on health care systems [3]. At the same time, it is also known that development of treatments for OA has not made comparable progress with that for many other musculoskeletal disorders, thus amplifying the concern on the future burden of the disease [2].

Pain is the defining clinical presentation of OA and represents the main motivation to seek medical care. It contributes to motor impairment and disability, but also impacts negatively in general quality of life, leads to sleep disruption, psychological stress and fatigue [4]. The better characterization and comprehension of OA pain mechanisms is essential for future therapy development and progress in clinical care.

1.1.1 Mechanisms of OA pain

The nature of OA pain is complex. There is an incongruity between structural changes, the physical impairment and levels of reported pain [5]. Individuals with joint structural changes consistent with OA can be asymptomatic; at the same time, patients with incapacitating pain may present with minimal radiographic changes [6 5]. Though this dissociation is not completely understood, the multiplicity of mechanisms responsible for OA pain may help to clarify its heterogeneous clinical presentation.

Local joint mechanical and inflammatory mechanisms, eliciting joint nociception were for a long time pointed as the key pain causatives. Later, the discovery of joint nociceptive sensitization, together with the reorganization of the spinal cord circuitry and impaired descending modulation of pain shed light into the involvement of peripheral and central nervous systems in OA pain [7]. Finally, overt the last years, brain mechanisms were proposed as a crucial part of development and maintenance of multiple chronic pain syndromes [8 9]. Nonetheless, brain mechanisms for the development and progression of OA pain are still minimally understood. The contribution of known or plausible mechanisms of OA pain is briefly explained below.

1.1.1.1 Activation and sensitization of joint afferents

The local pathological hallmark of OA is tissue injury and remodeling of the joint with accompanying structural changes: the progressive loss of articular cartilage leads to joint space narrowing and subchondral bone remodeling, osteophyte formation, bone marrow lesions and is accompanied by synovitis [10,11]. The aforenoted

local changes and the concurrent local and systemic response promote the infiltration of inflammatory cells, local production of enzymes and growth factors (e.g., TGF; NGF; MMP; ADAMSTS, FGF-1). Inflammation promotes further structural damage, and leads to nociceptor activation [12]. Progressive compressive forces and hypoxia stimulate vascular and nerve growth in the osteochondral bone and menisci that further contribute to nociception and constitute a current target for analgesic therapy [13,7] **(Figure 1.a)**.

The acute transduction of strong chemical and mechanical signals is pivotal for OA pain; however, nociceptors are plastic in their physiology and after damage occurs, they do not necessarily return to normal function. An increase in sensitivity and a reduction in stimulus threshold is often recorded after an injury, where, for example, lower mechanical pressure may elicit nociceptor activity. This phenomenon is often seen during chronic inflammation, and termed as sensitization – amplification of neuronal signaling within the nervous system that elicits pain hypersensitivity [12]. Inflammatory mediators (e.g., substance P, VIP, CGRP), contribute to nociceptor sensitization by reducing the firing threshold, making them more likely to respond to both noxious and non-noxious stimuli. Moreover, there is also evidence that during inflammation nociceptor fibers show increase mechano-sensitivity [12]. In addition to the classic nociceptor fibers being sensitized, there are a number of fibers in the joint that are not normally activated by noxious stimuli but become responsive when damage occurs - silent nociceptors[11]. The increased activity of low threshold units and the awakening of silent nociceptors may be at least partly responsible for the intensified nociception in OA.

Finally, though less information exists about the influence of local processes in the dorsal root ganglia (DRG) in OA, joint inflammation is known to increase

expression of local neuroinflammatory peptides which triggers molecular changes in the DRG and the early expression of neuronal injury markers (ATF-3; NYP) in animal models of OA[14, 15]. There is also evidence of local infiltration of macrophages into the DRG in animal models of chronic pain, associated with pain-like behaviors[16]. Signaling pathways activated in the DRG can exert effects in central spinal processes. This structure is thus central in linking the peripheral neuronal adaptation in OA and subsequent neural changes at the SC level [17].

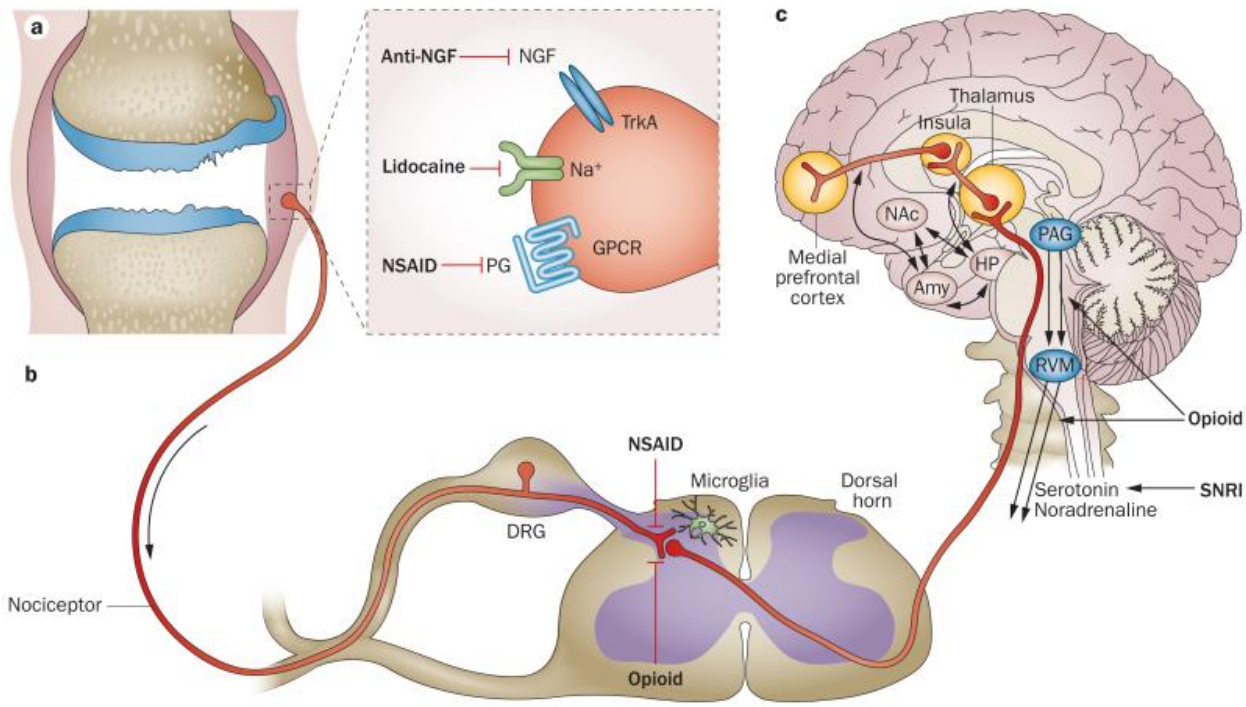

Figure 1. Mechanisms of OA pain and possible therapeutic targets. (a) Joint afferents are activated by mechanical and chemical stimuli; different analgesic drugs act in the periphery by targeting receptors expressed at nociceptor peripheral terminals; (b) afferent nociceptors synapse with second-order neurons in the dorsal horn; prostaglandins can also contribute to the SC sensitization, and NSAIDs can thus exert central analgesic effects; opioids also

contribute to the inhibition of nociceptive stimuli; (c) projection neurons relay nociceptive signals along the spinothalamic tract to the thalamus, and along the spinoreticulothalamic tract to the brainstem. From here, nociceptive signals are propagated for different areas of the brain, including the cortex. Descending pathways both facilitatory and inhibitory modulate pain transmission. Descending inhibitory pathways release noradrenaline and serotonin onto spinal circuits. SNRIs engage these descending inhibitory pathways. RVM neurons are opioid sensitive, and morphine has an analgesic effect through engaging descending inhibition. Amy, amygdala; DRG, dorsal root ganglion; GPCR, G-protein-coupled receptor; HP, hippocampus; NAc, nucleus accumbens; NGF, nerve growth factor; PAG, peri-aqueductal grey; PG, prostaglandin; RVM, rostral ventromedial medulla; SNRI, serotonin–noradrenaline reuptake inhibitor. Figure adapted from *Malfait and Schnitzer, 2013* [7].

1.1.1.2 Spinal mechanisms of OA pain

Continued nociceptor input can lead to prolonged hyperexcitability of nociception circuits in the spinal cord (SC), consisting in enhanced responses to mechanical stimulation of the joint, lowering of excitation threshold of high-threshold SC neurons and enlargement of its total receptive field [18], **Figure 2.b**.

Animal models of OA (both surgical and chemically induced arthritis) show a higher content of SC neuropeptides, namely substance P and CGRP. These peptides are thought to be released from sensitized nociceptors and facilitate hyperexcitability [19]. Moreover, there is evidence of SC microglia activation, that is time-dependent, taking a few days in a chemical induced OA (monoiodoacetate-induced arthritis, MIA) [20] and about 8 weeks in the surgical model (destabilization of medial meniscus, DMM) [21], thus reflecting the time course of OA development.

Additionally, it has been established that spinal cord microglia become activated

and contribute to the development of pain behaviors in animal models of peripheral nerve and SC injury; furthermore, the pharmacological inhibition of microglial cells can result in attenuated hyperresponsiveness of SC dorsal horn neurons results in lowering of pain related behaviors in animals [22]. This data shows microglia activation in SC is a prominent feature of neuropathic pain conditions and suggests that OA shares this mechanism [18].

Though less studied than peripheral mechanisms, it is known that spinal sensitization is often counteracted by local and descending inhibitory mechanisms, that seem to play an important role in OA pain [18].

1.1.1.3 Descending pain modulation

Descending pain control pathways operate in the CNS, mediating the inhibition and facilitation of nociceptive signals in spinal cord neurons. In short, bidirectional synaptic information, from supraspinal centers, both cortical (anterior cingulate cortex, ACC) and subcortical (hypothalamus, amygdala), radiate to and from the periaqueductal gray (PAG) in the midbrain [7]. The PAG has also reciprocal connections with midbrain areas, namely the rostral ventromedial medulla (RVM). Though the PAG does not directly project to the spinal cord, it relays the descending input though the RVM that exerts balance of inhibition and facilitation of nociceptive transmission at the spinal cord (through the release of noradrenaline and serotonin)[23] (**Figure 2.c**). Descending pain facilitatory and inhibitory systems work in concert, maintaining a baseline of sensory processing. Peripheral injury and inflammation can perturb this balance and favor facilitation, promoting and maintaining chronic pain [24]. In animal models of OA, serotoninergic descending facilitation contributes to

responses of spinal neurons to innocuous mechanical stimuli[25]. In humans, conditioned pain modulation (CPM) is defective in OA [26]. CPM is a serotoninergic physiological mechanism characterized by inhibition of pain in the initial site when a noxious stimulus is applied at a different site [27]. This data supports the impairment of descending pain modulation as an important pain mechanism in OA.

1.1.1.4 Supraspinal processing

The conventional view of the brain's import in OA pain is a state of continued activity in brain regions identified for acute pain. In short, ascending information from the joint nociceptors, spinal cord and midbrain reaches the thalamus, where its projections activate the primary and secondary somatosensory cortex (S1, S2; allowing for sensory processing), the ACC and posterior insula (involved in salience and aversiveness evaluation) and prefrontal cortex (PFC; related to cognitive tasks such as stimulus evaluation) [8].

The concept that the brain's representation of OA pain is more than a persistent state of acute pain was explored in some of the first neuroimaging studies in OA patients. Using positron emission tomography (PET) scans and functional magnetic resonance imaging (fMRI), the brain activity for spontaneous OA pain was contrasted to the one for acute experimental pain in the joint [28,29]. Pressure-evoked pain and related brain activity was minimally different between OA and healthy subjects, in contrast, spontaneous OA pain engaged prefrontal-limbic regions (medial and orbital prefrontal cortex, as well as bilateral nucleus accumbens (NAc) and Amygdala) [29]. Using a similar experimental protocol with a heat pain stimuli, OA spontaneous pain proved to be associated with increased activity in the cingulate,

thalamus and amygdala[28]. These findings pointed to a dissociation between mechanically induced and spontaneous OA knee pain, the latter engaging brain regions involved in cognitive and emotional assessment [28].

These were some of the initial findings challenging the standard view regarding brain representation of OA pain. Since then, a few important advances were made: there seem to be localized and global grey matter changes in OA, that relate to clinical pain characteristics[30,31] and a disruption of brain information sharing at a network level, driven mostly by prefrontal and limbic related regions [32,33].

Though innovative and necessary, studies looking at supraspinal processing of OA pain are still infrequent, and so far, large data samples evaluating OA pain mechanisms are missing. On the other hand, other chronic pain conditions have been better characterized from the brain point of view.

1.2 Brain mechanisms of chronic pain and its application in OA

1.2.1 Brain mechanisms of chronic pain – general concepts and challenges

Only relatively recently have we had the chance to probe into the functioning human brain: In the early 1990's non-invasive human brain imaging of physiological activity (functional MRI, fMRI), was developed [34,35]. This technology, and related measures (anatomical analysis using T1 data and diffusor tensor imaging (DTI) for studying brain white matter properties) have had a major impact revealing brain circuitry underlying acute and chronic pain [8,36].

Applying MRI technology to understand brain mechanisms of OA poses as a novel and exciting opportunity; nonetheless there are conceptual challenges in the

field of chronic pain research/brain imaging that should be addressed when applying present knowledge to the study of OA pain. These challenges are also opportunities to defy outdated concepts and theories that OA pain is the prototype of nociceptive pain (where the role of the brain is simply the continued encoding of nociceptive peripheral input into perceptual outputs).

Firstly, the great body of research both in human pain and animal models have targeted mostly peripheral nociceptive mechanisms and it is frequent to use models of acute pain to study chronic conditions. Consequently, the brain import has been mostly characterized from the viewpoint of nociceptive processing and acute pain: examining the dependence of noxious stimulation and acute pain perception on cognitive and emotional modulators [9]. It is essential to separate concepts of nociception, acute pain and chronic pain and its putative representation in the brain. Mechanistically these phenomena are interconnected, however they should translate very distinct brain states. Pain is a subjective conscious perceptive state that is distinct from nociception. While nociception reflects the neural encoding of tissue damage, pain refers to the subjective experience of actual or impending harm [37]. Multiple human neuroimaging studies show that pain and the noxious stimulation (nociception) are dissociable with regard to brain activity [38,39,40]. Pain should reflect the conscious awareness of the noxious sensation and is an outcome of cognitive-emotional processing. Though seemingly trivial, this concept should be acknowledged regarding OA: <u>pain should not be seen as directly dependent on the level of nociceptive joint damage</u>.

The challenge of distinguishing acute and chronic pain and their representation in the brain starts with the clinical definition of chronic pain, as it asserts that chronic pain is defined as “persistent or recurrent pain lasting longer than 3 months” [41]. It

does not incorporate underlying mechanisms, and at least suggests that chronic pain is the temporal extension of acute pain, implying commonly shared mechanisms between both. Multiple neuroimaging studies have demonstrated that brain anatomy and function are distorted in chronic pain[9]. Acute pain is a sign of tissue insult or of disease related tissue injury, while chronic pain is conceptualized as a pathological state [42]. This draws an important notion if we apply it to our knowledge of OA: continued joint pain after several months/years will potentially lead to neural plastic changes. Thus, OA pain also translates the cumulative peripheral and central adaptations associated with the burden of persistent/recurrent pain.

Finally, there is a general assumption that the peripheral injury is the primary controller of pain chronification from an acute state[43]. However, most patients that experience a similar injury exhibit different clinical outcomes. For the majority, pain subsides as the injury resolves within a normal healing period or with proper treatment. However, some patients develop chronic pain that may persist for years and do not respond to what are regarded as effective treatments [44]. Once again, one may apply this concept to OA: response to surgical treatment, namely total joint replacement (TJR), is not uniform, with a considerable number of patients presenting with persistent pain in the apparent absence of peripheral disease. This reinforces that injury alone is not sufficient to understand mechanisms of chronic pain and recovery.

1.2.2 From acute to chronic pain: the concept of predisposition and transition

An important notion in brain mechanisms of chronic pain developed about a

decade ago, with the concept of predisposition and transition from acute to chronic pain. Brain properties underlying the transition from a subacute pain state to chronic pain were characterized in a groundbreaking study in patients with low back pain [45] . Functional connectivity, or extent of information sharing measured with fMRI, between the medial prefrontal cortex (mPFC) and the nucleus accumbens (NAc) in the subacute pain phase, differentiated patients who recovered and patients who transitioned to chronic low back pain at 1 year (**Figure 2.C**). Remarkably, these results are consistent with animal models of chronic neuropathic pain – the same circuit causally controls neuropathic-like behaviors: optogenetic stimulation of the mPFC or the NAc reversed tactile allodynia [46]; up and down regulation of NAc dopamine D2 receptor controlled tactile allodynia [47]. Hence, there is strong evidence that the corticolimbic functional and structural properties have a causal relationship with the development of chronic pain after the painful acute phase installs.

The mesocorticolimbic circuit, composed by the mPFC, ventral tegmental area (VTA), NAc, amygdala and hippocampus, is one of the brain's major dopaminergic pathways, and is essential to mechanisms of reward and aversion, motivation-valuation, and regulating learning processes[48]. The fact that this circuit may be underlying the transition to chronic pain, suggests that the disorder may be viewed as a learning process, where increased NAc-mPFC connectivity reflects an aversive teaching that leads to sustained pain over time. Enhanced connectivity may reflect an increased emotional salience signal, associated with an abnormal dopaminergic outputs from the VTA, which would in turn modulate thalamocortical circuits, amplifying the value nociceptive inputs. [49]. It remains unclear whether alterations in this circuit is also prognostic of transition to chronic pain in other pain conditions, namely OA [9].

Other properties of this circuitry, namely corticolimbic white matter anatomical distortions (**Figure 2.A**) and white matter structural connectivity, together with limbic volumes (hippocampus, amygdala (**Figure 2.B**) and NAc), also differentiated subacute back pain patients transitioning to chronic pain [49,50]. The stability of structural measures, particularly white matter properties, 1 to 3 years after the acute phase, proposed that some of these properties may be preexisting, hardwired properties that place subjects at risk of developing chronic pain [49].

Given this evidence, we can hypothesize that the dynamics of the corticolimbic circuitry, which depend both on preexisting limbic brain properties and the reorganization following the inciting phase of OA determine the likelihood of pain recovering or persisting after the nociceptive drive ceases and apply these concepts in OA.

1.2.3 The brain in chronic pain

As explored above, some brain properties may predispose patients to chronic pain and others may reflect the transition from the acute to the chronic state (**Figure 2. D**). At the same time, brain anatomical and functional changes may also be a consequence of the ongoing pain over time [51].

One of the first reports of structural brain grey matter changes in chronic pain showed patients with CPB exhibited lower grey matter density (studied by voxel-based morphometry) in the mPFC when compared with healthy subjects [52]. Since then, multiple studies have shown morphological grey matter changes in chronic pain [53]. Different chronic pain syndromes share commonalities but also present specificity regarding to grey matter distortions – regions related to attention and salience are

affected transversely across conditions, however, sensory regions seem to be dependent on the specific condition[54]. Moreover, a specific pattern of whole brain grey matter reorganization (**Figure.2C**) was linked to each condition, reflecting a possible unique maladaptive physiological process dependent on the duration of chronic pain. It has also been shown that grey matter changes are reversible after successful treatment – both in hip OA[30,55] and CPB[56,57]. This data suggests that grey matter changes may be contingent on the ongoing chronic pain syndrome and reflect a consequence of chronic pain in the brain.

The underlying anatomical reorganization seen during chronic pain is also reflected in the properties of resting state (rs-fMRI) brain activity – brain activity in rest or task-negative state, when there is no explicit task being performed in the scanner [58]. Using rs-fMRI, the correlation between spontaneous activation patterns of brain regions can be measured, both between specific regions and at the whole brain level. This allows us to study the brain as a network, model sub-network properties and their relationships, and evaluate the state of information sharing. One of the first studies looking at network abnormalities in multiple chronic pain conditions showed functional connectivity changes within the default mode network (DMN) [33]. The general pattern of reorganization was common across multiple pain conditions (CBP, OA, complex regional pain syndrome (CRPS)), with subtle reorganization of spatial properties that were specific to each type of chronic pain. This frame of work was further characterized in OA [32], revealing a widespread network disruption in patients with persistent OA pain, primary driven by the anterior insular cortex. Overall, the extent of these reorganization patterns was a function of intensity and duration of chronic pain.

A distinct way to model functional connectivity, that has seen a more recent widespread use, is the application of mathematical properties of graph systems to model brain activity[59]. One of such properties is degree – for each unit of a network (e.g., a voxel; a region-of-interest) we can measure the number of connections it shares with other regions, its extent of information sharing. A whole-brain degree map then represents a special pattern of brain's information sharing. We can then contrast such maps with healthy control maps, and derive the overall deviation for patients – the slope of regression between each subjects relative to the healthy control mean [60]. This measure, named hub disruption index (K_D), can be interpreted as a measure of disruption of global information share. K_D has proven to be present in multiple chronic pain conditions (**Figure 2.F**), including OA, and in distinct demographic populations[61,31]. Moreover, K_D is proportional to the magnitude of chronic pain reported, it is not induced by acute thermal stimuli and is shown to emerge in time, together with clinical pain. Furthermore, this phenomenon was validated in an animal model of chronic pain (SNI)[31]. Other than the global disruption of information sharing, transversal to multiple chronic pain conditions, localized degree disruptions were also detected, showing specificities in distinct chronic pain conditions.

Overall, both structural and functional large-scale and localized disruptions can be seen as a consequence of the underlying pain in the brain, emerging with it. Large-scale adaptations seem to be transversal to chronic pain conditions, with localized different disruption patterns between syndromes. We can hypothesize that such structural and functional distortions develop with OA pain, relate to clinical pain characteristics, and consequently may change with the successful treatment of the disease.

1.2.4 Diagnostic vs Prognostics brain-based biomarkers for pain

The evidence and concepts so far expounded can be considered from the point of view of biomarkers – defined characteristics that are measured as an indicator of normal biological processes, pathogenic processes, or biological responses to an exposure or intervention [62]. Functional and structural Magnetic Resonance Imaging (fMRI/sMRI) are bringing us closer to develop brain-based markers of neural mechanisms and neuropathology that underlie chronic pain [63].

It is important to make a distinction in interpreting possible brain-biomarkers. These can be diagnostic, emergent in time and associated with the evolution of the disease, and thus useful in detecting or confirming the presence of a condition of interest; or prognostic, indicating an increased (or decreased) likelihood of a future clinical event, disease recurrence or progression, thus unveiling a predisposition [51].

Diagnostic biomarkers can be helpful in the identification of chronic pain, differentiating chronic pain from other related negative mood states, and in guiding therapy, as it is expected that they are reversible with appropriate therapeutic treatment. Prognostic biomarkers, on the other hand, can unravel causal mechanistic insights regarding brain circuitry predisposing to chronic pain, and further help guide treatment *a priori*.

Differentiating between prognostic and diagnostic brain-biomarkers is not straightforward. Most chronic pain conditions are studied cross-sectionally, leading to the mix of both markers. Longitudinal studies are much more informative, however, when there is no change in the clinical status of chronic pain (resolving/persisting), brain changes consequent and causal of chronic pain are still entangled. Studying the transition between an acute episode and chronification (as explored above)

allows us to define biomarkers for transition. Studying the effect of an intervention to treat the ongoing nociceptive stimuli, on the other hand, would allow us to extricate between diagnostic biomarkers, those present with the ongoing disorder and possibly reversible with treatment; and prognostic biomarkers, stable before and after the intervention, conferring *a priori* greater risk for chronic pain.

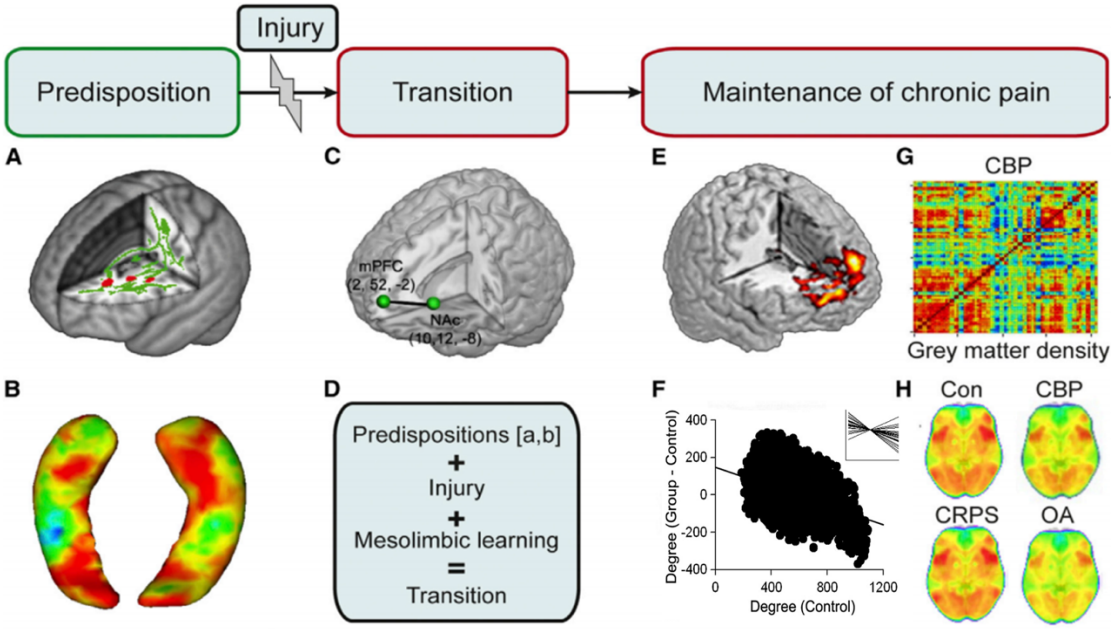

Figure 2. Brain properties adapting and predicting the transition to chronic pain. Brain structural and functional properties are suggested to both adapt with pain and impart risk for pain chronification. A. Specific brain white matter structural properties (red) associate with risk for developing chronic pain following an acute episode of back pain [64]; B. Limbic structural properties may also associate with risk for pain chronification (here, shape and size of the hippocampus) [65]. C. The strength of information exchange between the prefrontal cortex and accumbens determines long-term pain chronification [45]. D. The transition to a state of chronic pain is influenced by predisposing brain factors in combination with the injury-related

nociceptive signals. Mesolimbic adaptations, possibly underlying learning and emotional abnormalities in CP, together with predisposition and injury relate to the extent of accumbens-mPFC information exchange [66]. E. Ongoing pain-related brain activity patterns [67]; F. Hub disruption index (K_D), a measure of global information share disruption, is present in multiple chronic pain conditions and relates to clinical pain characteristics.[31] . G. Brain grey matter structural reorganization, here the similarity matrix, for CBP [68]; unique patterns are found for different types of CP. H. Distortions in information sharing in resting state brain activity shows chronic pain conditions specific patterns [33]. Figure adapted from *Baliki and Apkarian, 2015* [9] and *Mansour et al, 2016* [31].

1.3 Chronic pain in OA after total joint replacement

A common procedure to treat severe OA of the knee and hip is total joint replacement (TJR) surgery. This procedure is considered a safe and successful technique, when pharmacological and conservative treatments cannot provide adequate pain relief and level of functionality [4]. It is amongst the most commonly performed surgeries worldwide, and large increases in its demand are projected for the future [69,70]. Although TJR is seen as a highly successful surgery, offering substantial improvement in functional status and quality of life, 7 to 23% of all hip OA and 10 to 34% of knee OA patients report moderate to severe pain between 3 months and 5 years after surgery [71]. In addition to disruption in daily activities of life, chronic post-surgical pain has been associated with functional limitations, pain-related distress, depression, social isolation and overall lower quality of life [72,73].

Over the last years, multiple pre-operative clinical, demographic and psychological variables have been studied as possible risk factors for post-TKR pain.

Presurgical pain intensity, pre-operative function, psychological variables – anxiety, depression, pain catastrophizing, coping strategies, are amongst the most studied ones [74,75,76,77]. Female gender, younger age, medical co-morbidities, lower socioeconomic status, lower income and lower education and increased rates of opioid use before surgery, have also been proposed as individual risk factors for pain after TKR [75,78,79].

Post-operative risk factors for post-TKR pain have also been studied; acute postsurgical pain, early post-operative functional outcomes, post-operative mood parameters and opioid use after surgery have been liked with the negative outcome[73].

Though multiple studies evaluated such variables, evidence is conflicting and recently shown to be of low quality, even when studying large samples and considering multivariable models [80]. There is a large heterogeneity in outcome measures and study methodologies, and also in defining the pain outcomes. Moreover, many of the relationships reported are small in magnitude, and thus of debatable biological interest [80].

Other commonly studied predictors of post-TJR pain are quantitative sensory testing (QST): pressure pain thresholds (PPT) testing, sensitivity mapping, mechanical temporal summation and conditioned pain modulation [81]. These measures have been interpreted as clinical measures of central sensitization: e.g., OA knee patients with strong hyperalgesia exhibit higher temporal pain summation upon repetitive stimulation of the OA knee; patients with widespread pain beyond the joint exhibit lower pressure pain thresholds[26]. The presence of such indicators before surgery has been linked to a worse outcome[82,83]. However, the evidence regarding its validity and robustness as predictors of pain persistence after TJR, specially in knee OA is still conflicting [84].

Overall, the validity of clinical, psychological, demographic variables and QST measures as prognostics biomarkers in post-TJR pain is debated. Their widespread use limited, and the true value of these measures in need of comprehensive study. Moreover, such measures are mostly indirect markers of possible peripheral/central involvement in OA pain and do not further allow us to expound mechanisms of pain persistence.

Given all the exposed data, is it tempting to hypothesize that brain biomarkers, in the apparent absence of peripheral input, might help to explain pain persistence after a technically successful TJR.

1.4 Aims

The global aim of the present thesis was to provide new insights on brain mechanisms of OA pain, relate possible brain biomarkers to clinical metrics of OA pain and better understand its relevance for pain persistence after TJR. Four main goals were established:

1. Given the conflicting evidence on the value of clinical, psychological and sociodemographic variables as predictors of persistent OA pain after TJR [80], we sought to study how these parameters relate to OA pain and persistence of OA pain after TJR using a comprehensive multivariable approach. We hypothesize that distinct pain measurements relate to different clinical and biopsychological aspects of knee and hip OA pain, and propose to find stable predictors of surgery outcome **(Publication I)**.

2. The aforementioned data supports grey matter changes, both large scale and localized adaptations, to be associated with multiple chronic pain conditions. So far, structural grey matter reorganization in OA was shown, though in small samples and mostly using univariable methods [30]. We hypothesize that multivariable methods, accounting for the interrelationship of brain regions, translate brain structural adaptations in OA, and furthermore relate to clinical properties of the disease, thus testing grey matter properties as diagnostic brain biomarkers of hip and knee OA **(Publication II)**.

3. From a functional point of view, disruption of information share at a whole brain level has been associated with the development of chronic pain and proposed as a diagnostic biomarker of the disorder [31]. We hypothesize that similarly to other chronic pain conditions, there is a global distortion of information share in OA that is related to clinical properties of the disease. Furthermore, we query if local changes in information share underlie global disruptions, reflecting specific adaptive/maladaptive plasticity in OA pain **(Publication III).**

4. After studying structural and functional readaptations in OA pain, and its relations to clinical properties of the disease, we sought to study brain properties as predictors of OA pain after TJR. Given that spontaneous OA pain is known to engage limbic brain circuitry [29], and limbic brain functional connectivity properties are implicated in the transition to chronic pain in CBP [45], and finally, that corticolimbic white matter properties are seemingly

prognostic risk factors for pain chronification [49], we hypothesize that limbic circuitry is associated with pain persistence after TJR. We therefore study functional and structural properties of subcortical brain structures as predictors of pain persistence in OA (**Manuscript in preparation**).

1.5 References:

1. Loeser, R. F., Goldring, S. R., Scanzello, C. R. & Goldring, M. B. Osteoarthritis: A disease of the joint as an organ. *Arthritis Rheum.* **64**, 1697–1707 (2012).
2. Hunter, D. J., March, L. & Chew, M. Osteoarthritis in 2020 and beyond: a Lancet Commission. *The Lancet* **396**, 1711–1712 (2020).
3. Zhang, Y. & Jordan, J. M. Epidemiology of Osteoarthritis. *Clin. Geriatr. Med.* **26**, 355–369 (2010).
4. Neogi, T. The epidemiology and impact of pain in osteoarthritis. *Osteoarthritis Cartilage* **21**, 1145–1153 (2013).
5. Hannan, M. T., Felson, D. T. & Pincus, T. Analysis of the discordance between radiographic changes and knee pain in osteoarthritis of the knee. *J. Rheumatol.* **27**, 1513–1517 (2000).
6. Bedson, J. & Croft, P. R. The discordance between clinical and radiographic knee osteoarthritis: A systematic search and summary of the literature. *BMC Musculoskelet. Disord.* **9**, 116 (2008).
7. Malfait, A.-M. & Schnitzer, T. J. Towards a mechanism-based approach to pain management in osteoarthritis. *Nat. Rev. Rheumatol.* **9**, 654–664 (2013).
8. Apkarian, A. V., Bushnell, M. C., Treede, R.-D. & Zubieta, J.-K. Human brain mechanisms of pain perception and regulation in health and disease. *Eur. J. Pain* **9**, 463–463 (2005).
9. Baliki, M. N. & Apkarian, A. V. Nociception, Pain, Negative Moods, and Behavior Selection. *Neuron* **87**, 474–491 (2015).
10. Sofat, N., Ejindu, V. & Kiely, P. What makes osteoarthritis painful? The evidence for local and central pain processing. *Rheumatology* **50**, 2157–2165 (2011).

11. Fu, K., Robbins, S. R. & McDougall, J. J. Osteoarthritis: the genesis of pain. *Rheumatology* **57**, iv43–iv50 (2018).
12. Miller, R. E. *et al.* The Role of Peripheral Nociceptive Neurons in the Pathophysiology of Osteoarthritis Pain. *Curr. Osteoporos. Rep.* **13**, 318–326 (2015).
13. Mapp, P. I. & Walsh, D. A. Mechanisms and targets of angiogenesis and nerve growth in osteoarthritis. *Nat. Rev. Rheumatol.* **8**, 390–398 (2012).
14. Ferreira-Gomes, J., Adães, S., Sousa, R. M., Mendonça, M. & Castro-Lopes, J. M. Dose-Dependent Expression of Neuronal Injury Markers during Experimental Osteoarthritis Induced by Monoiodoacetate in the Rat. *Mol. Pain* **8**, 1744-8069-8–50 (2012).
15. Adães, S. *et al.* Injury of primary afferent neurons may contribute to osteoarthritis induced pain: an experimental study using the collagenase model in rats. *Osteoarthritis Cartilage* **23**, 914–924 (2015).
16. Raoof, R., Willemen, H. L. D. M. & Eijkelkamp, N. Divergent roles of immune cells and their mediators in pain. *Rheumatology* **57**, 429–440 (2018).
17. Tran, P. B., Miller, R. E., Miller, R. J. & Malfait, A.-M. Pain pathway activation in dorsal root ganglia and dorsal horn in a murine surgical model of osteoarthritis. *Osteoarthritis Cartilage* **22**, S417–S418 (2014).
18. Eitner, A., Hofmann, G. O. & Schaible, H.-G. Mechanisms of Osteoarthritic Pain. Studies in Humans and Experimental Models. *Front. Mol. Neurosci.* **10**, 349 (2017).
19. Schaible, H.-G. *et al.* Joint pain. *Exp. Brain Res.* **196**, 153–162 (2009).
20. Sagar, D. R. *et al.* The Contribution of Spinal Glial Cells to Chronic Pain Behaviour in the Monosodium Iodoacetate Model of Osteoarthritic Pain. *Mol. Pain* **7**, 1744-8069-7–88 (2011).

21. Tran, P. B., Miller, R. E., Ishihara, S., Miller, R. J. & Malfait, A. M. Spinal microglial activation in a murine surgical model of knee osteoarthritis. *Osteoarthritis Cartilage* **25**, 718–726 (2017).

22. Hains, B. C. Activated Microglia Contribute to the Maintenance of Chronic Pain after Spinal Cord Injury. *J. Neurosci.* **26**, 4308–4317 (2006).

23. Porreca, F. Chronic pain and medullary descending facilitation. *Trends Neurosci.* **25**, 319–325 (2002).

24. Ossipov, M. H., Morimura, K. & Porreca, F. Descending pain modulation and chronification of pain. *Curr. Opin. Support. Palliat. Care* **8**, 143–151 (2014).

25. Rahman, W. *et al.* Descending Serotonergic Facilitation and the Antinociceptive Effects of Pregabalin in a Rat Model of Osteoarthritic Pain. *Mol. Pain* **5**, 1744-8069-5–45 (2009).

26. Arendt-Nielsen, L. *et al.* Sensitization in patients with painful knee osteoarthritis. *Pain* **149**, 573–581 (2010).

27. King, C. D. A possible mechanism underlying conditioned pain modulation. *Pain* **155**, 1047–1048 (2014).

28. Kulkarni, B. *et al.* Arthritic pain is processed in brain areas concerned with emotions and fear. *Arthritis Rheum.* **56**, 1345–1354 (2007).

29. Parks, E. L. *et al.* Brain activity for chronic knee osteoarthritis: dissociating evoked pain from spontaneous pain. *Eur. J. Pain Lond. Engl.* **15**, 843.e1–14 (2011).

30. Gwilym, S. E., Filippini, N., Douaud, G., Carr, A. J. & Tracey, I. Thalamic atrophy associated with painful osteoarthritis of the hip is reversible after arthroplasty: A longitudinal voxel-based morphometric study. *Arthritis Rheum.* **62**, 2930–2940 (2010).

31. Mansour, A. *et al.* Global disruption of degree rank order: a hallmark of chronic pain. *Sci. Rep.* **6**, 34853 (2016).

32. Cottam, W. J., Iwabuchi, S. J., Drabek, M. M., Reckziegel, D. & Auer, D. P. Altered connectivity of the right anterior insula drives the pain connectome changes in chronic knee osteoarthritis: *PAIN* **159**, 929–938 (2018).

33. Baliki, M. N., Mansour, A. R., Baria, A. T. & Apkarian, A. V. Functional Reorganization of the Default Mode Network across Chronic Pain Conditions. *PLoS ONE* **9**, e106133 (2014).

34. Belliveau, J. *et al.* Functional mapping of the human visual cortex by magnetic resonance imaging. *Science* **254**, 716–719 (1991).

35. Ogawa, S., Lee, T. M., Kay, A. R. & Tank, D. W. Brain magnetic resonance imaging with contrast dependent on blood oxygenation. *Proc. Natl. Acad. Sci.* **87**, 9868–9872 (1990).

36. Martucci, K. T., Ng, P. & Mackey, S. Neuroimaging chronic pain: what have we learned and where are we going? *Future Neurol.* **9**, 615–626 (2014).

37. Mischkowski, D., Palacios-Barrios, E. E., Banker, L., Dildine, T. C. & Atlas, L. Y. Pain or nociception? Subjective experience mediates the effects of acute noxious heat on autonomic responses. *Pain* **159**, 699–711 (2018).

38. Apkarian, A. V., Darbar, A., Krauss, B. R., Gelnar, P. A. & Szeverenyi, N. M. Differentiating Cortical Areas Related to Pain Perception From Stimulus Identification: Temporal Analysis of fMRI Activity. *J. Neurophysiol.* **81**, 2956–2963 (1999).

39. Kong, J. *et al.* Using fMRI to dissociate sensory encoding from cognitive evaluation of heat pain intensity. *Hum. Brain Mapp.* **27**, 715–721 (2006).

40. Nickel, M. M. *et al.* Brain oscillations differentially encode noxious stimulus intensity and pain intensity. *NeuroImage* **148**, 141–147 (2017).

41. Treede, R.-D. *et al.* A classification of chronic pain for ICD-11: *PAIN* 1 (2015) doi:10.1097/j.pain.0000000000000160.

42. Raja, S. N. *et al.* The revised International Association for the Study of Pain definition of pain: concepts, challenges, and compromises. *Pain* **161**, 1976–1982 (2020).
43. Baron, R. Mechanisms of Disease: neuropathic pain—a clinical perspective. *Nat. Clin. Pract. Neurol.* **2**, 95–106 (2006).
44. Vachon-Presseau, E. *et al.* The Emotional Brain as a Predictor and Amplifier of Chronic Pain. *J. Dent. Res.* **95**, 605–612 (2016).
45. Baliki, M. N. *et al.* Corticostriatal functional connectivity predicts transition to chronic back pain. *Nat. Neurosci.* **15**, 1117–1119 (2012).
46. Lee, M. *et al.* Activation of Corticostriatal Circuitry Relieves Chronic Neuropathic Pain. *J. Neurosci.* **35**, 5247–5259 (2015).
47. Ren, W. *et al.* The indirect pathway of the nucleus accumbens shell amplifies neuropathic pain. *Nat. Neurosci.* **19**, 220–222 (2016).
48. Navratilova, E. & Porreca, F. Reward and motivation in pain and pain relief. *Nat. Neurosci.* **17**, 1304–1312 (2014).
49. Vachon-Presseau, E. *et al.* Corticolimbic anatomical characteristics predetermine risk for chronic pain. *Brain* **139**, 1958–1970 (2016).
50. Makary, M. M. *et al.* Loss of nucleus accumbens low-frequency fluctuations is a signature of chronic pain. *Proc. Natl. Acad. Sci.* **117**, 10015–10023 (2020).
51. Reckziegel, D. *et al.* Deconstructing biomarkers for chronic pain: context- and hypothesis-dependent biomarker types in relation to chronic pain. *PAIN* **160**, S37–S48 (2019).
52. Apkarian, A. V. Chronic Back Pain Is Associated with Decreased Prefrontal and Thalamic Gray Matter Density. *J. Neurosci.* **24**, 10410–10415 (2004).

53. Rodriguez-Raecke, R., Niemeier, A., Ihle, K., Ruether, W. & May, A. Structural Brain Changes in Chronic Pain Reflect Probably Neither Damage Nor Atrophy. *PLoS ONE* **8**, e54475 (2013).

54. Cauda, F. *et al.* Gray matter alterations in chronic pain: A network-oriented meta-analytic approach. *NeuroImage Clin.* **4**, 676–686 (2014).

55. Rodriguez-Raecke, R., Niemeier, A., Ihle, K., Ruether, W. & May, A. Brain Gray Matter Decrease in Chronic Pain Is the Consequence and Not the Cause of Pain. *J. Neurosci.* **29**, 13746–13750 (2009).

56. Čeko, M. *et al.* Partial recovery of abnormal insula and dorsolateral prefrontal connectivity to cognitive networks in chronic low back pain after treatment: Cognitive Networks in Chronic Back Pain. *Hum. Brain Mapp.* **36**, 2075–2092 (2015).

57. Seminowicz, D. A. *et al.* Effective Treatment of Chronic Low Back Pain in Humans Reverses Abnormal Brain Anatomy and Function. *J. Neurosci.* **31**, 7540–7550 (2011).

58. van den Heuvel, M. P. & Hulshoff Pol, H. E. Exploring the brain network: A review on resting-state fMRI functional connectivity. *Eur. Neuropsychopharmacol.* **20**, 519–534 (2010).

59. Bullmore, E. & Sporns, O. Complex brain networks: graph theoretical analysis of structural and functional systems. *Nat. Rev. Neurosci.* **10**, 186–198 (2009).

60. Achard, S. *et al.* Hubs of brain functional networks are radically reorganized in comatose patients. *Proc. Natl. Acad. Sci.* **109**, 20608–20613 (2012).

61. Huang, S. *et al.* Whole-brain functional network disruption in chronic pain with disk herniation: *PAIN* **160**, 2829–2840 (2019).

62. FDA-NIH Biomarker Working Group. BEST (Biomarkers, EndpointS, and other Tools) Resource. Silver Spring (MD): Food and Drug Administration (US); Bethesda (MD):

National Institutes of Health (US), www.ncbi.nlm.nih.gov/books/NBK326791/ (2021, accessed 20 March 2021).

63. Woo, C.-W. & Wager, T. D. Neuroimaging-based biomarker discovery and validation. *Pain* **156**, 1379–1381 (2015).
64. Mansour, A. R. *et al.* Brain white matter structural properties predict transition to chronic pain. *Pain* **154**, 2160–2168 (2013).
65. Mutso, A. A. *et al.* Abnormalities in Hippocampal Functioning with Persistent Pain. *J. Neurosci.* **32**, 5747–5756 (2012).
66. Mutso, A. A. *et al.* Reorganization of hippocampal functional connectivity with transition to chronic back pain. *J. Neurophysiol.* **111**, 1065–1076 (2014).
67. Baliki, M. N. *et al.* Chronic Pain and the Emotional Brain: Specific Brain Activity Associated with Spontaneous Fluctuations of Intensity of Chronic Back Pain. *J. Neurosci.* **26**, 12165–12173 (2006).
68. Baliki, M. N., Schnitzer, T. J., Bauer, W. R. & Apkarian, A. V. Brain Morphological Signatures for Chronic Pain. *PLoS ONE* **6**, e26010 (2011).
69. Kurtz, S., Ong, K., Lau, E., Mowat, F. & Halpern, M. Projections of Primary and Revision Hip and Knee Arthroplasty in the United States from 2005 to 2030: *J. Bone Jt. Surg.* **89**, 780–785 (2007).
70. Inacio, M. C. S., Graves, S. E., Pratt, N. L., Roughead, E. E. & Nemes, S. Increase in Total Joint Arthroplasty Projected from 2014 to 2046 in Australia: A Conservative Local Model With International Implications. *Clin. Orthop.* **475**, 2130–2137 (2017).
71. Beswick, A. D., Wylde, V., Gooberman-Hill, R., Blom, A. & Dieppe, P. What proportion of patients report long-term pain after total hip or knee replacement for osteoarthritis? A systematic review of prospective studies in unselected patients. *BMJ Open* **2**, e000435 (2012).

72. Gan, T. J. Poorly controlled postoperative pain: prevalence, consequences, and prevention. *J. Pain Res.* **Volume 10**, 2287–2298 (2017).

73. Wylde, V. *et al.* Chronic pain after total knee arthroplasty. *EFORT Open Rev.* **3**, 461–470 (2018).

74. Singh, J. A., Gabriel, S. & Lewallen, D. The impact of gender, age, and preoperative pain severity on pain after TKA. *Clin. Orthop.* **466**, 2717–2723 (2008).

75. Lewis, G. N., Rice, D. A., McNair, P. J. & Kluger, M. Predictors of persistent pain after total knee arthroplasty: a systematic review and meta-analysis. *Br. J. Anaesth.* **114**, 551–561 (2015).

76. Fortin, P. R. *et al.* Outcomes of total hip and knee replacement: preoperative functional status predicts outcomes at six months after surgery. *Arthritis Rheum.* **42**, 1722–1728 (1999).

77. Baert, I. A. C. *et al.* Does pre-surgical central modulation of pain influence outcome after total knee replacement? A systematic review. *Osteoarthritis Cartilage* **24**, 213–223 (2016).

78. Luong, M.-L. N., Cleveland, R. J., Nyrop, K. A. & Callahan, L. F. Social determinants and osteoarthritis outcomes. *Aging Health* **8**, 413–437 (2012).

79. Belard, A. *et al.* Battlefield to Bedside: Bringing Precision Medicine to Surgical Care. *J. Am. Coll. Surg.* **226**, 1093–1102 (2018).

80. Harmelink, K. E. M. *et al.* Are There Prognostic Factors for One-Year Outcome After Total Knee Arthroplasty? A Systematic Review. *J. Arthroplasty* **32**, 3840-3853.e1 (2017).

81. Frey-Law, L. A. *et al.* Pain sensitivity profiles in patients with advanced knee osteoarthritis. *Pain* **157**, 1988–1999 (2016).

82. Petersen, K. K., Arendt-Nielsen, L., Simonsen, O., Wilder-Smith, O. & Laursen, M. B. Presurgical assessment of temporal summation of pain predicts the development of chronic postoperative pain 12 months after total knee replacement. *Pain* **156**, 55–61 (2015).
83. Petersen, K. K., Graven-Nielsen, T., Simonsen, O., Laursen, M. B. & Arendt-Nielsen, L. Preoperative pain mechanisms assessed by cuff algometry are associated with chronic postoperative pain relief after total knee replacement. *Pain* **157**, 1400–1406 (2016).
84. Leung, Y. Y. *et al.* Pre-operative pressure pain thresholds do not meaningfully explain satisfaction or improvement in pain after knee replacement: a cohort study. *Osteoarthritis Cartilage* **27**, 49–58 (2019).

2. Research work

2.1 Publication I

Barroso J, Wakaizumi K, Reckziegel D, Pinto-Ramos J, Schnitzer T, Galhardo V, Apkarian AV. *Prognostics for pain in osteoarthritis: Do clinical measures predict pain after total joint replacement?* PLoS One. 2020 Jan 8;15(1): e0222370. doi: 10.1371/journal.pone.0222370. PMID: 31914126; PMCID: PMC6948829.

PLOS ONE

RESEARCH ARTICLE

Prognostics for pain in osteoarthritis: Do clinical measures predict pain after total joint replacement?

Joana Barroso[1,2,3], Kenta Wakaizumi[2,4], Diane Reckziegel[3], João Pinto-Ramos[5], Thomas Schnitzer[2,6], Vasco Galhardo[1], A. Vania Apkarian[2,3]*

1 Departamento de Biomedicina, Faculdade de Medicina, Universidade do Porto, Porto, Portugal; Instituto de Investigação e Inovação em Saúde—i3S, Universidade do Porto, Porto, Portugal, **2** Department of Physical Medicine and Rehabilitation, Northwestern University, Feinberg School of Medicine, Chicago, IL, United States of America, **3** Department of Physiology, Northwestern University, Feinberg School of Medicine, Chicago, IL, United States of America, **4** Shirley Ryan AbilityLab, Chicago, IL, United States of America, **5** Departamento de Medicina Física e de Reabilitação, Centro Hospitalar e Universitário de São João, Porto, Portugal, **6** Department of Rheumatology, Northwestern University, Feinberg School of Medicine, Chicago, IL, United States of America

* a-apkarian@northwestern.edu

Check for updates

OPEN ACCESS

Citation: Barroso J, Wakaizumi K, Reckziegel D, Pinto-Ramos J, Schnitzer T, Galhardo V, et al. (2020) Prognostics for pain in osteoarthritis: Do clinical measures predict pain after total joint replacement? PLoS ONE 15(1): e0222370. https://doi.org/10.1371/journal.pone.0222370

Editor: Yuanyuan Wang, Monash University, AUSTRALIA

Received: August 22, 2019

Accepted: December 13, 2019

Published: January 8, 2020

Peer Review History: PLOS recognizes the benefits of transparency in the peer review process; therefore, we enable the publication of all of the content of peer review and author responses alongside final, published articles. The editorial history of this article is available here: https://doi.org/10.1371/journal.pone.0222370

Copyright: This is an open access article, free of all copyright, and may be freely reproduced, distributed, transmitted, modified, built upon, or otherwise used by anyone for any lawful purpose. The work is made available under the Creative Commons CC0 public domain dedication.

Data Availability Statement: All relevant data are within the manuscript.

Funding: J.B. was funded through CCDRN [Norte-08-5369-FSE-000026], OARSI Collaborative

Abstract

A significant proportion of osteoarthritis (OA) patients continue to experience moderate to severe pain after total joint replacement (TJR). Preoperative factors related to pain persistence are mainly studied using individual predictor variables and distinct pain outcomes, thus leading to a lack of consensus regarding the influence of preoperative parameters on post-TJR pain. In this prospective observational study, we evaluated knee and hip OA patients before, 3 and 6 months post-TJR searching for clinical predictors of pain persistence. We assessed multiple measures of quality, mood, affect, health and quality of life, together with radiographic evaluation and performance-based tasks, modeling four distinct pain outcomes. Multivariate regression models and network analysis were applied to pain related biopsychosocial measures and their changes with surgery. A total of 106 patients completed the study. Pre-surgical pain levels were not related to post-surgical residual pain. Although distinct pain scales were associated with different aspects of post-surgical pain, multi-factorial models did not reliably predict post-surgical pain in knee OA (across four distinct pain scales) and did not generalize to hip OA. However, network analysis showed significant changes in biopsychosocial-defined OA personality post-surgery, in both groups. Our results show that although tested clinical and biopsychosocial variables reorganize after TJR in OA, their presurgical values are not predictive of post-surgery pain. Derivation of prognostic markers for pain persistence after TJR will require more comprehensive understanding of underlying mechanisms.

Introduction

Osteoarthritis is the most common cause of arthritis worldwide and a major source of chronic musculoskeletal pain. Although nociceptive inputs elicited by joint degeneration and chronic

Scholarship 2018 and Luso-American Development Foundation R&D@PhD scholarship grant. This research did not receive other specific funding from agencies in the public or commercial sectors.

Competing interests: The authors have declared that no competing interests exist.

inflammation are commonly recognized as contributing factors, current understanding of OA pain pathophysiology remains incomplete. In the last few years, a growing body of research indicates that altered peripheral and central nociceptive processes are influential [1]. This is substantiated by the discordance in joint structural damage and pain intensity [2], but also by the results of surgical treatment [3]. Total joint replacement (TJR) is an effective and safe intervention for advanced hip and knee OA; nevertheless, an important proportion of patients still report moderate to severe persistent pain post-TJR, not attributable to identifiable surgical or clinical complications. In the case of knee OA (KOA), persistent post-surgical pain is reported in about 20% of the patients. For hip OA (HOA), this number appears to be lower (up to 10%) [4].

Persistent post-TJR pain remains minimally understood. Post-surgical pain is defined as pain that occurs or intensifies after the procedure and lasts for at least 3 months [5]. However, in OA, long- lasting chronic pain pre-exists and is the main impetus for undergoing TJR, which complicates understanding post-surgical outcomes. Thus, it remains unclear the extent to which the post-surgical OA pain reflects residual presurgical pain, surgery induced pain, or some complex combination of both [6].

Regarding risk factors for pain persistence after TJR, those have been proposed, are mainly for KOA [7]. Pain intensity prior to surgery, disproportion between pain intensity and articular damage, neuropathic-like symptoms, psychosocial factors such as pain catastrophizing and poor coping strategies are commonly referenced as important predictive factors [8] [9] [10] [11]. Although these have been studied repeatedly, there is extensive variation of outcome measures used and there is no agreement on which measures are optimal to assess chronic pain after TJR [7]. The proposed risk factors across studies are often diverse, tested through univariate associations, based on different study designs and analysis methods, thus the quality of evidence on prognostic factors for recovery after total knee replacement (TKA) remains low [12].

Here, in a prospective cohort study, we test the hypothesis that presurgical pain and pain-related psychosocial parameters contribute to post-TJR pain in knee and hip OA. Our main aims are: 1) Test if baseline pain ratings relate to post-surgery pain levels; 2) examine how distinct pain measurement instruments relate to different clinical and biopsychological aspects of OA pain; 3) develop and evaluate models predictive of pain and pain relief after TJR; 4) use network analysis to assess the reorganization of pain related clinical and biopsychosocial properties of the personality of KOA and HOA patients after TJR.

Materials and methods

Study sample

KOA and HOA patients with clinical indications for primary arthroplasty surgery participated in this longitudinal observational study. The present report is part of a brain neuroimaging study, studying central mechanisms in osteoarthritis, which will be reported subsequently.

Enrollment took place at the Orthopedic Surgery Department of *Centro Hospitalar de São João*, a tertiary care hospital in Porto, Portugal. Study protocol was approved by the local Ethics Committee–*Comissão de Ética para a Saúde*, *Centro Hospitalar de São João*, and all participants provided informed written consent prior to partaking in the study. Sample size was determined by the number of patients waiting for surgery who met the eligibility criteria for the study, during a period of 20 months. Initial evaluation happened 1–3 months before TJR surgery and follow-up continued up to 6 months after surgery. A total of 95 knee OA and 25 hip OA patients, and 37 healthy control subjects were included (the last group not studied in this report).

Eligible patients met the following inclusion criteria: age between 45 and 75 years-old; diagnosis of HOA and KOA according to the clinical classification criteria of the *American College of Rheumatology*, and surgical indications for TJR (criteria for surgery selection was moderate to severe pain and quality of life impairment, after clinical and radiological evaluation and medical decision by a certified orthopedic surgeon in our center). Patients were excluded when there was evidence of secondary OA due to congenital or development diseases and inflammatory bone and articular diseases. Bilateral OA with predicted indication for contralateral arthroplasty in the following year, other chronic pain conditions (e.g., fibromyalgia; chronic pelvic pain) and chronic neurological or psychiatric disease (e.g., depression major, dementia, obsessive compulsive disorders, Parkinson's disease, demyelinating diseases, peripheral sensory neuropathy), were also exclusion criteria, as well as cognitive impairment. Previous history of stroke or traumatic brain injury was also exclusionary. Secondary OA following history of minor trauma or previous arthroscopy surgery due to ligamentous/meniscal injury was not an exclusion criterion.

Study design

This study comprised a total of 4 visits. Patients were initially assessed 1–3 months before surgery (V1). A second pre-surgical visit was held 2 to 6 weeks prior surgery (V2). Two post-surgical visits (V3-V4) occurred at 3 months and 6 months post-surgery. Specific data collected at each visit are shown in **Fig 1**. During visits 1, 3 and 4 patients were assessed for: (1) Clinical and socio-demographic properties; (2) physical function–performance-based tests; (3) radiographic evaluation, (4) pain, mood and health questionnaires; brain imaging was performed at visits 2 and 4.

Measures

Clinical and demographic assessment. Demographic profiling, acquired at V1, included age, education and professional status. Medical data concerning height and weight, pre-surgical co-morbid conditions, previous surgeries, general medication and smoking habits were recorded at patient interview and by clinical charts analysis. A clinical questionnaire regarding the history and evolution of knee pain assessed pain onset, duration and frequency; pain medication and previous non-pharmacological treatments. The Medicine Quantification Scale (MQS) was used to score type and dose of pain medication [13]

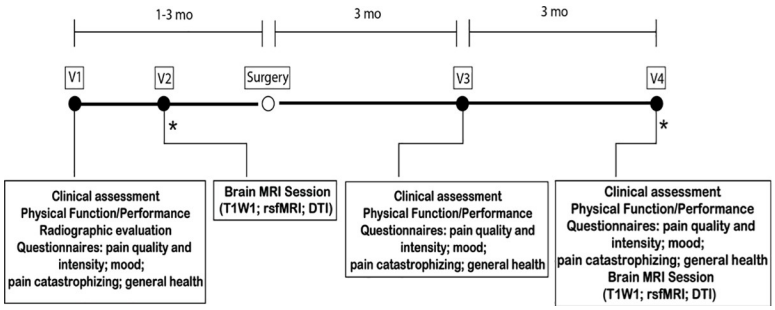

Fig 1. Experimental design, timeline and data collected. Knee and hip osteoarthritis patients entered a 4 visit (V1-V4), pre- and post-total joint replacement surgery, longitudinal, observational study. V1 and V2 occurred before surgery. V3 and V4 took place at 3 and 6 months after surgery. At each visit, participants underwent a series of assessments. *Brain MRI session. mo, months; MRI, magnetic resonance imaging; T1WI, T1-weighted imaging; rsfMRI, resting state functional magnetic resonance imaging; DTI, diffusion tensor imaging.

https://doi.org/10.1371/journal.pone.0222370.g001

At the post-surgical visits (V3-V4) a second clinical questionnaire assessing pain recovery, time to recovery, patient satisfaction, pain medication, use of health care services and rehabilitation protocol was administered.

Physical function–performance-based tests. Physical function was assessed with two different tests, depending on the activity measured. Ambulatory transitions were evaluated with the Timed up and go test (TUG) [14], and aerobic capacity/walking long distances with the six-minute walk test (6MWT) [15–17]. These tests were selected based on the *OARSI* 2013 recommendations [18].

Radiographic assessment. As part of standard hospital protocol, patients scheduled for TJR had bilateral joint radiographs during the 6 months before surgery. Knee OA radiographs were taken in two views: anterior-posterior (AP) weight-bearing with knee flexion at 20˚ and foot internal rotation at 5˚, and horizontal beam lateral view, with lateromedial projection, the patient in supine position and the knee flexed at 30˚. Hip OA patients had AP supine radiograph of the pelvis, with lower limbs internally rotated 15˚ degrees from the hip.

Radiographs were scored accordingly to the Kellgreen-Lawrence (KL) classification—grades 0 to 4 [19], by two trained radiologists. The first classified the whole sample, the second classified half of the subjects for inter-reliability measurement. Both researchers were blind to the clinical data of the patients when scoring. Inter-rater reliability was determined for KOA imaging only and the intra-class correlation coefficient of KL grading was 0.91 (95% confidence interval 0.80–0.93).

Questionnaires–Pain, mood and health. Seven questionnaires were administered by a trained clinician, during face-to-face interview. They were administered both before surgery (V1), and in the post-surgical visits (V3-V4). The repeated use of the same measures allowed us to track changes concerning intensity and quality of pain, emotion and affect, health and quality of life. All questionnaires were used in their Portuguese version, and validation data regarding their adequate context validity, internal consistency and test-retest reliability were consulted and hereby cited. We assessed: 1) KOOS, HOOS, validated injury and OA outcome scores for knee and hip [20–22]; 2) Brief Pain Inventory–Short Form (BPI) [23–25]; 3) McGill Pain Questionnaire (MPQ) [26, 27]; 4) Doleur Neuropathique en 4 Questions (DN4) [25, 28]; 5) Hospital Anxiety and Depression Scale (HADS) [29, 30]; 6) Pain Catastrophizing Scale (PCS) [25, 31]; and 7) SF36-item Short Form Survey (SF36) [32, 33].

Primary outcome variables. Primary outcome variables were part of the questionnaires/clinical assessments and consisted of 4 distinct pain intensity related scales/subscales: Numeric Rate Scale (NRS); BPI–Pain Severity; KOOS Pain and HOOS Pain, as clinically appropriate; SF36 Bodily Pain, here addressed specifically for knee/hip articular pain.

For each of the 4 outcome measures and for an aggregate of all four, we examined relationships for pain relief post-surgery on a per subject basis, by calculating residual pain: %residual pain = 100 –(100 *(average pain pre-surgery—post-surgery pain [at 3, or 6, months])/ average pain pre-surgery)). Thus, 100% residual pain = no change in a given pain measure between before and after surgery; 0% residual pain = complete relief from initial pain; while values >100% indicate worsening of pain post-surgery.

As the literature more commonly reports on the effect of pre-surgery baseline pain [9], we also examined and modeled influence of baseline pain on post-TJR pain.

Statistical analysis

All data from the reported measures were manually entered by the same researcher. Regarding missing data, if 30% or more was missing from a questionnaire (total or sub-score if

applicable), it should be excluded. If missing data were less than the threshold 30%, we used the mean of the total score/sub-score to fill in missing items.

Descriptive statistics were used to describe the study sample, with continuous variables presented as mean and standard deviations and categorical data as numbers and percentages. Comparisons between the two OA groups used independent sample t-tests or Chi-square(X^2) tests, for continuous parametrical variables and categorical data respectively.

Interrelationship of the primary outcome variables (all scored on a 0–10 score) was assessed through correlation analysis using Pearson product-moment tests. Fischer's z tests were used to evaluate differences between correlation coefficients at baseline, 3 and 6 months. The effects of time (pre-, 3- and 6-months post-surgery), type of OA and pain outcome measure on pain intensity were studied with a three-way mixed ANOVA. Following the initial procedure, two-way interactions and simple main effects were considered and pairwise comparisons with Bonferroni adjustments were performed.

Due to the high number of clinical and psychological measures collected, a data dimensionality reduction from all 19 subscales of 7 questionnaires and 2 physical performance scores was achieved using a principal component analysis (PCA) in KOA patients at baseline. This allows to reduce the data into fewer dimensions, while retaining underlying trends and patterns. Overall and individual Kaiser-Meyer-Olkin measures were 0.86 and >0.5 respectively. Threshold for component retention was set on eigenvalues >1.0, together with visual inspection of the scree plot for evaluation of the inflection point. A factor rotation on the obtained components was applied using a Promax oblique rotation technique. Threshold of factor loading was set on 0.5/-0.5 and components were labeled given the observed loadings. Due to the limited number of subjects available in the HOA group, we generated the component values using the same weights retrieved with PCA for the KOA, which enables direct comparison of TJR effects on network properties.

Different regression analysis techniques were used to model pain outcomes in KOA and HOA. For KOA, multifactorial regression models were generated using a stepwise forward and backward selection method, in an automatic step-by-step iterative construction of the model. Significance level to enter (α-to-enter) was set at 0.05 and α-to-remove at 0.10. To test if the models obtained in KOA replicated in HOA patients, and due to a smaller sample size in this group, we applied a multiple linear regression analysis in HOA, entering as independent variables the predictor factors uncovered for KOA, thus testing the extent of shared factors between the two conditions. For all regression models, assumptions of linearity, independence of observations, homoscedasticity and absence of multicollinearity were met, and residuals were approximately normally distributed in all models. Outliers were detected by examining studentized deleted residuals, any values greater than ± 3 standard deviations were removed. Throughout all models, no more than 3 cases were removed.

Correlation matrices of the clinical and psychological variables (questionnaires subscales and physical performance scores) were represented as binarized networks, constructed at the 25% stronger correlations for each matrix (KOA/HOA at baseline, 3- and 6-months post-surgery), and visualized using the software Cytoscape (v3.6.1, http://www.cytoscape.org). For each network, questionnaire measures were represented as nodes and the thresholded correlations as edges. Network communities were derived from the previous PCA. Two network graph measures were computed to characterize and quantify topological changes, using the Matlab Brain Connectivity Toolbox [34]. Clustering coefficient is a measure of the extent to which nodes in a graph tend to cluster together. Nodes have the trend to create groups characterized by a high density of connections. We computed local clustering coefficient of all nodes, and averaged them, reflecting the overall level of clustering in a network, from 0 (no clustering) to 1 (maximal clustering). The second calculated measure, modularity, refers to the

compartmentalization and interrelation of modules in a network. Modules can be defined as sets of nodes densely connected among themselves and poorly connected to other regions of the network. Using the Louvain community detection algorithm, averaged over 100 computed repetitions, we obtained values that vary from 0 (random network) and 1 (highly structured network).

We studied the changes in the strength of connectivity for all networks, calculating the change in correlation coefficients for all pairs of subscales from baseline to three and six months, and averaging these over the entire networks, obtaining the mean ΔR. For all inter and intra-group comparisons, regarding network measures and change in correlation coefficients, statistical probability was computed with 10,000 repeated random resampling.

All data were analyzed using the Statistical Package for the Social Sciences (IBM Corp. Released 2016. IBM SPSS Statistics for Windows, Version 24.0. Armonk, NY: IBM Corp), JMP software (JMP®, Version *14*. SAS Institute Inc., Cary, NC, 1989–2007) and MATLAB (MATLAB and Brain Connectivity Toolbox release 2016a, The Mathworks, Inc., Natick, Massachusetts, US).

Results

Recruitment, assessment and participant characteristics

A total of 94 KOA and 25 HOA patients were eligible and agreed to participate in this longitudinal, observational study. At 6 months, a total of 84 KOA and 22 HOA completed the study and were included in the analysis. Fig 2 presents patient and control participants flowchart and timeline. Causes for withdrawal included: revision arthroplasty due to periprosthetic infection or prosthesis displacement (n = 4); other co-morbidities (n = 2, concomitant oncological disease) and voluntary withdrawal (n = 12). Most included patients had a complete dataset, except 8% (n = 8) had missing data for at least one questionnaire and for those no more than 12% of each questionnaire was missing. The missing data were imputed using the mean for each scale/subscale.

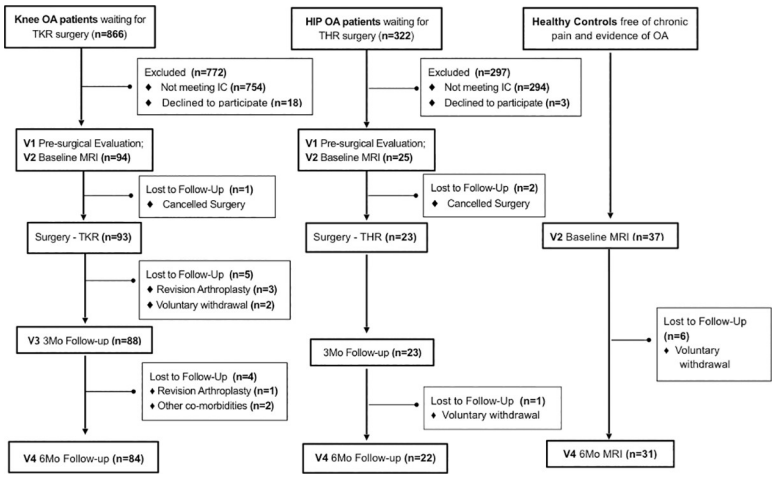

Fig 2. Recruitment and retention for KOA and HOA, and healthy control participants. The full battery of assessments was performed in osteoarthritis patients. Healthy individuals were recruited to act as controls in brain imaging analyses (not reported here). All patients were recruited from the same tertiary care hospital. Healthy participants were recruited from the general population in the Porto area. IC, Inclusion criteria; MRI, magnetic resonance imaging; KOA, knee osteoarthritis; HOA, hip osteoarthritis; THR, total hip replacement; TKR, total knee replacement.

https://doi.org/10.1371/journal.pone.0222370.g002

Table 1. Demographic characteristics of KOA and HOA patients.

	KOA(n = 84)	HOA(n = 22)	t/X2	p
Age, Mean±SD	65.6 ± 0.7	60 ± 1.6	4.005	**<0.001**
Gender, Count, %	75 (79.8) / 19 (20.2)	8 (32) / 17 (68)	21.37	**<0.001**
BMI, kg/m2, Mean±SD	30.3 ± 0.5	28.2 ± 0.7	2.027	**0.045**
Smoking Status, Count, %				
Active smoker	8 (8.5)	2 (8)		
Former smoker	14 (14.9)	6 (24)	1.176	0.556
Non-smoker	72 (76.6)	17 (68)		
Education Level, Count, (%)				
Primary school	74 (78.4)	17 (68)		
Secondary school	15 (16)	5 (20)	1.176	0.407
Graduate	5 (5.3)	3 (12)		
Professional Status, Count, (%)				
Retired	67 (70.5)	9 (36)		
Active	16 (16.8)	2 (8)	14.424	**0.006**
Medical leave	12 (12.6)	14 (56)		
Habitation, Count, (%)				
Alone	17 (18.1)	3 (12)	0.523	0.48
Cohabitation	77 (81.9)	22 (88)		

A total of 84 KOA and 22 HOA completed the study and were included in the analyses. Differences between groups were tested using T-test for continuous and parametric variables (t), and Chi-square tests for categorical data (X^2). P-values <0.05 were considered significant (bolded). BMI, body mass index; F/M = female/male; KOA, knee osteoarthritis; HOA, hip osteoarthritis.

https://doi.org/10.1371/journal.pone.0222370.t001

Table 1 describes HOA and KOA patients' demographic characteristics. Mean age of KOA patients was greater than that of HOA patients; the KOA group was predominantly female while the HOA group included mostly males. Body mass index (BMI) was higher in KOA than HOA patients. Smoking habits, educational level and habitation status were similar between HOA and KOA. Regarding occupational status, for the KOA group the most common status was retirement; HOA patients were mainly on medical leave, which relates to their differences in age.

Pain intensity as a function of type of pain measurement instrument, surgery, time, and OA joint involvement

We examined the pain intensity determined by our four pain outcome measures (NRS, KOOS pain, BPI pain severity, SF-36 pain), both at baseline and after surgery, in KOA and HOA patients, and then evaluated their interrelationship (Table 2). All pain magnitudes decreased post-surgery, correlations among measures generally strengthened. Mean post-surgical pain levels (across all measures) was lower in the HOA group than in the KOA group, and the pain intensity estimate was highest with the SF-36 pain scale.

A three-way ANOVA was conducted to determine the effects of time (pre-, 3, 6, months post-surgery), the four pain outcome measures, and the type of joint OA, on pain intensity. We found a non-significant three-way interaction between these variables. The two-way interactions were statistically significant between pain measures and time ($F(6,624) = 5.231$, $p<0.001$); type of OA and time ($F(2,624) = 4.096$, $p = 0.022$); but not type of OA and types of pain measures ($F(3,624) = 2.021$, $p = 0.129$). These results reveal that questionnaires show a similar rating pattern for hip and knee OA, but they vary in different ways over time.

Table 2. Pain in KOA and HOA patients pre- and post-surgery, characterized with four pain outcome measures.

Pain Outcome Measure					
Baseline					
Knee OA (n = 84)	**M**	**SD**	**(1)**	**(2)**	**(3)**
(1) BPI Pain Severity	4.79	1.5			
(2) NRS	6.53	1.67	.792**		
(3) KOOS Pain	6.49	1.49	.266**	.313**	
(4) SF-36 Pain	7.04	1.82	.162*	.288*	.475**
Hip OA (n = 22)					
(1) BPI Pain Severity	4.38	1.52			
(2) NRS	6.09	1.66	.801**		
(3) HOOS Pain	5.86	1.63	.564*	.405	
(4) SF-36 Pain	6.49	1.55	.547*	.474*	.631*
3 Months					
Knee OA (n = 84)	**M**	**SD**	**(1)**	**(2)**	**(3)**
(1) BPI Pain Severity	1.69	1.48			
(2) NRS	1.89	2.03	.922**†		
(3) KOOS Pain	2.45	1.96	.837**†	.809**†	
(4) SF-36 Pain	3.39	2.25	.750**†	.771**†	.774**†
Hip OA (n = 22)					
(1) BPI Pain Severity	0.54	1.05			
(2) NRS	0.55	1.06	.920**		
(3) HOOS Pain	0.79	0.88	.257	.159	
(4) SF-36 Pain	1.95	1.71	.329	.356*	.381*
6 Months					
Knee OA (n = 84)	**M**	**SD**	**(1)**	**(2)**	**(3)**
(1) BPI Pain Severity	1.70	1.53			
(2) NRS	2.01	1.9	.930**†		
(3) KOOS Pain	2.19	2.17	.813**†	.784**†	
(4) SF-36 Pain	2.98	2.26	.671*†	.652**†	.791**†
Hip OA (n = 22)					
(1) BPI Pain Severity	0.63	0.76			
(2) NRS	0.73	0.93	.961**†		
(3) HOOS Pain	0.80	0.77	.379	.280*	
(4) SF-36 Pain	1.98	1.87	.471*	.479*	.559**

Four scales were used (BPI Pain Severity, NRS, HOOS Pain, SF-36 Pain; all presented on a 0–10 scale) to assess pain pre-surgery (Baseline) and 3, and 6 months post-surgery. Mean (M), standard deviation (SD) and Pearson's product-moment correlations between the 4 scales are presented. For both OA groups the four measures decrease in amplitude after surgery and are correlated with each other, improving following surgery in the KOA group.

* $p<0.05$

** $p<0.01$.

† Significant increase in correlation from baseline, $p<0.05$.

KOA, knee osteoarthritis; HOA, hip osteoarthritis; BPI Severity, Brief Pain Inventory Pain: severity subscale; HOOS Pain, Hip Injury and Osteoarthritis Outcome Score: pain subscale; NRS, Numeric Rating Scale; SF36 Pain, Short-form (36) Health Survey: pain subscale.

https://doi.org/10.1371/journal.pone.0222370.t002

Moreover, decrease in pain over time is larger for HOA in comparison to KOA. These results are further characterized in S1 Fig.

Main effects of pain measurement types were statistically significant at baseline, 3 and 6 months ($F(3,315) = 66.6$, $p<0.001$; $F(3,315) = 51.03$, $p<0.001$; $F(3,315) = 41.02$, $p<0.001$). Pairwise comparisons revealed that at baseline, pain intensity estimates were lowest for BPI

pain severity, (mean differences—NRS: -1.72 [-2.44, -0.99], KOOS/HOOS: -1.436 [-2.158, -0.71], SF36: -2.06 [-2.78, -1.4], p<0.001). At 3 and 6 months after surgery pain intensity was higher when measured by SF-36 pain (mean differences at 3 months: NRS: 1.269 [0.509,2.03], BPI:1.566 [0.8,2.33], KOOS [0.24,1.76], p<0.003; at 6 months: NRS: 1.038 [0.23,1,81], BPI: 1.354 [0.57,2.14], p<0.003). Thus, one cannot assume that these different measurements are equivalent.

Joint involvement was also significant: KOA patients had higher levels of reported pain at baseline that HOA patients (mean difference: 0.55 [0.17,0.93], p = 0.005), while HOA surgery resulted in a larger decrease in pain intensity than KOA surgery (mean differences at 3 months: 1.462 [1.06,1.87] and 6 months: 1.21 [0.8,1.62], p value <0.001).

The main effect of time on pain intensity showed that from baseline to 3 months there is a large decrease in pain intensity. There was no change in pain intensity between 3 months and 6 months, revealing that pain levels were stable from 3 months onwards in both OA groups (mean differences, KOA: Baseline-3 months 3.8 [3.512,4.124] p<0.001; 3 months-6 months: 0.139 [-1.76,0.45], p = 0.8; HOA: Baseline-3 months 4.73 [4.133,5.332] p<0.001; 3 months-6 months: 0.112 [-0.512,0.736], p = 0.9).

Correlations between pain measure types pre-surgery were significantly positive in both OA groups, generally stronger in KOA than HOA, although these differences were relatively small. At 3- and 6-months post-surgery, the strength of the correlation of pain measures in the HOA group correlations were maintained; however, for the KOA, there was a strengthening of the correlations from baseline. Changes in correlations between pain measures by OA type, post-surgery imply that the characteristics of the pain itself is shifting distinctly post-surgery for each type of OA.

Pre-surgical pain levels mostly do not relate to post-surgical pain relief

For all 4 pain outcome measures, we examined the relationship between pre-surgical pain and a) residual pain after surgery (100% residual pain meaning no change; 0% residual pain rendering complete relief); b) absolute pain values after surgery, both for KOA and HOA at 3- and 6-months (Fig 3). We observed mostly weak and statistically not significant correlations between pre-surgical pain intensity and residual pain (except BPI pain at 3 months for KOA; NRS at 6 months for HOA; both were weakly negatively but statistically significantly related to pre-surgery values). Similarly, post-surgery pain was weakly and mostly not significantly related to pre-surgery pain (except KOOS at 3 months; and SF36 at 3 and 6 months, for KOA and HOA; all of these were statistically significantly positively related to pre-surgical measures). Both, residual pain and pain, show generally weak relationships with pre-surgery pain, and the relationships are often inconsistent with each other, indicating that pre-surgical pain levels are not consistent predictors of post-surgery measures.

OA related dimensions

Considering the broad battery of questionnaires and clinical measures collected, we sought to use a data dimensionality reduction approach to define dominant behavioral/clinical factors underlying OA pain and that were subject to change with surgery. To this end, we applied a PCA analysis to the questionnaires and physical performance tests at baseline, focusing on the larger group of KOA patients (n = 84). Pain intensity-related subscales were not included in this analysis, as they are the outcome measures to be modeled by PCA results. The correlations, organized by PCA results, are presented in **Fig 4A**. PCA identified 5 orthogonal components with eigenvalues>1.0, altogether explaining 69.9% of the variance (S2 Fig). Given the observed loadings (S1 Table), we labeled them as: 1) *Affect*, composed of anxiety and

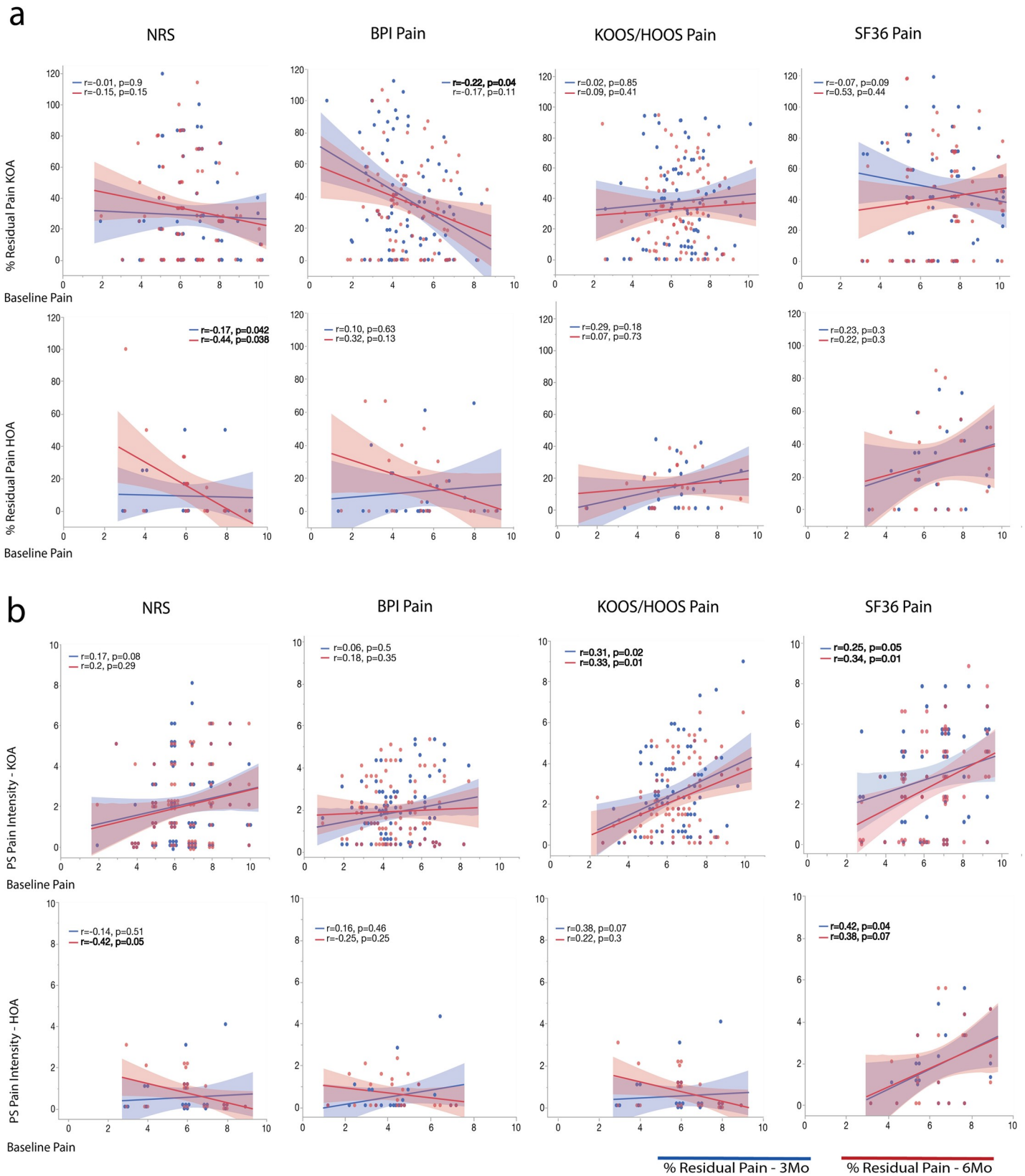

Fig 3. Influence of baseline pain levels on post-surgical residual pain. The scatterplots depict patients' percentage residual pain after surgery (% residual pain, where 100% = no change from pre-surgical levels, 0% = full recovery) **(a),** and post-surgery absolute pain intensity **(b)** relative to pre-surgical levels, as a function of pre-

surgical levels, for all four pain outcome measures for KOA and HOA, at 3 (blue) and 6 (red) months post-surgery. Symbols represent subjects. Shaded areas indicate 95% confidence intervals. Results in bold represent statistical significance at $p<0.05$. BPI Severity, Brief Pain Inventory Pain: severity subscale; HOOS Pain, Hip Injury and Osteoarthritis Outcome Score: pain subscale; NRS, Numeric Rating Scale; SF36 Pain, Short-form (36) Health Survey: pain subscale.

https://doi.org/10.1371/journal.pone.0222370.g003

depression subscales of HADS; *2) Pain Catastrophizing*, its highest factor loadings were the three maladaptive dimensions rumination, magnification and helplessness of PCS; 3) *Pain Quality*, dominated by the MPQ-sensory subscale and DN4, with high loadings regarding knee symptoms, knee related quality of life and sports and recreational ability; 4) *Health*, which was dominated by the SF-36 measures that quantify health status and health related quality of life; 5) *Physical Performance*, included high negative loading for 6MWT and high positive loading for TUG (**Fig 4B**). The factors approximate the distinct domains surveyed by the questionnaires and tasks: HADS, KOOS, PCS, SF-36, and the combination of TUG and 6WMT. These five factors were used in subsequent model building to predict pain and residual pain.

Modelling pain and TJR pain outcomes in OA

Next, we sought to model OA pain, using multi-factorial regressions (including only parameters that survived both forward and backward elimination), both at baseline and after surgery. Independent variables entered in our models are the five factors from the PCA results, together with relevant clinical/demographic variables: age, gender, educational level, body mass index, pain duration, and radiographic severity of OA.

Pre-surgery KOA pain is defined by its quality, across pain measures. Pre-surgery KOA pain could be successfully modeled for all four outcome measures (**Table 3**). All models reached statistical significance and accounted for 22–57% of variances of pain intensity. Pain

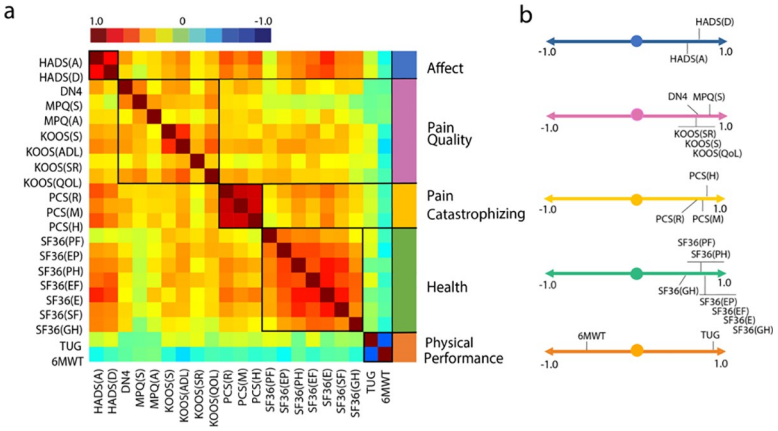

Fig 4. Principal component analysis identified five factors characterizing baseline KOA. Pain- and affect-related questionnaires, their subscales, and performance measures (prior to surgery) were examined together to identify dominant underlying factors. **a.** Correlation matrix ordered based on principal component analysis results (Pearson's r represented by color bar). The five identified components were labeled according to membership properties. **b.** Factor loadings are shown for the five components. To highlight dominant factors threshold of factor loading was set on 0.5/-0.5, after Promax oblique rotation. 6MWT, six minute walking test; DN4, The Neuropathic Pain 4 questions; HADS (A), The Hospital Anxiety and Depression Scale, Anxiety; HADS(D), The Hospital Anxiety and Depression Scale, Depression; KOOS, Knee Injury and Osteoarthritis Outcome Score, (ADL–Function in daily living), (S -Knee Symptoms), (SR–Function in sport and recreation), (QOL–knee related quality of life); MPQ, McGill Pain Questionnaire, (A–Affective score) (S–Sensory score); PCS, Pain Catastrophizing Scale, (R–Rumination subscale), (M–Magnification subscale), (H–Helplessness subscale); SF36, Short-form (36) Health Survey, (PF–Physical Functioning), (PH–physical role functioning), (EP–emotional role functioning), (EF–energy/fatigue), (E–emotional well-being), (SF–social functioning), (GH–general health); TUG, (Timed -up and go test).

https://doi.org/10.1371/journal.pone.0222370.g004

Table 3. Multiple regression models for KOA pain intensity at baseline for four different pain intensity measures.

Model	b	SE	β	t	p	Adjusted R^2
BPI Pain Severity						
Pain Quality	2.526	.670	.385	3.770	.000	
Pain Catastrophizing	1.430	.639	.229	2.239	.028	
						.275** F(2,92) = 18.816
NRS						
Pain Quality	0.851	0.162	0.479	5.258	.000	
						.229** F(1,93) = 27.652
KOOS Pain						
Pain Quality	11.499	1.126	.713	10.216	.000	
Physical Performance	2.426	1.123	.151	2.160	.033	
						.573** F(1,92) = 63.379
SF36 Pain						
Health	10.553	1.514	.602	6.970	.000	
Pain Quality	3.438	1.573	.189	2.186	.031	
						.513** F(2,92) = 50.504

KOA baseline pain intensity was explained by different pain-related characteristics, depending on the questionnaire used to capture pain intensity. While the pain quality factor was incorporated in all four regression models, additional unique influences were also identified for three of the four pain intensity scales. Displayed statistics are from the final step of each model. **b**, unstandardized regression coefficient; **SE**, standard error; **β**, standardized regression coefficient; **F**, obtained F-value; **t**, obtained t-value; $\mathbf{R^2}$, proportion of variance explained.

**$p \leq 0.01$. Displayed statistics are from the final step for each dependent variable. BPI Severity, Brief Pain Inventory Pain: severity subscale; HOOS Pain, Hip Injury and Osteoarthritis Outcome Score: pain subscale; NRS, Numeric Rating Scale; SF36 Pain, Short-form (36) Health Survey: pain subscale.

https://doi.org/10.1371/journal.pone.0222370.t003

quality emerged as the common dominant factor accounting for higher pain intensity throughout all scales. For NRS it was the only factor present in the model, whereas for the other 3 outcomes, additional factors were identified. BPI severity was predicted by higher levels of Pain Catastrophizing, KOOS Pain by worse Physical Performance, and SF-36 pain by worse Health Status.

Models predicting pain intensity and residual pain after surgery in KOA. Next, we sought to model absolute pain intensity after surgery and residual pain (reflecting within subject change from pre-surgery) for all four pain measures, using the parameters collected prior to surgery, thus searching for pre-surgery influences on post-surgical pain. Modeling was restricted to pain at 6 months post-surgery, since there were minimal differences between post-surgery pain at 3 and 6 months.

Results, (Table 4) demonstrated that only three of the four outcome measures for absolute post-surgical pain could be modeled, accounting for 0–24% of the variance, and obtained models were distinct for each pain measure. We obtained similar results when modeling residual pain 6 months post-surgery. Only three of the four pain measures could be modeled, accounting for even smaller 0–11% of the variance, and obtained models were distinct for each outcome measure, as well as from the models obtained for post-surgical pain. Note that obtained results seem paradoxical. Correlations between the four pain outcome measures increases post-surgery yet obtained, pre-surgery based, models diverge from each other, both for pain and for residual pain. A final attempt to model pain intensity as a composite variable

Table 4. Multiple regression models for post-surgical KOA pain intensity, and for percentage residual pain at 6-months post-surgery, for four different pain intensity measures.

Post-surgical Pain Intensity						
Model	**b**	**SE**	**β**	**t**	**p**	**Adjusted R^2**
BPI Pain Severity						
Affect	2.845	.670	.408	4.246	.000	.238** F(2,82) = 13.952
Pain Duration	.277	.096	.278	2.893	.005	
NRS						
No predictive model–no variables entered in the equation.						
KOOS Pain						
Affect	5.688	2.229	.284	2.522	.013	
Gender	9.756	4.320	.221	2.259	.027	
Health	4.246	2.026	.231	2.060	.043	
						.234** F(3,81) = 9.338
SF36 Pain						
Health	7.032	2.292	.310	3.068	.003	
Gender	15.176	5.520	.278	2.749	.007	
						.196* F(2,82) = 9.730
% Residual Pain						
Model	**b**	**SE**	**β**	**t**	**p**	**Adjusted R^2**
BPI Pain Severity						
Pain Duration	1.413	.536	.274	2.635	.01	
Health	7.681	3.451	.232	2.226	0.029	
						.114** F(2,82) = 6.267
NRS						
No predictive model–no variables entered in the equation.						
KOOS Pain						
Physical Performance	9.276	3.036	.321	3.055	.003	
						.092** F(1,83) = 9.335
SF36 Pain						
Gender	24.210	8.088	.316	2.993	.004	
						.088** F(1,83) = 8.959

Different explanatory models were elicited for absolute versus relative (% residual pain) pain intensity after surgery, with the variance explained by each model being overall lower for % residual pain than that for absolute pain intensity. Again, explanatory variables were also distinct considering the four different outcome measures. **b,** unstandardized regression coefficient; **SE,** standard error; **β**, standardized regression coefficient; **F**, obtain F-value; **t**, obtained t-value; **R^2**, proportion variance explained. Gender: male coded as 0, female coded as 1.

* $p \leq 0.05$

** $p \leq 0.01$. Displayed statistics are from the final step for each dependent variable.

BPI Severity, Brief Pain Inventory Pain: severity subscale; HOOS Pain, Hip Injury and Osteoarthritis Outcome Score: pain subscale; NRS, Numeric Rating Scale; SF36 Pain, Short-form (36) Health Survey: pain subscale.

https://doi.org/10.1371/journal.pone.0222370.t004

averaging the four outcomes was performed, without informative results and reported in S2 Table.

Do KOA models of pain and residual pain generalize to HOA?. Given the smaller data available in HOA (n = 22), and the large number of independent variables and four pain

outcome measures, we limited HOA modeling. We only tested the extent to which variables obtained in KOA modelling are meaningful for HOA. Therefore, regression models were constructed for HOA pre-surgical pain, 6-months absolute post-surgical pain and residual pain using only parameters identified for KOA. Pre-surgery, the multiple regression successfully modeled pain intensity for HOOS Pain (equivalent to KOOS pain), $F(2,22) = 24.308$, $p<0.005$, however only one of the two variables entered, Pain Quality, was significant ($\beta = .764$, $p = 0.005$). For SF-36 pain, the model obtained for KOA was also applicable, $F(2,22) = 23.55$, $p<0.001$. Here the factor Health ($\beta = .732$, $p<0.001$), but not Pain Quality was significant. NRS and BPI in HOA failed to be modeled. For absolute post-surgery pain and residual pain, variables identified on the KOA modelling were not significantly associated with any of the four pain scales in HOA.

Network analysis of pain dimensions

An alternative to regression-based modeling of the effects of TJR on OA pain is to examine properties of the correlation matrix identified pre-surgery (Fig 4) as a function of type of OA and time from surgery. Representing such correlation matrices as networks provides insights regarding organizational topography and changes in the inter-relationships between pain characteristics that define the OA state, as the variations in individual factor weights can be considered to define the OA-pain personality profile of such patients. Therefore, we calculated these networks pre-surgery, and three- and six-months post-surgery (Fig 5).

Regarding the pre-surgery KOA network, factors Affect, Pain Catastrophizing and Health presented salient edges (significantly high correlations) among them. Pain Quality showed a lower number of edges connecting with other factors (only through subscale KOOS-ADL). Physical performance was segregated from the other factors. For HOA, Affect and Pain Catastrophizing did not share any salient correlations. Pain Quality was highly correlated to Health and to a lesser extent to Pain Catastrophism. Physical performance was again segregated.

At six months after surgery topological differences were identified in both KOA and HOA groups. For the KOA network, Affect and Pain Catastrophizing no longer presented salient edges. Pain quality shared a higher number of edges with Affect and Health. Physical Performance continued to be isolated, sharing no edges with other components. For HOA, Pain Catastrophizing lost its prominent edges with Health and was only linked with Pain Quality. Physical Performance showed links with one variable in Pain Quality (HOOS Sports and Recreational) (Fig 5A).

To quantify topological changes in these network architectures we derived network measures and compared them between groups and as a function of time. We calculated change in strength of connectivity (change in correlation coefficients for all pairs of subscales, Δr-value) both for 3- and 6-months post-surgery. For further comparison intra- and inter-groups, we computed statistical probability using 10,000 permutations with random resampling.

Inside each group, there was a significant change in Δr-value, for both KOA and HOA, at 3 and 6 months, with no differences between 3 and 6 months in each group, indicating that post-surgical connectivity is stable in time. When comparing between KOA and HOA groups, connectivity change was larger for HOA both at 3 and 6 months (Fig 5B).

Lastly, we evaluated the clustering coefficient and modularity of the networks and assessed differences between groups. For both measures, KOA networks remained stable after treatment. HOA, on the other side, showed a significant change in both measures, from baseline to 3 and 6 months. From 3 to 6 months the networks remained stable (Fig 5C).

Overall, we observed that pain characterizing networks for KOA and HOA are quite distinct from each other prior to surgery while displaying similar topology; there is a significant

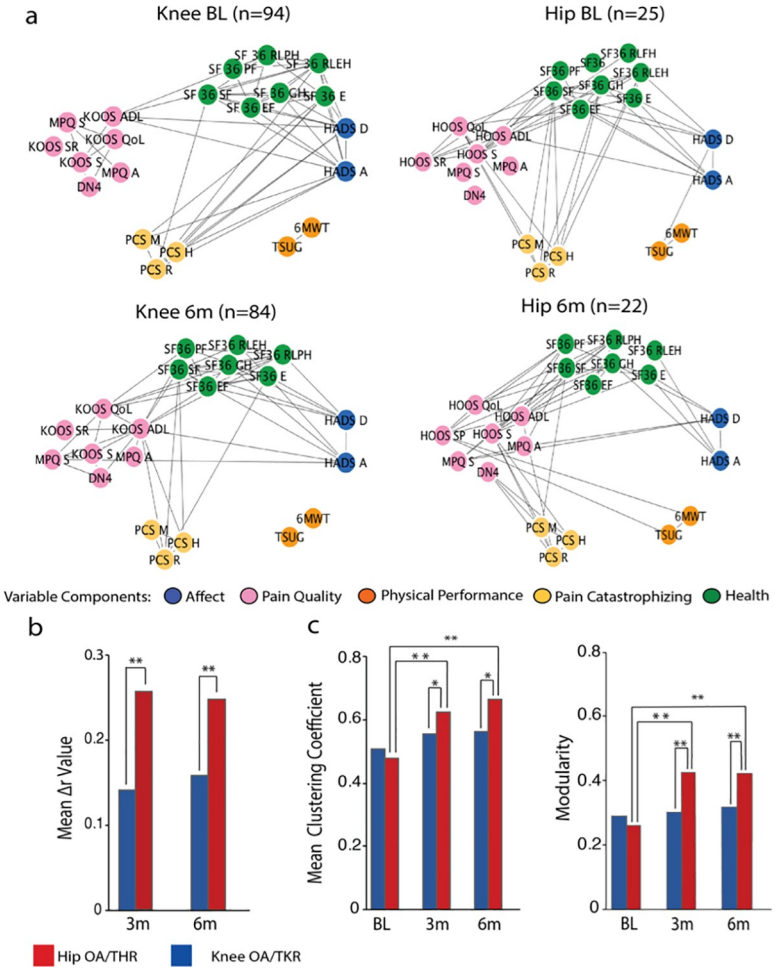

Fig 5. Network representation of OA pain characteristics. a) Network graphs depict interrelations between clinical and pain-related questionnaire subscale measures at baseline, and at 6 months post-surgery, for KOA and HOA patients. Network communities were derived from the PCA analysis. Links represent the top 25% correlations of each network. **b)** The bar graph displays mean change of global correlation coefficients (Pearson's Δr) for KOA and HOA, at 3- and 6-months post-surgery. Both groups had significant change in the overall interrelations between clinical and pain-related characteristics (KOA mean Δr 3months: 0.14, t = 13.37, mean Δr 6months: 0.16 t = 14.93, HOA mean Δr 3months:0.28, t = 8.72, mean Δr 6months:0.26 t = 9.23, $p<0.001$). The extent of change remained stable from 3 to 6 months post-surgery and was substantially higher in the HOA group at 3 months (t = 4.62, $p<0.001$) and 6 months (t = 3.44, $p<0.001$). **c)** Graph theory-based modularity and mean clustering coefficients for correlation networks at baseline, 3 and 6 months. The HOA networks shows significant topological reorganization 3 months (mcc: t = -8.19, modularity: t = -9.22, $p<0.001$) and 6 months after surgery (mcc, t = -10.62, modularity, t = -9.02, $p<0.001$), while KOA remains stable. BL, baseline; 3m, 3 months; 6m, 6 months; Statistical risk probability was computed under 10.000 times repeated random resampling. $^{**}p<0.001$, $^{*}p<0.05$.

https://doi.org/10.1371/journal.pone.0222370.g005

change in the overall interrelations between clinical and pain-related characteristics after surgery, more profoundly for HOA; and, topological properties show that network reorganization post-surgery is only significant for HOA.

Discussion

This study examined KOA and HOA pain prior and after TJR surgery. We used a systematic and structured approach, together with data reduction techniques, to investigate the properties of OA pain, its change with surgery, and factors that influence post-surgical OA pain. By using

four distinct pain intensity quantifying measures, two distinct types of joint OA, and measures collected at pre-, 3, and 6 months post-surgery, we examined the contribution of a large number of potential influences, many of which have been reported to be risk factors for OA pain persistence post-TJR. As available data were larger for KOA, we performed model building in this group and tested identified variables in HOA. Each of the four-pain intensity measures we used, demonstrated an overall decrease in OA pain after surgery in both OA groups, that was larger for HOA patients. A striking and perhaps unexpected result was how little OA pain changed from 3- to 6-months post-surgery in both groups. Neither the mean pain nor pain characteristics, as assessed by network properties, showed any important changes over this time period, although large changes were seen between pre-surgery and 3-months post-surgery. Our regression models showed that commonly assessed clinical and behavioral measures prior to surgery fail to reliably predict pain outcomes after TJR.

OA pain and persistent pain after TJR have been previously studied using multiple pain outcome scales. These can be divided in two major groups, general measures such as NRS, visual analog scale, SF-36 bodily pain and BPI pain severity, and OA specific measures as Western Ontario and McMaster Universities Osteoarthritis Index (WOMAC), KOOS/HOOS pain score and the Oxford Knee Score pain subscale [7, 35]. Such studies suggest that different pain outcomes relate to different facets of the pain experience in knee OA [36]. Using four different pain intensity outcomes, three of them from the category of general pain scales and one specific for OA (HOOS/KOOS), our results show that although correlations between these measures are positive and mostly significant (both at baseline and post-surgery), BPI pain severity tends to underestimate pain intensity and SF-36 pain tends to overrate pain intensity after surgery, both in KOA and HOA groups. Still, all four measures decreased 3-months post-surgery, and all remained unchanged between 3- and 6-months post-surgery.

Pain outcomes concerning persistency are commonly studied using primarily the absolute value of pain intensity after surgery, or dichotomizing the outcome using a fixed threshold that varies across studies [37–40]. Such approaches assume that the treatment has a constant effect. A change may show the health improvement in a more observable way. Here we chose to use both change (residual pain) and absolute value of pain. Both measures showed independence or minimal and inconsistent dependence on baseline values, implying pain relief post-surgery does not depend or inconsistently depend on entry scores.

An important remark concerning post-surgical pain and its risk prediction is that it relies on how it is defined and thus also on how one measures the pain outcomes. Chronic post-surgical pain is accepted as the pain that persists at least three months after surgery, different in characteristics from pre-operative pain, and without other causes such as infection or technical failure [5]. Our results are generally consistent with this definition and further advance the concept. Firstly, we observe that models characterizing OA pain at baseline do not generalize to pain post-surgery. Second, the amount of variance explained with the regression models for pain intensity decreased from pre-surgery (accounting for 23–57% of pain intensity variance), to post-surgery (accounting for 20–24% of variance), and further decreased when modeling residual pain (accounting for 9–11% of variance). Given that residual pain is a more direct measure of the influence of the surgical intervention than the absolute value of pain intensity, our models at best could only explain 11% of the variance of the surgery related OA pain. Third, studies report that pre-operative OA pain intensity has a strong influence on post-surgical outcomes [7]. It was recently argued that the evidence for this influence is of low-quality, even when studied in much larger number of OA patients [12], and our results support the failure of pre-operative pain as a predictor of post-surgical outcomes. Fourth, the network analysis shows large changes in the interrelationships between pain related characteristics post-surgery. Thus, our analysis, especially for KOA where we examined multiple models,

suggests that the post-operative pain is minimally related to the pre-operative pain properties. Our results in HOA, although not as strong, are also consistent with this notion.

Given the small sample size in HOA, we limited the statistical tests in this group. Models derived from KOA did not yield significance in the HOA group. Thus, HOA pain models remain to be studied in larger data sets in the future, and with additional parameters not included here. However, our results repeatedly confirm that pain relief is better in this group and this is accompanied with larger changes in the network properties. We observed larger changes in clustering coefficient and in modularity in HOA, implying that the pain personality in HOA is being fractured with pain relief, rendering different factors independent from each other. These findings are all consistent with earlier reports showing that the improvement in pain and physical function after arthroplasty is greater for hip than knee OA [3], even though symptomatic presentation of HOA is associated with more advanced radiological disease [41]. Determinants for persistent pain after THR are less studied, and evidence is limited and conflicting [42]. The full scope of the differences in TJR outcomes between both conditions requires further studies.

The primary focus of this paper was to find predictors for pain and pain persistency, and although we show that there is a high variability concerning scales and outcome definitions, some of the findings deserve further discussion. At baseline, we observed that across the four scales and the aggregated pain measure, Pain Quality (constituted mainly by neuropathic pain profile and sensory quality of MPQ) related to higher pain intensity. When we modelled residual pain after surgery, each scale unveiled different predictors. No homogeneous result could be retrieved.

It has been reported that the greatest improvement in patients undergoing TJR happens in the first 3 months after surgery [3]. Although a precise timeline for pain recovery is difficult to draw, our results support the finding that pain persistence at 3 months should be regarded as critical evidence for longer-term persistence of post-surgical pain.

An important weakness of the present study is the relatively small sample size and large number of variables tested. We acknowledge the increasing likelihood of type 2 errors and consider it as an important limitation that should be highlighted. It is possible that in larger samples stronger statistical relationships may be uncovered between presurgical clinical measures and post-TJR pain. However, we should note the literature where larger groups of subjects were studied indicate that these relationships are small in magnitude, and thus of debatable biological interest [12]. Nonetheless, we believe our results should be interpreted cautiously regarding generalizability, and the use of current methodology in larger samples would be of interest in the future.

The topic of reliability and sample size was recently discussed [43] in the field of neuroimaging but rendering important implications to other areas. The authors point that while sample size is recognized as a major determinant of statistical power, measurements of reliability are less commonly considered, that place an upper limit on the maximum detectable effect size. We measured inter-reliability regarding the radiographic assessment and used questionnaires with high context validity, internal consistency and test-retest reliability. Although we did not measure reliability directly, we believe this is an important remark, and data quality assessments are always important.

Another limitation is the imbalance of available data between KOA and HOA. Moreover, there were important demographic differences between the two groups which could not be corrected for due to the limited available sample in HOA. Thus, we cannot rule out the influence of these factors on the models derived from KOA and tested in HOA.

Regarding our sample characteristics, patients were enrolled in the same center, and the population included is ethnically homogeneous, thus caution is needed in generalizing the

present's study results to other populations. The follow-up time was limited to 6 months, what can also be regarded as a limitation. We also did not collect multiple measures that in the literature have been suggested to influence both baseline pain and post-surgical pain. For instance, measures of widespread hypersensitivity, temporal summation of pain and impaired endogenous pain inhibition assessed by quantitative sensory testing, have been suggested to contribute to poor pain relief following TKR [44, 45], however see [46]. It was also previously shown that OA patients present central nervous system structural and functional maladaptive changes [47, 48]. We will test the latter concept in this same group of participants using their brain imaging results.

In conclusion, our results show distinct pain scales relate to different aspects of the pain experience. Post-surgery residual pain scores show primarily independence from baseline pain. There is a reorganization of pain related biopsychosocial parameters that define the OA personality, and this change seems more profound in hip OA where pain relief is also larger.

Supporting information

S1 Fig. Pain intensity at baseline, 3 and 6 months for KOA and HOA. Interaction between the 2 OA groups, time (baseline, 3 months and 6 months), and measurement type (information present in Table 3). HOA patients presented larger pain relief than KOA. For both groups, pain intensity ratings did not show meaningful differences between 3- and 6-months post-surgery. Mo, months.
(TIF)

S2 Fig. Principal component analysis on correlations of pain related measures. a. Scree plot and percentage of variance explained by each component. The eigenvalues become lower than 1.0 at the fifth component, and the slope of eigenvalues flattens at this component. Components were retained only for eigenvalues higher than 1, corresponding to a percentage of variance higher than 5%. A total variance of 69.54% was explained by the 5 selected components
(TIF)

S1 Table. Principal Component Analysis–Factor loadings. Threshold of factor loading was set on 0.5/-0.5 after Promax oblique rotation (bold). 6MWT = 6 minute walking test; DN4 = The Neuropathic Pain 4 questions; HADS(A) = The Hospital Anxiety and Depression Scale, Anxiety; HADS(D) = The Hospital Anxiety and Depression Scale, Depression; KOOS = Knee Injury and Osteoarthritis Outcome Score, (ADL–Function in daily living), (S -Knee Symptoms), (SR—Function in sport and recreation), (QOL—knee related quality of life); MPQ = McGill Pain Questionnaire, (A–Affective score) (S–Sensory score); PCS = Pain Catastrophizing Scale, (R–Rumination subscale), (M–Magnification subscale), (H–Helplessness subscale); SF36 = Short-form (36) Health Survey, (PF–Physical Functioning), (PH–physical role functioning), (EP–emotional role functioning), (EF–energy/fatigue), (E–emotional well-being), (SF–social functioning), (GH–general health); TUG = Test stand-up and go.
(DOCX)

S2 Table. Multiple regression analysis for KOA pain intensity and % residual pain at 6-months post-surgery, using an aggregated variable for pain intensity (average of four pain intensity questionnaire measures). A composite measure of pain intensity was built averaging the four outcome scales. Prediction models of our aggregate pain intensity measure show differences across absolute and relative measures (% residual pain). Physical performance was a common predictive factor of both measures. No large effect size was captured in these models, rendering the 4 measures together are not capturing important predictive information. **b,** unstandardized regression coefficient; **SE** standard error; **β**, standardized regression

coefficient; **F**, obtain F-value; **t**, obtained t-value; $\mathbf{R^2}$, proportion variance explained. All statistics are from the final step of the model. $^{**}p \leq 0.01$. As the pre-surgical parameters predicting post-surgical pain or residual pain for four pain outcome measures captured distinct independent variables, we reasoned that each may be reflecting specific characteristics and thus combining all four measures would predict larger variance and incorporate the component characteristics. Therefore, we constructed the composite, average score, of all four pain outcome measures and studied its properties. We tested how pre-surgical factors predict 6-months post-surgical KOA pain, using our aggregate measure (S2 Table), again modeling pain and residual pain for KOA patients. For post-surgical aggregated pain severity, the model explained 19% of the variance and included worse health state, lower degree of structural articular damage, and poor results in the physical performance tests. For residual pain, the model explained 7% of the variance and Physical Performance was the only predictive factor. Using these variables to predict HOA post-surgical pain and residual pain we could not find any statistically significant models.
(DOCX)

Acknowledgments

We thank to Dr. Paulo Oliveira, for the clinical support and supervision of patients enrolled in the study and all the members of the Orthopedic Department of Centro Hospitalar Universitário de São João, Porto, for their support with data collection. Dr. Lina Melão and Dr. Patricia Leitão for the assistance in the radiographic classification. We are thankful to all Apkarian lab and Galhardo lab members that contributed to this study with their time and resources.

Author Contributions

Conceptualization: Joana Barroso, Vasco Galhardo, A. Vania Apkarian.

Data curation: Joana Barroso, João Pinto-Ramos.

Formal analysis: Joana Barroso, Kenta Wakaizumi.

Investigation: Joana Barroso.

Methodology: Joana Barroso, Vasco Galhardo, A. Vania Apkarian.

Resources: João Pinto-Ramos.

Supervision: A. Vania Apkarian.

Writing – original draft: Joana Barroso.

Writing – review & editing: Joana Barroso, Kenta Wakaizumi, Diane Reckziegel, Thomas Schnitzer, Vasco Galhardo, A. Vania Apkarian.

References

1. Neogi T. The epidemiology and impact of pain in osteoarthritis. Osteoarthritis Cartilage, 2013. 21(9): p. 1145–53. https://doi.org/10.1016/j.joca.2013.03.018 PMID: 23973124
2. Finan PH, Buenaver LF, Bounds SC, Hussain S, Park RJ, Haque UJ, et al. Discordance between pain and radiographic severity in knee osteoarthritis: findings from quantitative sensory testing of central sensitization. Arthritis Rheum, 2013. 65(2): p. 363–72. https://doi.org/10.1002/art.34646 PMID: 22961435
3. Bachmeier CJ, March LM, Cross MJ, Lapsley HM, Tribe KL, Courtenay BG, et al. A comparison of outcomes in osteoarthritis patients undergoing total hip and knee replacement surgery. Osteoarthritis Cartilage, 2001. 9(2): p. 137–46. https://doi.org/10.1053/joca.2000.0369 PMID: 11330253
4. Beswick AD, Wylde V, Gooberman-Hill R, Blom A, Dieppe P. What proportion of patients report long-term pain after total hip or knee replacement for osteoarthritis? A systematic review of prospective

studies in unselected patients. BMJ Open, 2012. 2(1): p. e000435. https://doi.org/10.1136/bmjopen-2011-000435 PMID: 22357571

5. Werner MU, Kongsgaard UE. Defining persistent post-surgical pain: is an update required? Br J Anaesth, 2014. 113(1): p. 1–4. https://doi.org/10.1093/bja/aeu012 PMID: 24554546
6. Erlenwei J, Muller M, Falla D, Przemeck M, Pfingsten M, Budde S, et al. Clinical relevance of persistent postoperative pain after total hip replacement—a prospective observational cohort study. J Pain Res, 2017. 10: p. 2183–2193. https://doi.org/10.2147/JPR.S137892 PMID: 28919814
7. Lewis GN, Rice DA, McNair PJ, Kluger M. Predictors of persistent pain after total knee arthroplasty: a systematic review and meta-analysis. Br J Anaesth, 2015. 114(4): p. 551–61. https://doi.org/10.1093/bja/aeu441 PMID: 25542191
8. Singh JA, Gabriel S, Lewallen D. The impact of gender, age, and preoperative pain severity of pain after TKA. Clin Orthop Relat Res, 2008. 466(11): p. 2717–23. https://doi.org/10.1007/s11999-008-0399-9 PMID: 18679762
9. Hochman JR, Gagliese L, Davis AM, Hawker GA. Neuropathic pain symptoms in a community knee OA cohort. Osteoarthritis Cartilage, 2011. 19(6): p. 647–54. https://doi.org/10.1016/j.joca.2011.03.007 PMID: 21440077
10. Forsythe ME, Dunbar MJ, Hennigar AW, Sullivan MJ, Gross M. Prospective relation between catastrophizing and residual pain following knee arthroplasty: two-year follow-up. Pain Res Manag, 2008. 13(4): p. 335–41. https://doi.org/10.1155/2008/730951 PMID: 18719716
11. Baert IA, Lluch E, Mulder T, Nijs J, Noten S, Meeus M. Does pre-surgical central modulation of pain influence outcome after total knee replacement? A systematic review. Osteoarthritis Cartilage, 2016. 24(2): p. 213–23. https://doi.org/10.1016/j.joca.2015.09.002 PMID: 26382109
12. Harmelink KEM, Zeegers AVCM, Hullegie W, Hoogeboom TJ, Nijhuis-van der Sanden MWG, Staal JB. Are There Prognostic Factors for One-Year Outcome After Total Knee Arthroplasty? A Systematic Review. J Arthroplasty, 2017. 32(12): p. 3840–3853 e1. https://doi.org/10.1016/j.arth.2017.07.011 PMID: 28927646
13. Harden RN, Weinland SR, Remble TA, Houle TT, Colio S, Steedman S, et al. Medication Quantification Scale Version III: update in medication classes and revised detriment weights by survey of American Pain Society Physicians. J Pain, 2005. 6(6): p. 364–71. https://doi.org/10.1016/j.jpain.2005.01.350 PMID: 15943958
14. Podsiadlo D, Richardson S. The timed "Up & Go": a test of basic functional mobility for frail elderly persons. J Am Geriatr Soc, 1991. 39(2): p. 142–8. https://doi.org/10.1111/j.1532-5415.1991.tb01616.x PMID: 1991946
15. Balke B. A Simple Field Test for the Assessment of Physical Fitness. Rep 63–6. Rep Civ Aeromed Res Inst US, 1963: p. 1–8. PMID: 14131272
16. Rejeski WJ, Ettinger WH Jr., Schumaker S, James P, Burns R, Elam JT. Assessing performance-related disability in patients with knee osteoarthritis. Osteoarthritis Cartilage, 1995. 3(3): p. 157–67. https://doi.org/10.1016/s1063-4584(05)80050-0 PMID: 8581745
17. Kennedy DM, Stratford PW, Wessel J, Gollish JD, Penney D. Assessing stability and change of four performance measures: a longitudinal study evaluating outcome following total hip and knee arthroplasty. BMC Musculoskelet Disord, 2005. 6: p. 3. https://doi.org/10.1186/1471-2474-6-3 PMID: 15679884
18. Dobson F, Hinman RS, Roos EM, Abbott JH, Stratford P, Davis AM, et al. OARSI recommended performance-based tests to assess physical function in people diagnosed with hip or knee osteoarthritis. Osteoarthritis Cartilage, 2013. 21(8): p. 1042–52. https://doi.org/10.1016/j.joca.2013.05.002 PMID: 23680877
19. Kellgren JH, Lawrence JS. Radiological assessment of osteo-arthrosis. Ann Rheum Dis, 1957. 16(4): p. 494–502. https://doi.org/10.1136/ard.16.4.494 PMID: 13498604
20. Roos EM, Toksvig-Larsen S. Knee injury and Osteoarthritis Outcome Score (KOOS)–validation and comparison to the WOMAC in total knee replacement. Health Qual Life Outcomes, 2003. 1: p. 17. https://doi.org/10.1186/1477-7525-1-17 PMID: 12801417
21. Goncalves RS, Cabri J, Pinheiro JP, Ferreira PL. Cross-cultural adaptation and validation of the Portuguese version of the Knee injury and Osteoarthritis Outcome Score (KOOS). Osteoarthritis Cartilage, 2009. 17(9): p. 1156–62. https://doi.org/10.1016/j.joca.2009.01.009 PMID: 19303082
22. Nilsdotter AK, Lohmander LS, Klassbo M, Roos EM. Hip disability and osteoarthritis outcome score (HOOS)—validity and responsiveness in total hip replacement. BMC Musculoskelet Disord, 2003. 4: p. 10. https://doi.org/10.1186/1471-2474-4-10 PMID: 12777182

23. Keller S, Bann CM, Dodd SL, Schein J, Mendoza TR, Cleeland CS. Validity of the brief pain inventory for use in documenting the outcomes of patients with noncancer pain. Clin J Pain, 2004. 20(5): p. 309–18. https://doi.org/10.1097/00002508-200409000-00005 PMID: 15322437

24. Daut RL, Cleeland CS, Flanery RC. Development of the Wisconsin Brief Pain Questionnaire to assess pain in cancer and other diseases. Pain, 1983. 17(2): p. 197–210. https://doi.org/10.1016/0304-3959(83)90143-4 PMID: 6646795

25. Azevedo L, Costa Pereira A, Dias C, Agualusa L, Lemos L, Romão J, et al. Tradução, adaptação cultural e estudo multicêntrico de validação de instrumentos para rastreio e avaliação do impacto da dor crónica (Translation, cultural adaptation and multicentric validation study of chronic pain screening and impact assessment instruments. Dor, 2007. 15: p. 6–65.

26. Melzack R. The McGill Pain Questionnaire: major properties and scoring methods. Pain, 1975. 1(3): p. 277–99. https://doi.org/10.1016/0304-3959(75)90044-5 PMID: 1235985

27. Byrne M, Troy A, Bradley LA, Marchisello PJ, Geisinger KF, Van der Heide LH, et al. Cross validation of the factor structure of the McGill Pain Questionnaire. Pain, 1982. 13(2): p. 193–201. https://doi.org/10.1016/0304-3959(82)90029-x PMID: 6214754

28. Bouhassira D, Attal N, Alchaar H, Boureau F, Brochet B, Bruxelle J, et al.Comparison of pain syndromes associated with nervous or somatic lesions and development of a new neuropathic pain diagnostic questionnaire (DN4). Pain, 2005. 114(1–2): p. 29–36. https://doi.org/10.1016/j.pain.2004.12.010 PMID: 15733628

29. Zigmond AS, Snaith RP. The hospital anxiety and depression scale. Acta Psychiatr Scand, 1983. 67 (6): p. 361–70. https://doi.org/10.1111/j.1600-0447.1983.tb09716.x PMID: 6880820

30. Pais-Ribeiro J Silva I, Ferreira T, Martins A, Meneses R, Baltar M. Validation study of a Portuguese version of the Hospital Anxiety and Depression Scale. Psychol Health Med, 2007. 12(2): p. 225–35; quiz 235–7. https://doi.org/10.1080/13548500500524088 PMID: 17365902

31. Sullivan MJL, Bishop SR, Pivik J. The Pain Catastrophizing Scale: Development and validation. Psychological Assessment, 1995. 7: p. 524–532.

32. McHorney CA, Ware JE Jr., Raczek AE. The MOS 36-Item Short-Form Health Survey (SF-36): II. Psychometric and clinical tests of validity in measuring physical and mental health constructs. Med Care, 1993. 31(3): p. 247–63.

33. Ferreira PL. Development of the Portuguese version of MOS SF-36. Part I. Cultural and linguistic adaptation. Acta Med Port, 2000. 13(1–2): p. 55–66. PMID: 11059056

34. Rubinov M, Sporns O. Complex network measures of brain connectivity: uses and interpretations. Neuroimage, 2010. 52(3): p. 1059–69. https://doi.org/10.1016/j.neuroimage.2009.10.003 PMID: 19819337

35. Kim DH, Pearson-Chauhan KM, McCarthy RJ, Buvanendran A. Predictive Factors for Developing Chronic Pain After Total Knee Arthroplasty. J Arthroplasty, 2018. 33(11): p. 3372–3378. https://doi.org/10.1016/j.arth.2018.07.028 PMID: 30143334

36. Creamer P, Lethbridge-Cejku M, Hochberg MC. Determinants of pain severity in knee osteoarthritis: effect of demographic and psychosocial variables using 3 pain measures. J Rheumatol, 1999. 26(8): p. 1785–92. PMID: 10451078

37. Wylde V, Dixon S, Blom AW. The role of preoperative self-efficacy in predicting outcome after total knee replacement. Musculoskeletal Care, 2012. 10(2): p. 110–8. https://doi.org/10.1002/msc.1008 PMID: 22368121

38. Pinto PR, McIntyre T, Ferrero R, Almeida A, Araujo-Soares V. Risk factors for moderate and severe persistent pain in patients undergoing total knee and hip arthroplasty: a prospective predictive study. PLoS One, 2013. 8(9): p. e73917. https://doi.org/10.1371/journal.pone.0073917 PMID: 24058502

39. Valdes AM, Doherty SA, Zhang W, Muir KR, Maciewicz RA, Doherty M. Inverse relationship between preoperative radiographic severity and postoperative pain in patients with osteoarthritis who have undergone total joint arthroplasty. Semin Arthritis Rheum, 2012. 41(4): p. 568–75. https://doi.org/10.1016/j.semarthrit.2011.07.002 PMID: 21868060

40. Sullivan M, Tanzer M, Reardon G, Amirault D, Dunbar M, Stanish W. The role of presurgical expectancies in predicting pain and function one year following total knee arthroplasty. Pain, 2011. 152(10): p. 2287–93. https://doi.org/10.1016/j.pain.2011.06.014 PMID: 21764515

41. Dabare C, Le Marshall K, Leung A, Page CJ, Choong PF, Lim KK. Differences in presentation, progression and rates of arthroplasty between hip and knee osteoarthritis: Observations from an osteoarthritis cohort study-a clear role for conservative management. Int J Rheum Dis, 2017. 20(10): p. 1350–1360. https://doi.org/10.1111/1756-185X.13083 PMID: 28493422

42. Vissers MM, Bussmann JB, Verhaar JA, Busschbach JJ, Bierma-Zeinstra SM, Reijman M. Psychological factors affecting the outcome of total hip and knee arthroplasty: a systematic review. Semin Arthritis Rheum, 2012. 41(4): p. 576–88. https://doi.org/10.1016/j.semarthrit.2011.07.003 PMID: 22035624

43. Zuo XN, Xu T, Milham MP. Harnessing reliability for neuroscience research. Nat Hum Behav, 2019. 3 (8): p. 768–771. https://doi.org/10.1038/s41562-019-0655-x PMID: 31253883

44. Petersen KK, Arendt-Nielsen L, Simonsen O, Wilder-Smith O, Laursen MB. Presurgical assessment of temporal summation of pain predicts the development of chronic postoperative pain 12 months after total knee replacement. Pain, 2015. 156(1): p. 55–61. https://doi.org/10.1016/j.pain.0000000000000022 PMID: 25599301

45. Petersen KK, Graven-Nielsen T, Simonsen O, Laursen MB, Arendt-Nielsen L. Preoperative pain mechanisms assessed by cuff algometry are associated with chronic postoperative pain relief after total knee replacement. Pain, 2016. 157(7): p. 1400–6. https://doi.org/10.1097/j.pain.0000000000000531 PMID: 27331347

46. Leung YY, Lim Z, Fan Q, Wylde V, Xiong S, Yeo SJ, et al. Pre-operative pressure pain thresholds do not meaningfully explain satisfaction or improvement in pain after knee replacement: a cohort study. Osteoarthritis Cartilage, 2019. 27(1): p. 49–58. https://doi.org/10.1016/j.joca.2018.09.003 PMID: 30243947

47. Baliki MN ,Schnitzer TJ, Bauer WR, Apkarian AV. Brain morphological signatures for chronic pain. PLoS One, 2011. 6(10): p. e26010. https://doi.org/10.1371/journal.pone.0026010 PMID: 22022493

48. Baliki MN, Mansour AR, Baria AT, Apkarian AV. Functional reorganization of the default mode network across chronic pain conditions. PLoS One, 2014. 9(9): p. e106133. https://doi.org/10.1371/journal.pone.0106133 PMID: 25180885

2.2 Publication II

Barroso J, Vigotsky AD, Branco P, Reis AM, Schnitzer TJ, Galhardo V, Apkarian AV. *Brain gray matter abnormalities in osteoarthritis pain: a cross-sectional evaluation*. Pain. 2020 Sep 1;161(9):2167-2178. doi: 10.1097/j.pain.0000000000001904. PMID: 32379222; PMCID: PMC7745790.

Research Paper

PAIN

VIDEO

Brain gray matter abnormalities in osteoarthritis pain: a cross-sectional evaluation

Joana Barroso[a,b,c], Andrew D. Vigotsky[d], Paulo Branco[c], Ana Mafalda Reis[e], Thomas J. Schnitzer[b,f,g], Vasco Galhardo[a], A. Vania Apkarian[b,c,g,*]

Abstract

The interaction between osteoarthritis (OA) pain and brain properties remains minimally understood, although anatomical and functional neuroimaging studies suggest that OA, similar to other chronic pain conditions, may impact as well as partly be determined by brain properties. Here, we studied brain gray matter (GM) properties in OA patients scheduled to undergo total joint replacement surgery. We tested the hypothesis that brain regional GM volume is distinct between hip OA (HOA) and knee OA (KOA) patients, relative to healthy controls and moreover, that these properties are related to OA pain. Voxel-based morphometry group contrasts showed lower anterior cingulate GM volume only in HOA. When we reoriented the brains (flipped) to examine the hemisphere contralateral to OA pain, precentral GM volume was lower in KOA and HOA, and 5 additional brain regions showed distortions between groups. These GM changes, however, did not reflect clinical parameters. Next, we subdivided the brain into larger regions, approximating Brodmann areas, and performed univariable and machine learning-based multivariable contrasts. The univariable analyses approximated voxel-based morphometry results. Our multivariable model distinguished between KOA and controls, was validated in a KOA hold-out sample, and generalized to HOA. The multivariable model in KOA, but not HOA, was related to neuropathic OA pain. These results were mapped into term space (using Neurosynth), providing a meta-analytic summary of brain anatomical distortions in OA. Our results indicate more subtle cortical anatomical differences in OA than previously reported and also emphasize the interaction between OA pain, namely its neuropathic component, and OA brain anatomy.

Keywords: Osteoarthritis, Chronic pain, Structural brain anomalies, Gray matter volume, VBM

1. Introduction

Osteoarthritis (OA) is the most common form of arthritis worldwide, one of the most prevalent sources of chronic musculoskeletal pain,[43] and a leading cause of disability.[14,42] Pain is the defining symptom and primary complaint of OA,[37] and its consequences include fatigue, sleep disruption, reduced activity, and psychological stress.[27] Understanding the mechanisms of pain in OA is thus critical for the management of the disease.

Traditionally, OA was considered the hallmark of nociceptive pain, explained by mechanical and biochemical activation of afferents innervating the affected joint.[29,63] Recent studies show evidence for peripheral sensitization of nociceptors[59] and central sensitization, associated with nociceptive-mediated transmission strengthening and dysfunction of descending modulator pathways in OA.[41] In addition, neuropathic-like symptoms,[19,28] negative affect, anxiety, and catastrophizing have been related with pain severity,[1,57] suggesting linkage between the brain's emotional circuitry and OA pain.

We[6,7,38,46] and other researchers[16,25,39] have provided evidence for brain anatomical and functional abnormalities in OA. Brain activity for ongoing OA pain[46] shows similar activity patterns as observed in chronic back pain (CBP).[6,26] Disruption of information sharing,[38] and brain morphological distortions are reported both in OA and in CBP.[7] Given that transition from subacute to CBP is predicted by brain anatomical and functional parameters[8,62] and chronification of back pain is accompanied by anatomical and functional reorganization,[26] a similar concept can be formulated for OA pain, namely, brain parameters in part predefine risk and consequently reorganize with OA pain. Here, we attempt to address this issue from the viewpoint of brain morphology. Hip OA (HOA) and knee OA (KOA) have distinct clinical characteristics, pain properties, and joint replacement surgery outcomes. For both conditions, pain is poorly related to joint structural damage.[18] Our main hypothesis is that KOA and HOA exhibit brain gray matter (GM) distortions when contrasted with healthy controls, and GM properties should also be different between the 2 conditions.

GM indices indicate morphologic brain abnormalities in OA,[2,25,34,39] but their clinical import is not yet understood. Although promising, these data are primarily derived from small samples at

Sponsorships or competing interests that may be relevant to content are disclosed at the end of this article.

[a] *Departamento de Biomedicina, Faculdade de Medicina, Instituto de Investigação e Inovação em Saúde-i3S, Universidade do Porto, Porto, Portugal, Departments of* [b] *Physical Medicine and Rehabilitation and,* [c] *Physiology, Feinberg School of Medicine, Northwestern University, Chicago, IL, United States,* [d] *Departments of Biomedical Engineering and Statistics, Northwestern University, Evanston, IL, United States,* [e] *Unilabs Boavista, Porto, Portugal, Departments of* [f] *Rheumatology and,* [g] *Anesthesia, Feinberg School of Medicine, Northwestern University, Chicago, IL, United States*

**Corresponding author. Address: Feinberg School of Medicine, Northwestern University, Tarry Bldg. 7-705, Chicago, IL 60611, United States. Tel.: (312) 503-0404; fax (312)503-5101. E-mail address: a-apkarian@northwestern.edu (A.V. Apkarian).*

Supplemental digital content is available for this article. Direct URL citations appear in the printed text and are provided in the HTML and PDF versions of this article on the journal's Web site (www.painjournalonline.com).

PAIN 161 (2020) 2167–2178

© 2020 International Association for the Study of Pain

http://dx.doi.org/10.1097/j.pain.0000000000001904

distinct stages of OA progression, and evidence is discrepant as GM changes exhibit little overlap between studies. Moreover, previous literature fails to find robust associations between clinical properties of OA and brain structural changes.[2,39] Our second objective is to study the association between brain morphological distortions and OA clinical properties.

We study brain morphological distortions and their relationship with clinical outcomes in a large population of advanced KOA, and a smaller group of HOA, in contrast to healthy controls. We study GM properties at whole-brain voxel-wise scale and after subdividing gray matter to regions of interest (ROIs) and apply both univariable and multivariable machine-learning analysis to explore the multidimensional basis of these alterations. Finally, we perform a reverse inference mapping of obtained results to terms (using Neurosynth), providing a meta-analytic summary of results and linking brain anatomy to the psychological domain.

2. Patients and methods

2.1. Subjects

Advanced HOA and KOA patients with indication for total joint replacement were recruited in the Orthopedic Department of *Centro Hospitalar e Universitário de São João*, Porto, together with healthy controls from the same geographical area. Participant recruitment was finished at the time of this report. Sample size was determined by the number of patients waiting for surgery who met the eligibility criteria during a period of 20 months. Controls were recruited in the end of the patient recruitment phase and intended to be one-third of the patient number in the largest OA group.

Inclusion criteria for OA patients were: (1) age between 45 and 75 years; (2) diagnosis of HOA and KOA according to the clinical classification criteria of the American College of Rheumatology[3]; (3) surgical indication for total joint replacement. Exclusion criteria included: (1) secondary OA due to congenital and development diseases or inflammatory and autoimmune articular diseases; (2) bilateral OA with indication for contralateral arthroplasty in the following year or bilateral knee pain with less than or equal to 4 points difference on the numeric pain rating scale between knees; (3) other chronic pain conditions (eg, fibromyalgia; chronic pelvic pain), (4) chronic neurological or psychiatric disease; (5) previous history of stroke or traumatic brain injury.

Controls were subjects without chronic conditions, musculoskeletal disorders, and neurological disorders, from the same geographic area, age range, and social and educational background as the patients.

Clinical, demographic, and biopsychosocial measures were obtained 2 to 6 weeks before surgery and repeated at 3, 6, and 12 months after surgery, together with brain imaging collection (magnetic resonance imaging [MRI]). The study was approved by the local ethics committee, and all participants provided informed consent before partaking in the study. In this article, we are reporting baseline cross-sectional data from presurgical state. Longitudinal data results will follow in future work.

2.2. Clinical and behavioral measures

Demographic and clinical data were obtained at the initial interview and by clinical chart assessment. Bilateral radiographs of involved joints were performed as part of the standard hospital protocol and scored accordingly to the Kellgren–Lawrence classification[32] by 2 trained radiologists. Physical performance was assessed with 2 distinct tasks—timed up and go test[47] and 6-minute walking test (6MWT).[9,50]

All patients completed the following questionnaires: Knee and Hip Injury and Osteoarthritis Score (KOOS; HOOS)[21,44,52]; Hospital Anxiety and Depression Scale (HADS)[45,67]; Pain Catastrophizing Scale[5,58]; and *Doleur Neuropathique en 4 questions*—Neuropathic pain scale (DN4).[5,12] All questionnaires were used in their Portuguese validated versions.

2.3. Brain imaging

High-resolution, MPRAGE type T1-anatomical brain images were acquired with a 3.0 T Siemens Magnetom Spectra scanner (Siemens Medical, Erlagen, Germany). Acquisition parameters: isometric voxel size = 1 × 1 × 1 mm, TR = 2500 ms, TE = 3.31 ms, flip angle = 9°, in-plane matrix resolution = 256 × 256, number of slices, = 160; field of view = 256 mm. Total time of acquisition was 6 minutes.

2.4. Gray matter properties and statistical analyses

GM properties were extracted, and analyses were performed using tools from the Oxford Center for Functional Magnetic Resonance Imaging Software Library (FMRIB, Oxford OK; FSL version 5.0.10, https://fsl.fmrib.ox.ac.uk/fsl)[31]; Matlab (MATLAB 2018a; The MathWorks, Natick, 2018), and RStudio (RStudio Team (2016); RStudio: Integrated Development for R. RStudio, Inc, Boston, MA URL http://www.rstudio.com).

2.4.1. Total gray matter volume estimation

SIENAx (2.6) from FSL[55,56] was used to calculate estimates of volumes of interest, after automated brain extraction and tissue segmentation. We compared total gray matter (GM) volume across groups using an analysis of covariance (ANCOVA), controlling for intracranial volume, age, and sex. Differential relationships between GM and age were assessed using linear regression, controlling for sex and total intracranial volume (TICV), in which a group interaction indicated a difference in slopes.

2.4.2. Voxel based morphometry

Regional GM density was analyzed with voxel-based morphometry (VBM) using tools from FSL. In brief, images were skull stripped using Brain Extraction Tool[55] and tissue-type segmented into GM, white matter, and cerebrospinal fluid using FMRIBs Automated Segmentation Tool.[66] A study-specific GM template was created using 72 gray-matter-segmented native images (24 subjects of each group; KOA and controls were randomly selected to minimize size of population bias). Steps towards the template creation included: affine registering the GM partial volume images (FLIRT)[30] and left-to-right x-axis flipping to produce a symmetrical image followed by nonlinear registration (FNIRT)[4] to standard space. The native space GM volume images were then normalized into this template using a nonlinear registration (FNIRT) and corrected for the contraction/enlargement due to the nonlinear component of the transformation using the Jacobian. Finally, GM images were concatenated and smoothed with an isotropic Gaussian kernel (FWHM = 8 mm). Cerebellum was excluded from the analyses because the foci of this study were neocortical and subcortical structures.

A second group for parallel VBM analysis was created by midline flipping the scans of patients with left-sided OA (knee = 45; hip = 10), in accordance with previous OA and unilateral pain conditions studies.[24,36] Brains were flipped along the x-axis

Copyright © 2020 by the International Association for the Study of Pain

before nonlinear registration to the study template. All subsequent steps were identical.

Gray matter differences in OA groups and controls were assessed through a one-way between-subjects ANCOVA, using age, sex, and TICV, plus laterality of OA for the flipped data analysis as covariates of no interest. Permutation-based testing (n = 5000 permutations) was performed using FSL's randomize toolbox.[64] Threshold-free cluster enhanced uncorrected *P*-values were obtained,[54] and $\alpha = 0.001$ was used as threshold for statistical significance of group differences. A minimum cluster size of 66 voxels (number of voxels contained within the 8 mm smoothing kernel) was used as a secondary threshold. Post hoc analyses of VBM results using Tukey HSD tests for multiple comparisons of means were conducted for the identified clusters.

The association of significant clusters with clinical variables was examined using partial correlations, with age, sex, and TICV as covariates.

In addition to assessing simple group differences, we sought to understand their relationship with clinical variables. Thus, the association of significant clusters with clinical variables was examined using partial Pearson correlations, which controlled for age, sex, and TICV.

2.4.3. Regional Brodmann area parcellation-based analysis of gray matter GM morphometry volume

Next, we calculated GM volume for 90 cortical and subcortical ROIs approximating Brodmann areas, defined anatomically by the Automated Anatomical Labeling atlas (Neurofunctional Imaging Group [GIN-IMN] http://www.gin.cnrs.fr/en/tools/aal/).[61] Cerebellum and vermis areas were excluded from the analysis. A list of regions, labeling, and respective coordinates can be found in Table S1 (available online as supplemental digital content at http://links.lww.com/PAIN/B8).

The volume of each ROI was calculated as the mean GM volume of all voxels within the ROI for each subject. Volumes were calculated both for native brains and x-axis-flipped brains depending on laterality of OA. Univariable analyses were conducted using one-way ANCOVA test for each region contrasting the 3 groups: KOA, HOA, and controls, while controlling for age, sex, and TICV. For the flipped brain analysis, laterality was also added as a covariate. Again, an $\alpha = 0.001$ was used a threshold for statistical significance of group differences. Multiple comparison correction was performed using a false discovery rate-adjusted *P*-value of 0.05.

Next, a multidimensional approach using a L1-regularized logistic regression (ie, least absolute shrinkage and selection operator [LASSO])[60] was performed. First, we divided our KOA sample into 2 distinct sets, training (n = 46) and test (n = 45). This was performed using the Kennard–Stone algorithm,[33] which allowed us to select samples with a uniform distribution over a multivariate predictor space (here: age, sex, pain levels, and behavioral variables). Second, using the KOA training set, we performed a logistic model with a LASSO penalty to predict group membership (ie, knee vs controls), based on the GM volumes of all 90 ROIs. In addition, we added age, sex, and TICV to the full model. Ten-fold cross-validation was used to choose the hyperparameter, λ, which minimized binomial deviance over a default grid size of 100.[20] Finally, models were evaluated in the KOA test group and HOA group by constructing receiver operating characteristic curves and computing areas under the curve (AUC).

Later, Neurosynth term-based reverse inference was used to decode the identified AAL regions for the flipped brain model. This meta-analytical tool contains a database with activation coordinates for a total of 14,371 functional MRI studies (September 2019), paired with their associated cognitive and anatomical terms (http://neurosynth.org/decode/).[22,48,65] The decoder takes in the voxel-wise representation of the ROI, cross-references it with the full database, and returns a list of terms and correlation values, which indicates the strength of terms associated with delineated brain regions, in contrast to the rest of the brain. Here, we retrieved the top 40 nonanatomical terms (of about 1700 terms generated) showing the greatest correlation with the model's ROIs. Next, to further elucidate the contribution of each region in the model, the correlation for each ROI was weighted by its LASSO-derived coefficient and ranked. Terms were visualized using a word-cloud (MATLAB 2018a and Text Analytical Toolbox, The MathWorks, Natick, 2018).

Finally, we aimed to test whether the OA classification models were associated with OA clinical variables.

For this, using the KOA testing group, we linearly modeled each clinical variable of interest with the variables retrieved from the LASSO. For statistically significant relationships ($P < 0.05$), the relative importance of each independent variable was calculated using the sequential sums of squares over all orderings of regressors,[35] and confidence intervals computed over 1000 bootstraps for each regressor.[23] Finally, statistically significant regression models were tested in the KOA validation group and HOA group by calculating Pearson correlation coefficient between predicted and real values.

3. Results

3.1. Demographic and clinical characteristics

A total of 91 KOA patients, 24 HOA patients, and 36 healthy controls were included in the study. Patient and control groups were similar concerning education, habitation profile, marital status, and smoking habits. Age and sex were statistically significantly different among the 3 groups: age was higher in the KOA group and HOA had a lower representation of females.

Pain intensity as well as affective measures and performance-based tasks did not statistically significantly differ among OA groups. The KOA group, however, presented a longer pain duration and a higher probability of neuropathic pain than the HOA group, which in contrast exhibited higher radiographic structural damage (**Table 1**).

3.2. Total gray matter characterization

Total neocortical gray matter volumes (TGM) were compared between the 3 groups (OA and controls), while controlling for TICV, age, and sex. TGM was not statistically significantly different between the 3 groups ($F(2,145) = 0.07$, $P = 0.79$)). Women showed greater TGM than men (controlling for group, TIVC, and age) (**Fig. 1A**). The effect of age on TGM was calculated for each group separately (after correcting for sex). TGM decreased with age (**Fig. 1B**) and the interaction between age and group was not statistically significant ($F(2,145) = 2.62$, $P = 0.078$), showing approximately similar trends for the 3 groups.

3.3. Hip osteoarthritis patients exhibit lower GM volume in anterior cingulate/paracingulate cortex

To identify regional differences in GM volume between OA groups and controls, we performed a whole-brain, voxel-wise, one-way ANCOVA for VBM outcomes (**Fig. 1C**). Statistically significant differences in GM volume in the right and left anterior cingulate

Table 1

Demographic and clinical characteristics of osteoarthritis patients and controls.

	Controls		Knee OA		Hip OA		*P*
Subjects, n, %	36	23	91	60	24	16	
Age (y), mean, SD	59.2	8	65.5	6.5	59.7	8.2	<0.001†
Female, n, %	20	55.5	72	79.1	8	33.3	<0.001†
BMI (kg/m^2), mean, SD	27.8	4.6	30.4	4.9	28.3	3.7	0.06
Education, n, %							0.12
Primary education	21	58.3	71	78	16	66.7	
Secondary education	8	22.2	15	16.5	5	20.8	
Post-secondary education	7	19.5	5	4.5	3	12.5	
Smoking, n, %	8	22.2	8	8.8	2	8.3	0.09
Habitation, n, %							
Alone	6	16.7	17	18.7	3	12.5	
Cohabitation	30	83.3	74	81.3	21	87.5	
Marital status, n, %				6			0.9
Married	27	66.7	65	71.4	17	70.8	
Never married	3	8.3	5	5.5	2	8.3	
Divorced	2	5.6	7	7.7	2	8.3	
Widowed	4	11.1	14	15.4	3	12.5	
Pain duration (y), mean, SD	—	—	7.7	6	5.1	4.3	0.015*
Pain intensity (NRS), mean, SD	—	—	6.6	1.7	6	1.6	0.1
KOOS/HOOS, mean, SD	—	—	61.2	20	50.8	15	0.011*
Symptom	—	—	63.7	15.6	55.9	17.8	0.061
Pain ADL SR	—	—	62.6	16.4	58.8	18.1	0.354
QoL	—	—	91.9	13.9	83.6	18.6	0.049*
	—	—	79.5	15.3	71.1	20.3	0.061
HADS, mean, SD							0.354
Anxiety	—	—	8.8	5	6.8	4.4	0.061
Depression	—	—	7.1	4.1	6	4.6	0.354
PCS, mean, SD			8.3	4.8	7.5	4.	0.41
Rumination magnification	—	—	5	3.7	4.4	3.4	0.43
Helplessness	—	—	10	7.5	8.4	6.2	0.34
DN4, mean, SD	—	—	2.8	2.2	1.8	1.5	0.029*
Physical performance tasks, mean, SD							
TUG, seg	—	—	13.6	4.2	270.8	68.4	0.4
6MWT, meters	—	—	14.4	4.7	270.6	98.5	0.9
Radiographic KL, n, %							<0.001†
Grade 1	—	—	2	1.8	0	0	
Grade 2	—	—	21	23.1	0	0	
Grade 3	—	—	43	39.1	6	25	
Grade 4	—	—	25	22.8	18	75	

To identify demographic difference between groups, ANOVA and t-tests were performed for continuous data, controls and OA groups, and between OA groups, respectively. χ^2 tests were performed for categorical data.
* $P < 0.05$.
† $P < 0.001$.
6MWT, 6-Minute Walking Test; ADL, activities of daily living; ANOVA, analysis of variance; BMI, body mass index; DN4, Douleur Neuropathique en 4 questions; HADS, Hospital Anxiety and Depression Scale; HOOS, Hip Injury and Osteoarthritis Outcome Score; KOOS, Knee Injury and Osteoarthritis Outcome Score; KL, Kellgren–Lawrence scale; NRS, numeric pain rating; PCS, Pain Catastrophizing Scale; SR, sports and recreation; TUG, stand up and go test; QoL, quality of life.

cortex/paracingulate gyri were identified, differentiating the 3 groups (**Table 2**). Post hoc analyses (Tukey HSD test) revealed statistically significantly reduced regional volume only for HOA when compared with KOA and controls ($P < 0.001$). Knee osteoarthritis and controls did not show a statistically significant difference within this cluster ($P = 0.34$).

3.4. Hip osteoarthritis and knee osteoarthritis patients exhibit lower GM volume in primary motor cortex contralateral to osteoarthritis pain

Next, we sought to isolate the effects of OA pain on regional GM volumes. To this end, we first realigned the OA brains relative to the body part with OA pain. That is, brains were flipped across the midsagittal plane for left-side OA patient (x-axis flipping), such that the left hemisphere would correspond to the body side contralateral to OA pain for all patients. We then performed whole-brain, voxel-wise analyses using one-way ANCOVAs across the 3 groups for VBM outcomes. Using the same criteria for statistical significance as above (ie, $\alpha = 0.001$), we identified 5 statistically significant clusters (**Fig. 2A** and **Table 2**). Post hoc analysis of these clusters revealed: (1) relative to healthy controls, both OA groups exhibited lower volumes in left primary motor cortex (precentral cortex), as well as in the left temporal pole; and (2) relative to healthy controls, KOA, but not HOA, had lower GM volume in the precuneus cortex and increased GM volume in the

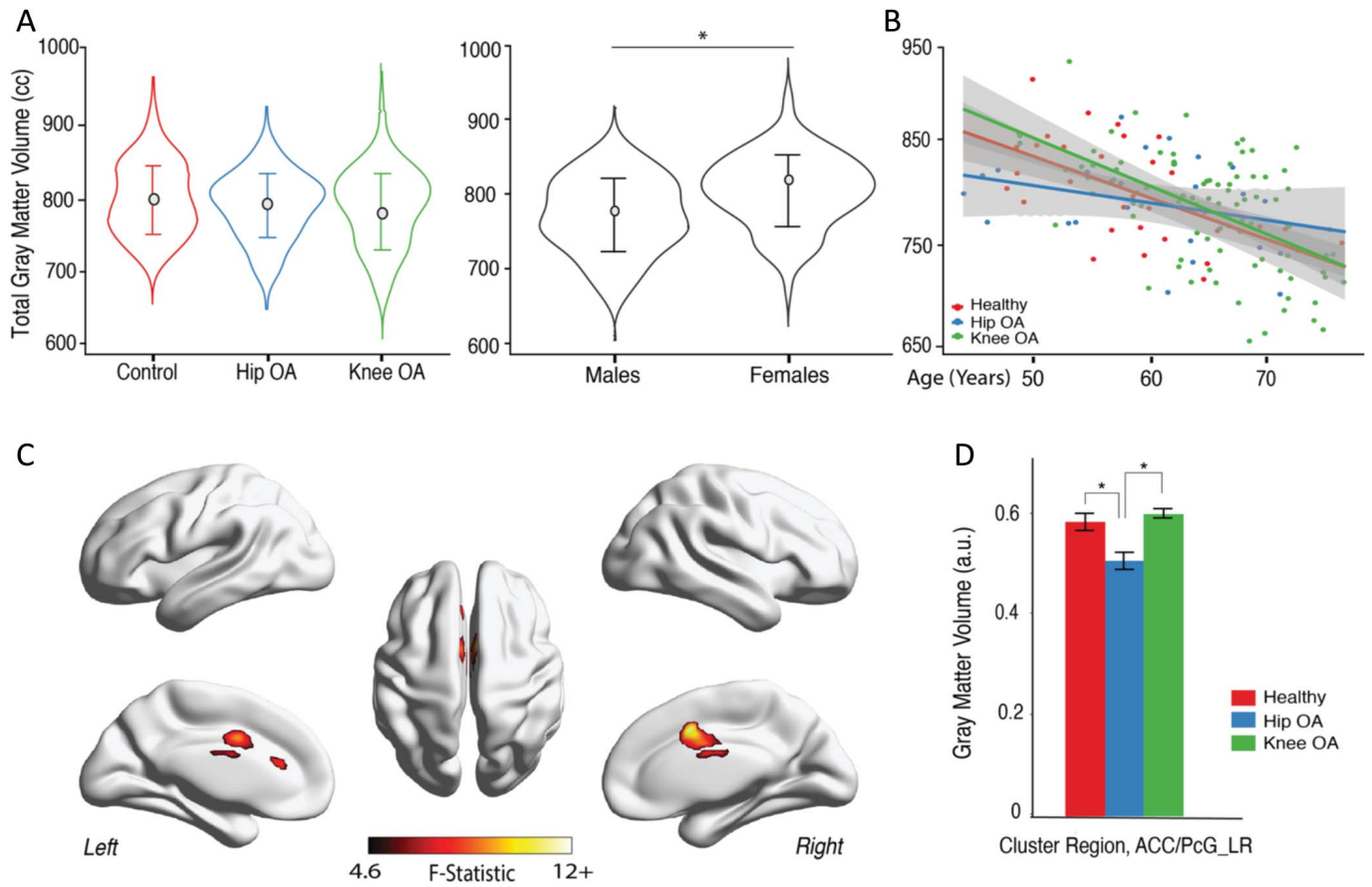

Figure 1. Whole-brain cortical gray matter changes reflect lower volumes in anterior cingulate, paracingulate gyri in HOA. (A) Average total neocortical gray matter (TGM) matter volume was not different between healthy controls, HOA, and KOA patients (age, sex, and intracranial volume were used as confound variables ($F(2,145) = 0.07$, $P = 0.79$)). TGM differed by sex across groups, when controlling for total IC volume and age ($F(1,145) = 15.7$, $P < 0.001$), with females showing higher volumes. (B) Scatterplot represents total neocortical GM in relation to age for each subject, color-coded by group; slopes were computed for each group, showing decrease of TGM with age, for all groups ($P < 0.05$; R2: controls = 0.52; KOA = 0.37; HOA = 0.17). (C) Gray matter morphological changes assessed by voxel-based morphometry (VBM). The 3 groups were contrasted together, using a 1-way between-subjects ANCOVA, with age, sex, and total ICV as covariates of no interest. Shown is the F-test statistical map, clustering determined using uncorrected *P*-value binarized at value of 0.001 and cluster size >66 voxels. Only cingulate/paracingulate gyri showed regional GM volume difference between the groups. (D) Post hoc results for GM volume comparisons in the identified region—anterior cingulate/paracingulate gyri (ACC/PcG_LR). Bars represent the mean gray matter volume and error bars represent the standard error. Tukey HSD test showed regional GM volume was lower in HOA from KOA and healthy subjects at $P < 0.001$. Knee osteoarthritis and controls did not show a statistically significant difference ($P = 0.34$). *$P < 0.001$. ANCOVA, analysis of covariance; HOA, hip osteoarthritis; KOA, knee osteoarthritis.

medial frontal gyrus. In addition, we identified lower GM volume in the anterior cingulate cortex (ACC_LR) for the HOA group relative to KOA and controls. This cluster considerably overlapped (Sørensen–Dice coefficient = 0.71) with the ACC cluster we obtained in the nonflipped analysis. The unthresholded statistical maps for native space and flipped analysis can be accessed in Neurovault.org (https://identifiers.org/neurovault.collection:6002).

Overall, by aligning the brain in relation to body side with OA pain, we observe more statistically significant clusters and stronger effects of GM volume differences between the groups. Importantly, we are able to identify the primary motor cortex region contralateral to the OA pain with lower GM volume in both knee and HOA patients.

3.5. Lack of relationship between clinical variables for clusters identified by voxel-based morphometry

To elucidate the clinical relevance of the GM volume differences among HOA, KOA, and healthy controls (6 clusters, before and after brain flipping), we correlated clinical characteristics of OA with GM volumes. The relationship between cluster GM volumes and clinical variables was calculated using partial correlations, controlling for age, sex, and TICV. We did not find any statistically significant relationships ($|r| \leq 0.28$; (Table S2, available online as supplemental digital content at http://links.lww.com/PAIN/B8).

3.6. Univariable and multivariable GM volume relationships associated with osteoarthritis, after parceling the brain into Brodmann areas

The above analyses were done at the voxel level. To reduce dimensionality, we studied GM properties across the groups and as a function of clinical characteristics after parceling the brain into ROIs approximating Brodmann areas (AAL atlas). GM volume differences were studied at this larger scale by subdividing the brain into 90 predefined regions (approximating 45 left and 45 right brain Brodmann areas) and calculating the mean GM volume for each ROI. Reduced dimensionality enabled studying OA-related brain volume differences with a multivariable approach, which considers the inter-relationships between regional GM volumes.

Table 2

Clusters for GM volume differences in HOA, KOA, and healthy controls for whole brain analysis with and without brain flipping based on OA body side dominance (x-axis).

Peak MNI coordinate region (Harvard-Oxford Cortical Structural atlas)	Peak (max) F value	No. of voxels	Peak MNI coordinate
Nonflipped brain (Fig. 1C)			
Paracingulate gyrus (20%); cingulate gyrus, anterior division (14%); juxtapositional lobule cortex (7%)	12.4	888	(12,8,8)
Cingulate gyrus, anterior division (93%)	8.58	51	(−2,32,16)
Flipped brain (Fig. 2A)			
Cingulate gyrus, anterior division (9%), posterior division (4%)	18.8	1224	(8,−8,32)
Precentral gyrus (54%)	7.55	136	(−28,−18,70)
Temporal pole (34%)	9.06	122	(34,8,−34)
Precuneous cortex (49%), intracalcarine cortex (72%)	13.2	84	(12,−58,10)
Middle frontal gyrus (42%), superior frontal gyrus (2%)	10.3	76	(30,24,50)
Middle frontal gyrus (23%), superior frontal gyrus (2%)	8.45	30	(−38,2,64)
Frontal orbital cortex (88%)	10.5	27	(−22,26,−20)
Heschl gyrus (22%)	10.9	24	(−42,−28,8)
Precentral gyrus (64%), middle frontal gyrus (2%)	6.72	14	(−52,−4,50)

All identified clusters from VBM GLM analysis, TFCE uncorrected $P < 0.001$. Cluster peak coordinates (x,y,z) are displayed according to MNI atlas, labels accordingly to the Oxford-Harvard Structural Cortical Atlas (http://fsl.fmrib.ox.ac.uk/fsl/fslwiki/Atlases). We accepted clusters greater than 66 voxels in size for post hoc analysis, given the Gaussian Kernel (FWHM = 8 mm) used for smoothing.
HOA, hip osteoarthritis; KOA, knee osteoarthritis; OA, osteoarthritis; VBM, voxel-based morphometry.

First, differences in GM volume across the 3 groups were examined for each ROI in the native and appropriately flipped brains (rendering OA pain to be left body side lateralized) using a one-way ANCOVA (**Figs. 3A and B**). Multiple regions that attained statistical significance were identified ($P < 0.001$): left putamen in the native brain analysis; bilateral pallidum, precentral left cortex, and 2 right frontal regions (rectus and lingual gyrus) for the flipped brain analysis. After FDR correction for multiple comparisons, only left precentral cortex yielded statistical significance ($F = 5.9$, corrected $P < 0.05$). Post hoc analysis for this ROI showed decreased volume for both OA groups when compared with controls (Tukey HSD tests, $P < 0.01$), but not between OA groups ($P = 0.73$), showing a pattern concordant with the results obtained in the voxel-wise analysis.

We next sought to study GM volumetric differences in a multivariable space using logistic regression to classify OA patients and controls based on 90 ROIs. To enforce sparsity and reduce overfitting, we used L1 regularization (LASSO) to drive coefficients towards zero. We took advantage of the large number of KOA patients and subdivided this group into training and test groups to ensure generalizability and unbiasedness. Results obtained in the training group were tested on the hold-out

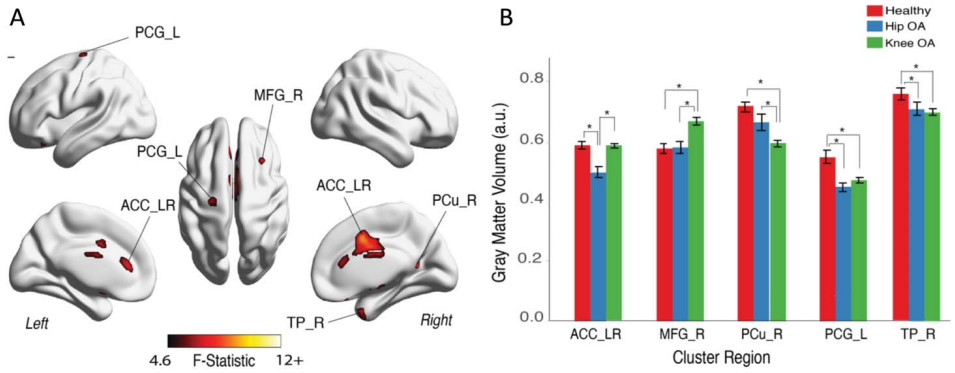

Figure 2. Primary motor cortex, contralateral to OA pain, showed lower volume in both HOA and KOA patients. (A) Gray matter morphological changes assessed by voxel-based morphometry (VBM) after aligning the brain in relation to OA pain (brain x-axis left-to-right flipping for left sided KOA and HOA, which renders the left hemisphere to be contralateral to OA in all patients). The 3 groups were contrasted together, using a 1-way between-subjects ANCOVA, controlling for age, sex, total ICV, and brain flipping. Shown is the F-test statistic map clustering determined using a TFCE uncorrected *P*-value binarized mask at value of 0.001 and cluster size >66 voxels. Multiple brain regions showed changes in regional volume (B). Post hoc results for GM volume differences for significant clusters, adjusted for age, sex, and TICV (Tukey HSD tests at $P < 0.001$); bars represent the mean gray matter volume and error bars represent the standard error. Left primary motor cortex (precentral gyrus; PCG_L) and right temporal pole (TP_R) presented lower GM volume in both OA groups. Bilateral anterior cingulate cortex (ACC_LR) showed lower GM volume only in HOA, when contrasted with the other 2 groups. In the KOA group, GM volume was greater for middle frontal gyrus cluster on the right (MFG_R) and lower for right precuneus cortex (PC_R). Further information on thresholded clusters can be found in Table 2. *$P < 0.001$. HOA, hip osteoarthritis; KOA, knee osteoarthritis; OA, osteoarthritis; TICV, total intracranial volume.

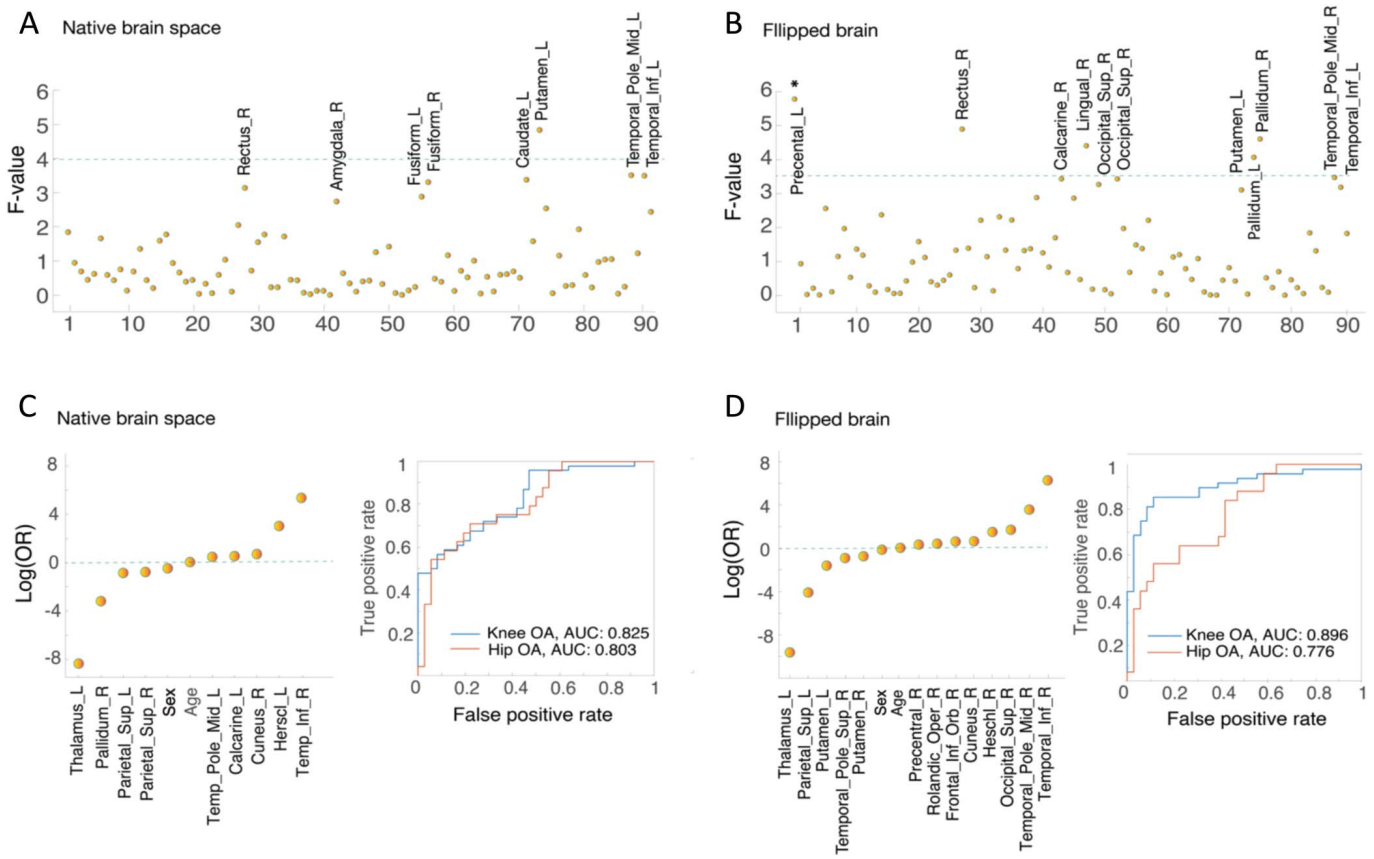

Figure 3. Univariable and multivariable analysis of regional GM differences between groups. Cortex was subdivided into 90 ROIs approximating Brodmann areas, using the AAL atlas; A and B plots show the F-value for each ROI across group comparison in native space, without brain flipping (A) and after flipping the brains (B) based on OA body side dominance (x-axis). Age, sex, TICV, and OA side in lateralized analysis were entered as covariates of no interest. Green line indicates uncorrected significance threshold at $P < 0.01$ ($F(3,148) > 4$ and $F(4,127) > 3.5$ for A and B); brain regions above and close to uncorrected threshold are labeled and include subcortical regions, temporal, and frontal regions. Primary motor cortex was identified solely in the flipped brain analysis (B) and was the only region surviving FDR correction for multiple comparisons (*$P < 0.05$). (C and D) The coefficient estimates (log(odds)) in KOA training group after LASSO regularization with lambda selection through 10-fold cross-validation for native (C) and in flipped volumes (D). Receiver operating characteristic for classification by logistic regression for the test KOA group and HOA group are also reported (blue = KOA; red = HOA). Areas under the curve showed values between 0.77 and 0.90, suggesting that generated models were not overfit and selected parameters are relevant predictors of OA-related brain morphological properties. HOA, hip OA; KOA, knee OA; OA, osteoarthritis; LASSO, least absolute shrinkage and selection operator; ROI, region of interest; TICV, total intracranial volume.

test group. **Figures 3C and D** show multivariable model results for the training KOA sample in native space (**Fig. 3C** left panel) and for flipped brain analyses (**Fig. 3D** left panel). Age and sex, although having small influences (0.24-0.06 log(OR)) were captured in both models. In addition, the combination of lower GM volumes of the left thalamus and parietal superior left cortex and higher GM volumes of temporal inferior gyrus together were strong predictors for KOA classification in both models. The flipped brain model captured additional regions not observed in the native analysis, including lower GM volumes in bilateral putamen, and higher GM volumes in right precentral gyrus and in frontal inferior orbicular gyrus.

We tested the performance of the classification models in the KOA hold-out sample to test validity of obtained results, and in HOA sample to test for generalization from KOA to HOA. For the hold-out KOA group, an AUC of 0.82 (nonflipped analysis) and 0.89 (flipped brain analysis) was attained. When evaluated in the HOA group, logistic regression presented an AUC of 0.8 and 0.77 for nonflipped and flipped analyses, respectively. Receiver operating characteristic curves are displayed in **Figure 3C** (right panel) and **Figure 3D** (right panel). Probability plots for each model are presented in Figure S1 (available online as supplemental digital content at http://links.lww.com/PAIN/B8).

Finally, we tested the model's performance for classifying among OA groups. The obtained AUC's were 0.65 and 0.76 for the nonflipped and flipped models, respectively (probability plots, Figure S2, available online as supplemental digital content at http://links.lww.com/PAIN/B8). Multivariable models seem both valid and generalizable from KOA to HOA, with the flipped model showing higher specificity for KOA.

3.7. Neuropathic pain associated with multivariable model for knee osteoarthritis

Given that the flipped brain multivariable model could better distinguish between OA and healthy controls, also showing higher specificity for knee OA, we further examined this model (**Fig. 4A**). First, we used Neurosynth database meta-analytical decoding to identify psychological/task terms associated with brain activity in these regions. We decoded the regions as absolute values, reflecting only location (**Fig. 4B**), and also using weighted values to account relative contribution of different regions in the model (**Fig. 4C**). The top 5 terms associated with the model for location only were: dementia, personality, gestures, social interaction, and interpersonal relations. When incorporating the model coefficient of each area, the main terms identified were pain, anticipatory, finger tapping, index finger, and integrate.

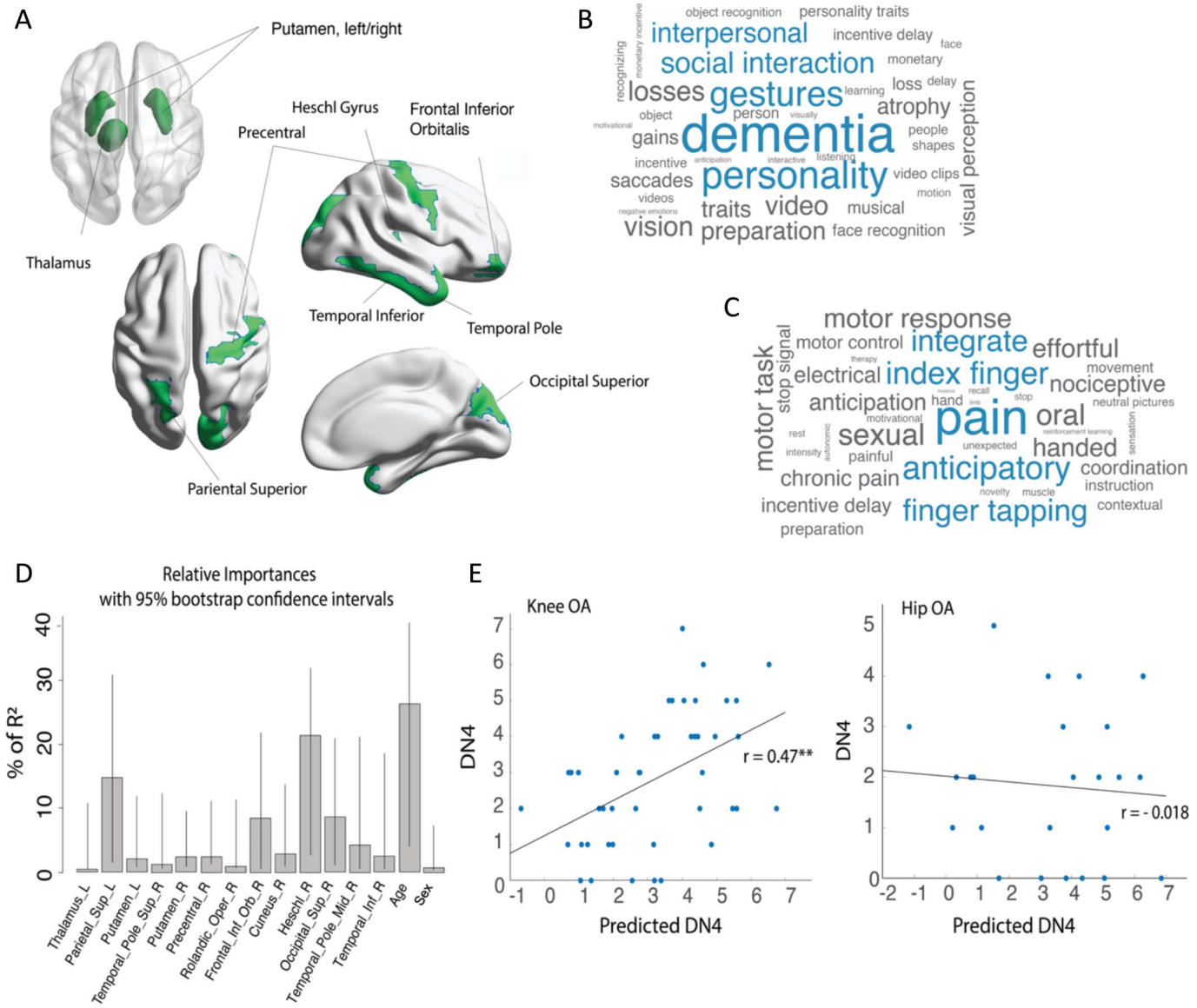

Figure 4. Neuropathic pain profile was associated with KOA multivariable brain volume changes. (A) Graphic representation of the AAL ROIs identified in the multivariable analysis (flipped brain). (B and C) plots show the top 40 (of about 1700) correlated psychological/task terms using Neurosynth reverse inference decoder for the brain regions (B) and weighted regions, given the model estimate coefficients (C). The size of a term in each word cloud is proportional to the correlation strength of term/region. Blue color represents top 5 correlations. (D–E) A multiple regression model using the logistic regression/LASSO results for flipped brain KOA classification predicted neuropathic pain score (DN4) in a subsample of KOA patients (training sample, n = 45). This result was validated on a KOA hold-out sample (test sample, n = 46), but not in the HOA group. (C) The relative importance of all predictive variables where % of R^2 is normalized to sum 100%. Bars correspond to 1000 bootstrap confidence intervals at 95%. (E) The validation of the obtained regression model in KOA testing sample and HOA groups. Predicted neuropathic pain scale (DN4) strongly and significantly correlated with the actual score in the KOA test group, but not in the HOA. DN4 (Douleur Neuropathique en 4 questions); $^{**}P < 0.001$. HOA, hip osteoarthritis; KOA, knee osteoarthritis; LASSO, least absolute shrinkage and selection operator; ROI, region of interest.

In an unbiased approach, we tested the model's association with clinical aspects of pain and mobility in OA. Using the KOA training sample (n = 45), and the predictors obtained from the LASSO, multiple regression models were built for each clinical variable of interest (ie, pain duration; pain intensity; HADS anxiety; HADS depression; Pain Catastrophizing Scale; 6MWT; timed up and go; DN4 and KOOS subscales). Only one model yielded statistical significance: neuropathic pain scale, DN4 ($F(1,45) = 2.29$; Adj R2 = 0.29; $P = 0.03$). Details for all generated models can be found in Table S3 (available online as supplemental digital content at http://links.lww.com/PAIN/B8). Finally, because several models were generated and thus spuriousness of the DN4 model is highly feasible, we sought to better characterize and unbiasedly validate the DN4 model. To do so, we first calculated the relative importance for each predictor variable and computed its respective 95% confidence interval using 1000 bootstrap replicates (**Fig. 4D**). Age, parietal superior cortex, Heschl/S2 gyrus, and frontal inferior orbitalis cortex presented the highest percentage of explained variance, with smaller contributions from other brain regions. We then validated the model in the KOA hold-out sample (n = 45), where the correlation between DN4 and predicted DN4 was statistically significant and strong ($r = 0.47$, $P < 0.001$). The model failed to replicate in the HOA group ($r = -0.018$, $P = 0.93$; **Fig. 4E**). Therefore, the obtained multivariable model reflects neuropathic pain characteristics, and the model is valid for neuropathic pain in KOA but does not generalize to HOA.

4. Discussion

Our univariate analyses highlight primarily lower GM volume in HOA in the anterior cingulate, and lower GM volume in the precentral cortex in both KOA and HOA contralateral to OA pain. In addition, the multivariable analysis reveals GM distortions captured as a multidomain system that integrates cortical and subcortical structures, shared between KOA and HOA. Reverse inference of this multidomain distortion, from functional brain space to psychological and task-related terms, identified 2 sets of concepts: (1) for unweighted location analysis associated terms included dementia, personality, gestures, social interaction, and interpersonal relations; (2) when the same analysis was performed taking into consideration the weights of contributing regions, the top associated concepts were: pain, anticipatory, finger tapping, index finger, and integrate. We found that the multivariable set of regions was associated with patient-reported neuropathic pain in KOA, but not in HOA patients. Importantly, the latter group has shorter pain duration and lower neuropathic pain scores. Our univariable analysis demonstrates more widespread and stronger GM distortions when taking into account the laterality of OA; however, no statistically significant relationships were found between univariable (VBM) results and clinical variables, similar to previous reports in the field.[2,39]

Brain structural changes using GM indices in chronic pain have been reported by multiple groups, primarily using VBM. Disparate regions, both directions of GM change, and even null findings are reported.[13] Our study was designed with the purpose of characterizing brain structural properties in the largest OA population reported to date. Our results are, in part, consistent with earlier reports: decreased GM in ACC seen in HOA has also been described in the past[51]; decreased precentral GM seen here in KOA and HOA is consistent with a report of functional remodeling of the motor cortex in KOA patients.[53] Importantly, we did not observe significant GM changes (univariable analysis) in brain areas previously reported for OA VBM studies, including both subcortical (thalamus,[25] amygdala and nuclei accumbens,[34] and caudate nuclei[39]) and cortical areas (insular cortex and dorsolateral prefrontal cortex[51]). Incongruent findings across studies may relate to the heterogeneity of OA pain at distinct stages of the disease, but also to the potential inherent limitations of VBM; eg, the sensitivity of VBM to imaging parameters and scanner differences, in addition to analytical details, such as spatially normalizing atypical brains and limitations of univariate techniques.[7,40]

Our multivariable analysis indicates the existence of a common set of brain distortions between KOA and HOA that differentiate these patients from healthy controls: 9 to 13 brain areas, composed of both cortical and subcortical regions. There is accumulating evidence that chronic pain leads to whole-brain global reorganization.[13] Tested specifically in OA patients, pain was associated with whole-brain degree rank order disruption,[38] and changes in large-scale brain network temporal dynamics.[16] Bridging this concept to morphologic brain reorganization in OA, we examined the GM volumetric distortions in a multidimensional space, accounting for the interrelationship between regions. Classification models were generated in a KOA sample, both in native and flipped brain space, and tested in hold-out KOA and HOA groups. Interestingly, the native space model yielded similar accuracy for knee and hip patients. Accuracy improved for the KOA group in the flipped brain space.

To better characterize this model, we identified the terms in the brain imaging literature associated with these regions using Neurosynth Image Decoder and selected the top 40 (of about 1300 terms) nonanatomical terms. The method uses meta-analysis (exploring around 14,000 brain imaging studies) to identify psychological and task-related terms associated with the collection of brain regions included in the multivariable model. The reverse association for the unweighted multivariable model identifies cognitive, interpersonal, and social interaction concepts, not obviously related to OA. Remarkably, when the weighted multivariable model was examined, the top term was pain (chance probability of this observation is near 1 in 1300 = 0.0008); additional pain-related terms, including chronic pain as well as motor-related terms, were also captured. This result is noteworthy because Neurosynth explores brain activity in a heterogeneous population and yet identifies pain and motor properties in the weighted multivariable model.

When studying the relationship between clinical measures and LASSO-derived multivariable models, we show that neuropathic pain probability, measured with the DN4 scale, is associated with the set of identified variables in the KOA group. Using an unbiased approach, we demonstrated that this result validates in the KOA sample but fails to generalize for HOA patients. This finding deserves a thorough examination: (1) KOA patients show a higher probability of neuropathic pain than HOA, fact that has been previously described[11]; (2) interestingly, in our sample, KOA patients also showed a longer pain duration, but less severe radiographic damage.

These results are concordant with Dabare et al.,[17] who showed that HOA symptomatology clinically presents later with more advanced disease than KOA, and patients are likely to undergo arthroplasty earlier from the time of presentation. Our findings suggest that, together with longer pain duration, there is the emergence of a neuropathic pain profile that can be clinically identified and linked to brain GM morphological properties. Our present result cannot unequivocally establish whether the multivariable GM distortion is a prognostic or diagnostic of neuropathic pain. However, the temporal dissociation between knee and hip pain and radiographic damage, together with a shared GM multivariable model, suggests that the model is more likely to be prognostic risk factor for developing signs of neuropathic pain in OA.

In a recent report based on the same KOA and HOA patient cohort, we examined the relationship between OA pain and clinical parameters.[10] Although multiple models could be derived for different measures of OA pain, these were not consistent and thus were deemed unstable and uninformative. Here, we queried the univariate and multivariable GM distortions associated with OA regarding their relationship to clinical characteristics. Univariate brain distortions were more prominent in the hemisphere contralateral to OA pain, and the neuropathic pain scale was related to the multivariable model, yet the majority of clinical parameters associated with OA were unrelated to GM distortions. This raises the question whether observed GM distortions can be seen as prognostic or diagnostic. Within the conceptual construct of the four-stage model for transition to chronic pain,[49] formulated based on a longitudinal study of back pain patients,[8] we have proposed a set of criteria that would differentiate between prognostic and diagnostic biomarkers for chronic pain: prognostic biomarkers should be preexisting factors that influence transition to chronic pain but are not modulated by pain. Conversely, diagnostic biomarkers are emergent in time with the transition to chronic pain and should reflect pain and related clinical characteristics. If we presume that the transition to chronic pain for OA, relating to its persistence after joint replacement surgery, follows the same general model as in back pain, then a lack of relationship

between clinical parameters and GM abnormalities suggests these are more likely to be prognostic in nature. This notion should be especially true for brain regions or multivariable models that show distortions shared between KOA and HOA as the impact of OA pain in HOA is distinct from that for KOA,[10] which in turn should differentially distort GM in areas reflecting diagnostic consequences.

This study does not come without limitations. Results from the VBM analysis should be cautiously interpreted because identified clusters result from uncorrected whole-brain analysis; however, our report is in line with previous publications on brain morphometry in chronic pain, reporting group comparisons at uncorrected $P < 0.001$.[2] We limit reporting only large cluster GM abnormalities (>66 voxels) to minimize false-positive findings. Another important limitation that has to be highlighted is the imbalance in the number of subjects between OA groups and controls. Although such an imbalance limits our statistical power,[15] our knee group was sufficient to construct the multivariable models using half of the knee patients. However, this is in contrast to the control group, which was not large enough to split, and thus, it was used in both the training and test set. Another shortcoming of this study is the fact that controls are not perfectly matched regarding age and sex with our KOA group; however, we account for the effect of these variables in all stages of our analysis. Finally, socioeconomic and cultural differences regarding attitudes of coping and/or suffering with OA pain may also underlie differences in VBM results when contrasting our findings with other studies.

In conclusion, our results show decreased GM in HOA in the ACC and decreased GM in precentral cortex in both KOA and HOA; however, these GM differences are not strongly correlated with clinical variables in OA. Moreover, we derived a multivariable model based on GM distortion that differentiated OA patients from healthy subjects. Importantly, this model was associated with the neuropathic scale in KOA, and in reverse inference, it was linked with pain and motor control in the brain imaging literature. We reason that observed GM distortions may reflect a priori risks for chronicity of OA pain rather than being consequential to the development of the disease.

Conflict of interest statement

The authors have no conflicts of interest to declare.

Acknowledgements

The authors thank to Dr Paulo Oliveira, for the clinical support and supervision of patients enrolled in the study, and all the members of the Orthopedic Department of Centro Hospitalar Universitário de São João, Porto, for their support with data collection. The authors thank Unilabs Boavista and Dr Nuno Martins for all the support in imaging data acquisition. The authors are thankful to all Apkarian laboratory and Galhardo laboratory members who contributed to this study with their time and resources.
J. Barroso was funded through CCDRN [Norte-08-5369-FSE-000026], OARSI Collaborative Scholarship 2018 and Luso-American Development Foundation R&D scholarship grant. Neuroimage data acquisition was provided by Unilabs Boavista and the Grünenthal Young Pain Researcher 2017 Grant, Portugal. This material is based upon work supported by the National Science Foundation Graduate Research Fellowship under Grant No. DGE-1324585.

Appendix A. Supplemental digital content

Supplemental digital content associated with this article can be found online at http://links.lww.com/PAIN/B8.

Supplemental video content

A video abstract associated with this article can be found at http://links.lww.com/PAIN/B9.

Article history:
Received 24 January 2020
Received in revised form 16 March 2020
Accepted 1 April 2020
Available online 4 May 2020

References

[1] Akin-Akinyosoye K, Frowd N, Marshall L, Stocks J, Fernandes GS, Valdes A, McWilliams DF, Zhang W, Doherty M, Ferguson E, Walsh DA. Traits associated with central pain augmentation in the Knee Pain in the Community (KPIC) cohort. PAIN 2018;159:1035–44.
[2] Alshuft HM, Condon LA, Dineen RA, Auer DP. Cerebral cortical thickness in chronic pain due to knee osteoarthritis: the effect of pain duration and pain sensitization. PLoS One 2016;11:e0161687.
[3] Altman R, Asch E, Bloch D, Bole G, Borenstein D, Brandt K, Christy W, Cooke TD, Greenwald R, Hochberg M, Howell D, Kaplan D, Koopman W, Longley S, Mankin H, McShane DJ, Medsger T Jr, Meenan R, Mikkelsen M, Hochberg W, Mqscowitz, Murphy W, Rothschild B, Segal M, Sokoloff L, Wolfe F. Development of criteria for the classification and reporting of osteoarthritis. Classification of osteoarthritis of the knee. Diagnostic and Therapeutic Criteria Committee of the American Rheumatism Association. Arthritis Rheum 1986;29:1039–49.
[4] Andersson JLR, Jenkinson M, Smith S. Non-linear registration, aka spatial 524 normalisation. FMRIB Tech Rep 2010:TR07JA2. Available at: https://www.fmrib.ox.ac.uk/datasets/techrep/tr07ja2/tr07ja2.pdf
[5] Azevedo LCP. Tradução, adaptação cultural e estudo multicêntrico de validação de instrumentos para rastreio e avaliação do impacto da dor crónica (Translation, cultural adaptation and multicentric validation study of chronic pain screening and impact assessment instruments). Dor 2007;15:6–65.
[6] Baliki MN, Geha PY, Jabakhanji R, Harden N, Schnitzer TJ, Apkarian AV. A preliminary fMRI study of analgesic treatment in chronic back pain and knee osteoarthritis. Mol Pain 2008;4:47.
[7] Baliki MN, Schnitzer TJ, Bauer WR, Apkarian AV. Brain morphological signatures for chronic pain. PLoS One 2011;6:e26010.
[8] Baliki MN, Petre B, Torbey S, Herrmann KM, Huang L, Schnitzer TJ, Fields HL, Apkarian AV. Corticostriatal functional connectivity predicts transition to chronic back pain. Nat Neurosci 2012;15:1117–19.
[9] Balke B. A simple field test for the assessment of physical fitness. Rep 63-6. Rep Civ Aeromed Res Inst US 1963:1–8. Available at: https://www.faa.gov/data_research/research/med_humanfacs/oamtechreports/1960s/media/am63-06.pdf
[10] Barroso J, Wakaizumi K, Reckziegel D, Pinto-Ramos J, Schnitzer T, Galhardo V, Apkarian AV. Prognostics for pain in osteoarthritis: do clinical measures predict pain after total joint replacement? PLoS One 2020;15:e0222370.
[11] Blikman T, Rienstra W, van Raay J, Dijkstra B, Bulstra SK, Stevens M, van den Akker- Scheek I. Neuropathic-like symptoms and the association with joint-specific function and quality of life in patients with hip and knee osteoarthritis. PLoS One 2018;13:e0199165.
[12] Bouhassira D, Attal N, Alchaar H, Boureau F, Brochet B, Bruxelle J, Cunin G, Fermanian J, Ginies P, Grun-Overdyking A, Jafari-Schluep H, Lanteri-Minet M, Laurent B, Mick G, Serrie A, Valade D, Vicaut E. Comparison of pain syndromes associated with nervous or somatic lesions and development of a new neuropathic pain diagnostic questionnaire (DN4). PAIN 2005;114:29–36.
[13] Cauda F, Palermo S, Costa T, Torta R, Duca S, Vercelli U, Geminiani G, Torta DM. Gray matter alterations in chronic pain: a network-oriented meta-analytic approach. Neuroimage Clin 2014;4:676–86.
[14] Centers for Disease Control and Prevention (CDC). Prevalence and most common causes of disability among adults—United States, 2005. MMWR Morb Mortal Wkly Rep 2009;58:421–6.

[15] Cohen J. Statistical power analysis for the behavioral sciences. 2nd ed. Hillsdale, NJ: Lawrence Erlbaum Assoc Publ. 2018, p. 558.
[16] Cottam WJ, Iwabuchi SJ, Drabek MM, Reckziegel D, Auer DP. 559 Altered connectivity of the right anterior insula drives the pain connectome changes in chronic knee osteoarthritis. PAIN 2018;159:929–38.
[17] Dabare C, Le Marshall K, Leung A, Page CJ, Choong PF, Lim KK. Differences in presentation, progression and rates of arthroplasty between hip and knee osteoarthritis: observations from an osteoarthritis cohort study-a clear role for conservative management. Int J Rheum Dis 2017;20:1350–60.
[18] Finan PH, Buenaver LF, Bounds SC, Hussain S, Park RJ, Haque UJ, Campbell CM, Haythornthwaite JA, Edwards RR, Smith MT. Discordance between pain and radiographic severity in knee osteoarthritis: findings from quantitative sensory testing of central sensitization. Arthritis Rheum 2013;65:363–72.
[19] Fingleton C, Smart K, Moloney N, Fullen BM, Doody C. Pain sensitization in people with knee osteoarthritis: a systematic review and meta-analysis. Osteoarthritis Cartilage 2015;23:1043–56.
[20] Friedman J, Hastie T, Tibshirani R. Regularization paths for generalized linear models via coordinate descent. J Stat Softw 2010;33:1–22.
[21] Goncalves RS, Cabri J, Pinheiro JP, Ferreira PL. Cross-cultural adaptation and validation of the Portuguese version of the Knee injury and Osteoarthritis Outcome Score (KOOS). Osteoarthritis Cartilage 2009; 17:1156–62.
[22] Gorgolewski KJ, Varoquaux G, Rivera G, Schwartz Y, Sochat VV, Ghosh SS, Maumet C, Nichols TE, Poline JB, Yarkoni T, Margulies DS, Poldrack RA. NeuroVault.org: a repository for sharing unthresholded statistical maps, parcellations, and atlases of the human brain. Neuroimage 2016; 124:1242–4.
[23] Grömping U. Relative importance for linear regression in R: the package relaimpo. J Stat Softw 2006;17:1–27.
[24] Gustin SM, Peck CC, Wilcox SL, Nash PG, Murray GM, Henderson LA. Different pain, different brain: thalamic anatomy in neuropathic and non-neuropathic chronic pain syndromes. J Neurosci 2011;31:5956–64.
[25] Gwilym SE, Filippini N, Douaud G, Carr AJ, Tracey I. Thalamic atrophy associated with painful osteoarthritis of the hip is reversible after arthroplasty: a longitudinal voxel-based morphometric study. Arthritis Rheum 2010;62:2930–40.
[26] Hashmi JA, Baliki MN, Huang L, Baria AT, Torbey S, Hermann KM, Schnitzer TJ, Apkarian AV. Shape shifting pain: chronification of back pain shifts brain representation from nociceptive to emotional circuits. Brain 2013;136:2751–68.
[27] Hawker GA. Experiencing painful osteoarthritis: what have we learned from listening? Curr Opin Rheumatol 2009;21:507–12.
[28] Hochman JR, Davis AM, Elkayam J, Gagliese L, Hawker GA. Neuropathic pain symptoms on the modified painDETECT correlate with signs of central sensitization in knee osteoarthritis. Osteoarthritis Cartilage 2013; 21:1236–42.
[29] IASP. IASP Terminology 2018 [definitions of pain terminology]. 2018. Available at: http://www.ias-pain.org/Edication/Content.aspx?Itemnumber=1698. Accessed September 2019.
[30] Jenkinson M, Bannister P, Brady M, Smith S. Improved optimization for the robust and accurate linear registration and motion correction of brain images. Neuroimage 2002;17:825–41.
[31] Jenkinson M, Beckmann CF, Behrens TE, Woolrich MW, Smith SM. Fsl. Neuroimage 2012;62:782–90.
[32] Kellgren JH, Lawrence JS. Radiological assessment of osteo-arthrosis. Ann Rheum Dis 1957;16:494–502.
[33] Kennard RW, Stone LA. Computer aided design of experiments. Technometrics 1969;11:137–48.
[34] Lewis GN, Parker RS, Sharma S, Rice DA, McNair PJ. Structural brain alterations before and after total knee arthroplasty: a longitudinal assessment. Pain Med 2018;19:2166–76.
[35] Lindeman RH, Merenda PF, Gold RZ. Introduction to bivariate and multivariate analysis. Glenview: Scott Foresman, 1980. p. 119.
[36] Maeda Y, Kettner N, Sheehan J, Kim J, Cina S, Malatesta C, Gerber J, McManus C, Mezzacappa P, Morse LR, Audette J, Napadow V. Altered brain morphometry in carpal tunnel syndrome is associated with median nerve pathology. Neuroimage Clin 2013;2:313–19.
[37] Malfait AM, Schnitzer TJ. Towards a mechanism-based approach to pain management in osteoarthritis. Nat Rev Rheumatol 2013;9:654–64.
[38] Mansour A, Baria AT, Tetreault P, Vachon-Presseau E, Chang PC, Huang L, Apkarian AV, Baliki MN. Global disruption of degree rank order: a hallmark of chronic pain. Sci Rep 2016;6:34853.
[39] Mao CP, Bai ZL, Zhang XN, Zhang QJ, Zhang L. Abnormal subcortical brain morphology in patients with knee osteoarthritis: a cross-sectional study. Front Aging Neurosci 2016;8:3.
[40] Mechelli A, Price CF. Voxel-based morphometry of the human brain: methods and applications. Curr Med Imaging Rev 2005;1:9.
[41] Murphy SL, Phillips K, Williams DA, Clauw DJ. The role of the central nervous system in osteoarthritis pain and implications for rehabilitation. Curr Rheumatol Rep 2012;14:576–82.
[42] Murray CJ, Vos T, Lozano R, Naghavi M, Flaxman AD, Michaud C, Ezzati M, Shibuya K, Salomon JA, Abdalla S, Aboyans V, Abraham J, Ackerman I, Aggarwal R, Ahn SY, Ali MK, Alvarado M, Anderson HR, Anderson LM, Andrews KG, Atkinson C, Baddour LM, Bahalim AN, Barker-Collo S, Barrero LH, Bartels DH, Basanez MG, Baxter A, Bell ML, Benjamin EJ, Bennett D, Bernabe E, Bhalla K, Bhandari B, Bikbov B, Bin Abdulhak A, Birbeck G, Black JA, Blencowe H, Blore JD, Blyth F, Bolliger I, Bonaventure A, Boufous S, Bourne R, Boussinesq M, Braithwaite T, Brayne C, Bridgett L, Brooker S, Brooks P, Brugha TS, Bryan-Hancock C, Bucello C, Buchbinder R, Buckle G, Budke CM, Burch M, Burney P, Burstein R, Calabria B, Campbell B, Canter CE, Carabin H, Carapetis J, Carmona L, Cella C, Charlson F, Chen H, Cheng AT, Chou D, Chugh SS, Coffeng LE, Colan SD, Colquhoun S, Colson KE, Condon J, Connor MD, Cooper LT, Corriere M, Cortinovis M, de Vaccaro KC, Couser W, Cowie BC, Criqui MH, Cross M, Dabhadkar KC, Dahiya M, Dahodwala N, Damsere-Derry J, Danaei G, Davis A, De Leo D, Degenhardt L, Dellavalle R, Delossantos A, Denenberg J, Derrett S, Des Jarlais DC, Dharmaratne SD, Dherani M, Diaz-Torne C, Dolk H, Dorsey ER, Driscoll T, Duber H, Ebel B, Edmond K, Elbaz A, Ali SE, Erskine H, Erwin PJ, Espindola P, Ewoigbokhan SE, Farzadfar F, Feigin V, Felson DT, Ferrari A, Ferri CP, Fevre EM, Finucane MM, Flaxman S, Flood L, Foreman K, Forouzanfar MH, Fowkes FG, Fransen M, Freeman MK, Gabbe BJ, Gabriel SE, Gakidou E, Ganatra HA, Garcia B, Gaspari F, Gillum RF, Gmel G, Gonzalez- Medina D, Gosselin R, Grainger R, Grant B, Groeger J, Guillemin F, Gunnell D, Gupta R, Haagsma J, Hagan H, Halasa YA, Hall W, Haring D, Haro JM, Harrison JE, Havmoeller R, Hay RJ, Higashi H, Hill C, Hoen B, Hoffman H, Hotez PJ, Hoy D, Huang JJ, Ibeanusi SE, Jacobsen KH, James SL, Jarvis D, Jasrasaria R, Jayaraman S, Johns N, Jonas JB, Karthikeyan G, Kassebaum N, Kawakami N, Keren A, Khoo JP, King CH, Knowlton LM, Kobusingye O, Koranteng A, Krishnamurthi R, Laden F, Lalloo R, Laslett LL, Lathlean T, Leasher JL, Lee YY, Leigh J, Levinson D, Lim SS, Limb E, Lin JK, Lipnick M, Lipshultz SE, Liu W, Loane M, Ohno SL, Lyons R, Mabweijano J, MacIntyre MF, Malekzadeh R, Mallinger L, Manivannan S, Marcenes W, March L, Margolis DJ, Marks GB, Marks R, Matsumori A, Matzopoulos R, Mayosi BM, McAnulty JH, McDermott MM, McGill N, McGrath J, Medina-Mora ME, Meltzer M, Mensah GA, Merriman TR, Meyer AC, Miglioli V, Miller M, Miller TR, Mitchell PB, Mock C, Mocumbi AO, Moffitt TE, Mokdad AA, Monasta L, Montico M, Moradi-Lakeh M, Moran A, Morawska L, Mori R, Murdoch ME, Mwaniki MK, Naidoo K, Nair MN, Naldi L, Narayan KM, Nelson PK, Nelson RG, Nevitt MC, Newton CR, Nolte S, Norman P, Norman R, O'Donnell M, O'Hanlon S, Olives C, Omer SB, Ortblad K, Osborne R, Ozgediz D, Page A, Pahari B, Pandian JD, Rivero AP, Patten SB, Pearce N, Padilla RP, Perez-Ruiz F, Perico N, Pesudovs K, Phillips D, Phillips MR, Pierce K, Pion S, Polanczyk GV, Polinder S, Pope CA, Popova S, Porrini E, Pourmalek F, Prince M, Pullan RL, Ramaiah KD, Ranganathan D, Razavi H, Regan M, Rehm JT, Rein DB, Remuzzi G, Richardson K, Rivara FP, Roberts T, Robinson C, De Leon FR, Ronfani L, Room R, Rosenfeld LC, Rushton L, Sacco RL, Saha S, Sampson U, Sanchez-Riera L, Sanman E, Schwebel DC, Scott JG, Segui-Gomez M, Shahraz S, Shepard DS, Shin H, Shivakoti R, Singh D, Singh GM, Singh JA, Singleton J, Sleet DA, Sliwa K, Smith E, Smith JL, Stapelberg NJ, Steer A, Steiner T, Stolk WA, Stovner LJ, Sudfeld C, Syed S, Tamburlini G, Tavakkoli M, Taylor HR, Taylor JA, Taylor WJ, Thomas B, Thomson WM, Thurston GD, Tleyjeh IM, Tonelli M, Towbin JA, Truelsen T, Tsilimbaris MK, Ubeda C, Undurraga EA, van der Werf MJ, van Os J, Vavilala MS, Venketasubramanian N, Wang M, Wang W, Watt K, Weatherall DJ, Weinstock MA, Weintraub R, Weisskopf MG, Weissman MM, White RA, Whiteford H, Wiebe N, Wiersma ST, Wilkinson JD, Williams HC, Williams SR, Witt E, Wolfe F, Woolf AD, Wulf S, Yeh PH, Zaidi AK, Zheng ZJ, Zonies D, Lopez AD, AlMazroa MA, Memish ZA. Disability-adjusted life years (DALYs) for 291 diseases and injuries in 21 regions, 1990-2010: a systematic analysis for the Global Burden of Disease Study 2010. Lancet 2012;380:2197–223.
[43] Neogi T. The epidemiology and impact of pain in osteoarthritis. Osteoarthritis Cartilage 2013;21:1145–53.
[44] Nilsdotter AK, Lohmander LS, Klassbo M, Roos EM. Hip disability and osteoarthritis outcome score (HOOS)—validity and responsiveness in total hip replacement. BMC Musculoskelet Disord 2003;4:10.
[45] Pais-Ribeiro J, Silva I, Ferreira T, Martins A, Meneses R, Baltar M. Validation study of a Portuguese version of the Hospital Anxiety and Depression Scale. Psychol Health Med 2007;12:225–35; quiz 235–7.

[46] Parks EL, Geha PY, Baliki MN, Katz J, Schnitzer TJ, Apkarian AV. Brain activity for chronic knee osteoarthritis: dissociating evoked pain from spontaneous pain. Eur J Pain 2011;15:843.e1–14.
[47] Podsiadlo D, Richardson S. The timed "Up & Go": a test of basic functional mobility for frail elderly persons. J Am Geriatr Soc 1991;39: 142–8.
[48] Poldrack R. Can cognitive processes be inferred from neuroimaging data? Trends Cogn Sci 2006;10:59–63.
[49] Reckziegel D, Vachon-Presseau E, Petre B, Schnitzer TJ, Baliki MN, Apkarian AV. Deconstructing biomarkers for chronic pain: context- and hypothesis-dependent biomarker types in relation to chronic pain. PAIN 2019;160:S37–48.
[50] Rejeski WJ, Ettinger WH, Schumaker S, James P, Burns R, Elam JT. Assessing performance701 related disability in patients with knee osteoarthritis. Osteoarthritis Cartilage 1995;3:157–67.
[51] Rodriguez-Raecke R, Niemeier A, Ihle K, Ruether W, May A. Structural brain changes in chronic pain reflect probably neither damage nor atrophy. PLoS One 2013;8:e54475.
[52] Roos EM, Toksvig-Larsen S. Knee injury and Osteoarthritis 705 Outcome Score (KOOS)—validation and comparison to the WOMAC in total knee replacement. Health Qual Life Outcomes 2003;1:17.
[53] Shanahan CJ, Hodges PW, Wrigley TV, Bennell KL, Farrell MJ. Organisation of the motor cortex differs between people with and without knee osteoarthritis. Arthritis Res Ther 2015;17:164.
[54] Smith S, Nichols T. Threshold-free cluster enhancement: addressing problems of smoothing, threshold dependence and localisation in cluster inference. NeuroImage 2009;44:83–98.
[55] Smith SM, Zhang Y, Jenkinson M, Chen J, Matthews PM, Federico A, De Stefano N. Accurate, robust, and automated longitudinal and cross-sectional brain change analysis. NeuroImage 2002;17:479–89.
[56] Smith SM, Jenkinson M, Woolrich MW, Beckmann CF, Behrens TEJ, Johansen-Berg H, Bannister PR, De Luca M, Drobnjak I, Flitney DE, Niazy RK, Saunders J, Vickers J, Zhang Y, De Stefano N, Brady JM, Matthews PM. Advances in functional and structural MR image analysis and implementation as FSL. NeuroImage 2004;23:S208–19.
[57] Somers TJ, Keefe FJ, Pells JJ, Dixon KE, Waters SJ, Riordan PA, Blumenthal JA, McKee DC, LaCaille L, Tucker JM, Schmitt D, Caldwell DS, Kraus VB, Sims EL, Shelby RA, Rice JR. Pain catastrophizing and pain-related fear in osteoarthritis patients: relationships to pain and disability. J Pain Symptom Manage 2009;37:863–72.
[58] Sullivan MJL, Bishop SR, Pivik J. The pain catastrophizing scale: development and validation. Psychol Assess 1995;7:524–32.
[59] Thakur M, Dickenson AH, Baron R. Osteoarthritis pain: nociceptive or neuropathic? Nat Rev Rheumatol 2014;10:374–80.
[60] Tibshirani R. Regression shrinkage and selection via the lasso. J R Stat Soc Ser B Methodol 1996;58:267–88.
[61] Tzourio-Mazoyer N, Landeau B, Papathanassiou D, Crivello F, Etard O, Delcroix N, Mazoyer B, Joliot M. Automated anatomical labeling of activations in SPM using a macroscopic anatomical parcellation of the MNI MRI single-subject brain. NeuroImage 2002;15:273–89.
[62] Vachon-Presseau E, Tétreault P, Petre B, Huang L, Berger SE, Torbey S, Baria AT, Mansour AR, Hashmi JA, Griffith JW, Comasco E, Schnitzer TJ, Baliki MN, Apkarian AV. Corticolimbic anatomical characteristics predetermine risk for chronic 739 pain. Brain 2016;139:1958–70.
[63] Wieland HA, Michaelis M, Kirschbaum BJ, Rudolphi KA. Osteoarthritis—an untreatable disease? Nat Rev Drug Discov 2005;4: 331–44.
[64] Winkler AM, Ridgway GR, Webster MA, Smith SM, Nichols TE. Permutation inference for the general linear model. NeuroImage 2014; 92:381–97.
[65] Yarkoni T, Poldrack RA, Nichols TE, Van Essen DC, Wager TD. Large-scale automated synthesis of human functional neuroimaging data. Nat Methods 2011;8:665–70.
[66] Zhang Y, Brady M, Smith S. Segmentation of brain MR images through a hidden Markov random field model and the expectation-maximization algorithm. IEEE Trans Med Imaging 2001;20:45–57.
[67] Zigmond AS, Snaith RP. The hospital anxiety and depression scale. Acta Psychiatr Scand 1983;67:361–70.

2.3 Publication III

Barroso J, Wakaizumi K, Reis AM, Baliki M, Schnitzer TJ, Galhardo V, Apkarian AV. *Reorganization of functional brain network architecture in chronic osteoarthritis pain*. Hum Brain Mapp. 2021 Mar;42(4):1206-1222. doi: 10.1002/hbm.25287. PMID: 33210801; PMCID: PMC7856636.

Received: 15 August 2020 | Revised: 12 October 2020 | Accepted: 2 November 2020

DOI: 10.1002/hbm.25287

Check for updates

RESEARCH ARTICLE

WILEY

Reorganization of functional brain network architecture in chronic osteoarthritis pain

Joana Barroso[1,2,3,4] | Kenta Wakaizumi[5,6] | Ana Mafalda Reis[7] | Marwan Baliki[5,3] | Thomas J. Schnitzer[3,8,9] | Vasco Galhardo[1,2] | Apkar Vania Apkarian[3,4,9]

[1]Departamento de Biomedicina, Faculdade de Medicina, Universidade do Porto, Porto, Portugal

[2]Instituto de Investigação e Inovação em Saúde - i3S, Universidade do Porto, Porto, Portugal

[3]Department of Physical Medicine and Rehabilitation, Northwestern University, Feinberg School of Medicine, Chicago, Illinois

[4]Department of Physiology, Northwestern University, Feinberg School of Medicine, Chicago, Illinois

[5]Shirley Ryan Ability Lab, Chicago, Illinois

[6]Department of Anesthesiology, Keio University School of Medicine, Tokyo, Japan

[7]Unilabs Boavista, Porto, Portugal

[8]Department of Internal Medicine/Rheumatology, Northwestern University, Feinberg School of Medicine, Chicago, Illinois

[9]Department of Anesthesia, Northwestern University, Feinberg School of Medicine, Chicago, Illinois

Correspondence
Apkar Vania Apkarian, Northwestern University, Feinberg School of Medicine, Tarry Bldg. 7-705, Chicago, IL 60611.
Email: a-apkarian@northwestern.edu

Funding information
CCDRN, Grant/Award Number: Norte-08-5369-FSE-000026; Unilabs Boavista and the Grünenthal Young Pain Researcher 2017 Grant; Luso-American Development Foundation R&D@PhD Scholarship Grant; OARSI Collaborative Scholarship 2018

Abstract

Osteoarthritis (OA) manifests with chronic pain, motor impairment, and proprioceptive changes. However, the role of the brain in the disease is largely unknown. Here, we studied brain networks using the mathematical properties of graphs in a large sample of knee and hip OA (KOA, *n* = 91; HOA, *n* = 23) patients. We used a robust validation strategy by subdividing the KOA data into discovery and testing groups and tested the generalizability of our findings in HOA. Despite brain global topological properties being conserved in OA, we show there is a network wide pattern of reorganization that can be captured at the subject-level by a single measure, the hub disruption index. We localized reorganization patterns and uncovered a shift in the hierarchy of network hubs in OA: primary sensory and motor regions and parahippocampal gyrus behave as hubs and insular cortex loses its central placement. At an intermediate level of network structure, frontoparietal and cingulo-opercular modules showed preferential reorganization. We examined the association between network properties and clinical correlates: global disruption indices and isolated degree properties did not reflect clinical parameters; however, by modeling whole brain nodal degree properties, we identified a distributed set of regions that reliably predicted pain intensity in KOA and generalized to hip OA. Together, our findings reveal that while conserving global topological properties, brain network architecture reorganizes in OA, at both global and local scale. Network connectivity related to OA pain intensity is dissociated from the major hub disruptions, challenging the extent of dependence of OA pain on nociceptive signaling.

KEYWORDS

brain networks, brain topology, chronic pain, graph properties, osteoarthritis

1 | INTRODUCTION

Osteoarthritis (OA) is one of the most prevalent sources of chronic musculoskeletal pain (Neogi, 2013), and a leading cause of disability worldwide (Centers for Disease Control and Prevention, 2009; Murray et al., 2012). Pain is the hallmark symptom of the disease, contributing to reduced mobility and psychological stress, and representing the main motivation to seek medical care (Hawker, 2009). When compared to other chronic painful conditions, OA pain is unique in numerous ways: there is an extraordinary interpatient

This is an open access article under the terms of the Creative Commons Attribution License, which permits use, distribution and reproduction in any medium, provided the original work is properly cited.
© 2020 The Authors. *Human Brain Mapping* published by Wiley Periodicals LLC.

variability in clinical symptoms and structural manifestations, and a heterogeneous response to treatment interventions (Deveza, Nelson, & Loeser, 2019). It is not clear to what extent pain is a reflection of afferent nociceptive signaling, represents central adaptive or maladaptive processes, and/or is contingent on psychological and emotional dimensions (Neogi, 2013). Evidence derived from rodent models of OA shows nervous system reorganization, mostly highlighting peripheral changes in nociceptors and spinal cord circuitry (Miller et al., 2015; Miller, Block, & Malfait, 2017); however, the contribution of the brain in the development and progression of OA pain remains minimally explored.

Individual brain regions are functionally specialized, and information exchange between brain areas is fundamental for integrated perceptual states. All cognitive-emotional functions require such integration (van den Heuvel & Sporns, 2013). Thus, functional resting-state brain network properties reflect both disease and normal abilities of information integration in the brain. By describing brain networks as graphs, essentially comprising sets of nodes (neuronal elements/brain regions) and edges (their interconnections), we can study key organizational features of the brain's network architecture: locally, at the each node level; globally, both by considering whole-brain mean nodal properties, and by calculating graph disruption indices—global metrics sensitive to the reorganization of nodes within the network (Mansour et al., 2016).

Using this theoretical framework, we (Huang et al., 2019; Mansour et al., 2016) and other groups (De Pauw et al., 2020; Kaplan et al., 2019) have studied brain networks' global topological properties in chronic pain. It has been shown, for diverse clinical conditions, that CP is associated with large-scale brain functional changes. Specifically for OA pain, we have recently shown that brain gray matter distortions are distributed across cortical and subcortical structures and relate to pain correlates (Barroso et al., 2020). Moreover, differences in brain modular organization in OA were previously reported in the insula and parietal cortices (Mansour et al., 2016), and the anterior insula was proposed as a key element driving changes in brain network temporal dynamics in chronic OA pain patients (Cottam, Iwabuchi, Drabek, Reckziegel, & Auer, 2018). Here, we hypothesize that together with a global disturbance, local network metrics should be altered in several regions/networks for which structural/functional properties have shown abnormalities in OA, and moreover, that the community/subnetwork organization should also reflect the disease process.

In addition, there is good evidence that brain-network organizational properties are closely related to function, both in health and in disease (Stam, 2014). Graph disruption indices and local topological changes were previously related to pain intensity and other dimensions of clinical pain (De Pauw et al., 2020; Kaplan et al., 2019; Mansour et al., 2016). We therefore theorize that global and local network disruptions in OA will relate with pain and other key clinical correlates of the disease, potentially reflecting adaptive and maladaptive brain anatomical and physiological plasticity.

In order to test our hypotheses, using resting state functional MRI data from a large sample of long-duration, severe OA pain patients, we modeled large-scale brain networks as graphs. We investigated differences between knee OA (KOA) patients and healthy controls (HC) at multiple levels of network topographic structure. Moreover, we evaluated the associations between brain topological properties and clinical correlates of the disease. To ensure that outcomes were robust and applicable to KOA cohorts at large, we validated our findings in a KOA hold out sample, and further tested generalizability in a hip OA (HOA) sample.

2 | MATERIALS AND METHODS

2.1 | Participants

This study included 95 KOA and 24 HOA patients with indication for total arthroplasty and 36 HC participants. Patients were recruited in the Orthopedic Department of *Centro Hospitalar e Universitário de São João*, Porto, Portugal. HC were healthy subjects from the same geographic area, age range, social and educational background as the OA patients.

The following inclusion criteria for OA were applied: (a) age between 45 and 75 years; (b) diagnosis of OA according to the clinical classification criteria of the American College of Rheumatology (4); (c) surgical indication for arthroplasty. Exclusion criteria included: (a) secondary OA due to congenital and development diseases or inflammatory and auto-immune articular diseases; (b) bilateral OA with indication for contralateral arthroplasty in the following year or bilateral knee pain with less than or equal to four points difference on the numeric pain rating scale (NRS) between knees; (c) other chronic pain conditions (e.g., low back pain; fibromyalgia; chronic pelvic pain; chronic headache/migraine); (d) chronic neurological or psychiatric disease (e.g., multiple sclerosis and other demyelinating diseases; peripheral neuropathy; bipolar and related disorders; neurodevelopment disorders); and (e) previous history of stroke or traumatic brain injury. Controls were included if matching patients demographic characteristics regarding age, gender, and educational level. Exclusion criteria for this group were the same as for patients, in addition to the diagnosis of OA in any joint, or undiagnosed joint pain.

All OA patients were evaluated 2–6 weeks prior to surgery with a clinical examination, questionnaires, and a brain MRI. HC underwent a clinical examination and completed a brain MRI. All subjects provided informed consent prior to participating in the study, and all methods were carried out in accordance with the local Ethics Committee (*Comissão de Ética para a Saúde*, *Centro Hospitalar e Universitário de São João*) and the Helsinki declaration.

After brain imaging quality control, a total of 91 KOA, 23 HOA, and 35 HC were considered for formal analysis. OA patients were subdivided in three groups: KOA discovery (n = 46); KOA validation (n = 45), here using the Kennard–Stone algorithm (5), which allowed us to select samples with a uniform distribution over a multivariate predictor space (age, sex, pain levels, and behavioral variables); and HOA. The first set, the KOA discovery group, was used in the primary

analysis of the paper; the KOA validation and the HOA groups were used to assess the external validity of the main findings.

2.2 | Clinical parameters

Clinical and demographic parameters were obtained at the initial interview, after consenting the patient, and by clinical chart assessment. All patients completed a battery of questionnaires assessing multiple domains: NRS for pain; Knee and Hip Injury and Osteoarthritis Score (KOOS) (Gonçalves, Cabri, Pinheiro, & Ferreira, 2009; Roos & Toksvig-Larsen, 2003); Hospital Anxiety and Depression Scale (HADS) (Pais-Ribeiro et al., 2007; Zigmond & Snaith, 1983); Pain Catastrophizing Scale (PCS) (Azevedo, 2007; Sullivan, Bishop, & Pivik, 1995); *Doleur Neuropathique en 4 questions*—Neuropathic pain scale (DN4) (Azevedo, 2007; Bouhassira et al., 2005). All questionnaires were used in their Portuguese validated versions. We also assessed physical performance by applying two distinct tasks: timed up and go test (TUG) (Podsiadlo & Richardson, 1991) and 6-min walking test (6MWT) (Balke, 1963; Rejeski et al., 1995). Finally, joint X-rays were also assessed by two trained radiologists and classified using the Kellgren–Lawrence scale (Kellgren & Lawrence, 1957).

Regarding these parameters, descriptive statistics were used to describe the study sample, with continuous variables presented as mean and *SD*s, and categorical data as numbers and percentages. Comparisons between HC, KOA, and HOA groups were done with analysis of variable and independent sample *t* tests or chi-square (X^2) tests, for continuous parametrical variables and categorical data, respectively.

2.3 | Magnetic resonance imaging data acquisition

For all participants, MPRAGE type T1-anatomical brain images were acquired with a 3.0 T Siemen Magnetom Spectra scanner (Siemens Medical, Erlagen, Germany). Acquisition parameters: isometric voxel size = 1 × 1 × 1 mm, TR = 2,500 ms, TE = 3.31 ms, flip angle = 9°, in-plane matrix resolution = 256 × 256, number of slices = 160; field of view = 256 mm.

Resting-state fMRI (rs-fMRI) images were acquired at the same session and scanner, with the following parameters: Multi-slice T2*-weighted echo-planar images with repetition time TR = 2,500 ms; echo time TE = 30 ms; flip angle = 90 °; voxel size = 3.4 × 3.4 × 3.0; in-plane resolution = 64 × 64, number of volumes 300; number of slices = 40 (slices covered the whole brain from the cerebellum to the vertex), with interleaved ordering. The time of acquisition lasted 12 min and 39 s, and patients were instructed to keep their eyes open and to remain still during the acquisition.

2.4 | rs-fMRI data preprocessing

Preprocessing of each subject's time series of rs-fMRI volumes was performed using the FMRIB Expert Analysis Tool (www.fmrib.ox.ac.uk/fsl) (Smith et al., 2004) and in-house software and encompassed the following steps: discarding the first four (10 s) volumes to eliminate saturation effects and achieve steady-state magnetization; skull extraction using BET; slice time correction; motion correction; spatial smoothing with a full width at half maximum Gaussian kernel of 5 mm; high pass temporal filtering (0.1 Hz) for correcting low frequency signal drift. Afterward, several sources of noise were removed from the data: we regressed the six parameters obtained by rigid body correction of head motion, global signal averaged over all voxels of the brain, white matter signal averaged over all voxels of eroded white matter region, and ventricular signal averaged over all voxels of eroded ventricle regions. Next, in order to further remove motion artifacts, we performed a motion-volume censoring procedure: we calculated a composite motion score based on normative thresholds (volumes with frame-wise displacement larger than 0.5 mm, derivative variance root mean square after Z-normalization larger than 2.3 and deviation of volume intensity within the predefined gray matter mask larger then 2.3); then, we scrubbed the detected volume (volume = i) and adjacent four volumes (i-2,i-1, i, i + 1, i + 2) (Power et al., 2014; Power, Barnes, Snyder, Schlaggar, & Petersen, 2012). Finally, and because we are interested in low-frequency fluctuations of rs-fMRI signal, we applied a Butterworth filter (0.008–0.1 Hz) to the scrubbed time-series. Finally, all preprocessed rs-fMRI data were normalized to standard MNI space, using nonlinear registration (FNIRT) (ref: https://www.fmrib.ox.ac.uk/datasets/techrep/tr07ja1/tr07ja1.pdf). The registered brains were visually inspected to ensure optimal registration.

2.5 | Quality control of rs-fMRI data

To ensure optimal quality of the data after preprocessing a two-step procedure was performed. First, the number of censored motion values was evaluated as this reflects the extent of a subject's motion during scanning; a subject reached the criterion for exclusion if he/she had less than 200 volumes after censoring (8 min of rs-fMRI scanning). Mean and *SD* of volume censoring was 30 ± 7.3, and maximal volume censoring was 51. Thus, no subjects were excluded given this criterion.

Second, a functional connectivity outlier detection was implemented: for each subject the resting-state functional connectivity was calculated across 256 regions of interest (ROIs) (Power et al., 2011), then the correlation coefficients of all subjects in each group (KOA, total sample; HC) was calculated separately; finally the average of each column was calculated, representing the mean correlation coefficient across subjects of the correlation coefficient across the 256 ROIs. Subjects with low average within-group correlation (<2 *SD*s from the average in each group) were identified as outliers and excluded from the analysis. A total of four KOA patients, one HOA patient, and one HC subject were excluded given this criterion.

2.6 | Brain graph calculation and construction

Brain networks can be mathematically described as graphs, comprising sets of nodes (N, ROIs) and edges (M, or connections, here equivalent

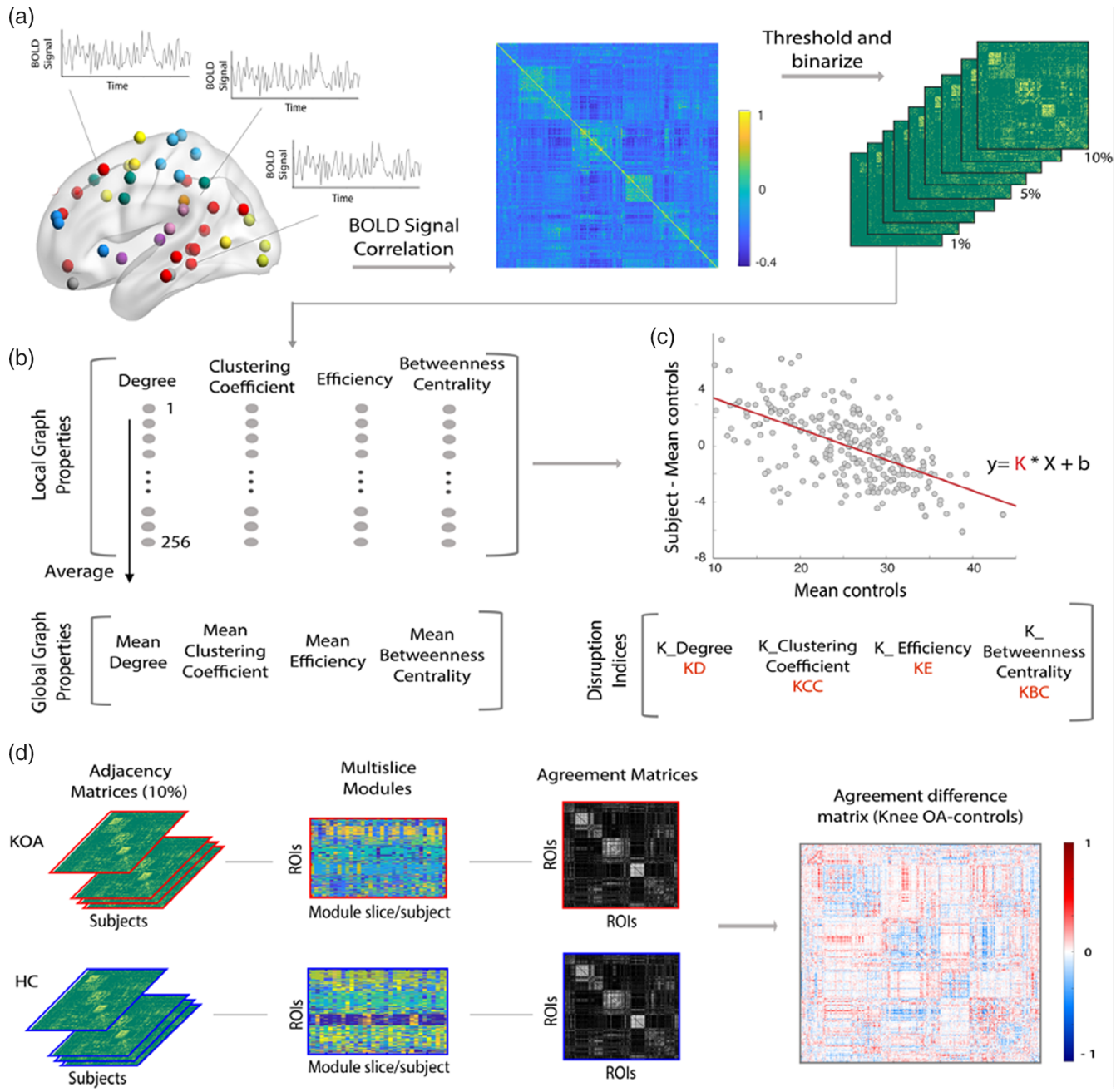

FIGURE 1 Methodological overview of the computation pipeline for global and nodal graph properties, hub disruption indices and modular reorganization analysis. (a) For each subject included in the study, brain was parcellated in 256 regions of interest (ROIs) from a 264 parcellation Scheme (eight ROIs corresponding to the cerebellum were excluded). For each ROI, blood oxygenation level-dependent signal (BOLD) was extracted as an average over voxels within 10-mm diameter spheres with center at defined peak coordinate. Next, a 256 × 256 Pearson's full correlation matrix was computed between all pairs of ROIs time-series; nine adjacency matrices were then calculated at different link densities (2–10%). (b) Graph properties (degree, clustering coefficient, efficiency, and betweenness centrality) were estimated using the Brain Connectivity Toolbox: First, we calculated nodal (local level) properties; latter, by averaging each property across the 256 ROIs we computed the corresponding global measurement. (c) Hub disruption indices were calculated for each subject as the gradient of a straight line fitted to a scatterplot of the nodal property of interest, for example, degree, minus the same nodal property on average in HC ([osteoarthritis [OA] patient—HC group], y-axis), versus the mean nodal property in the HC group (x-axis). (d) Modular reorganization was studied by calculating multislice modularity and agreement matrices separately for knee OA (KOA) and controls (agreement: 0 to 1). A difference agreement matrix was then considered, by subtracting controls agreement matrix to KOA (diff. agreement: −1 to 1). A positive entrance value (red) indicates higher likelihood for the two corresponding ROIs to be in the same module in KOA, but not in the control group. The opposite for negative entrance values (blue). Near zero values reveals pairs of ROIs that behave similarly in both groups. A permutational-based random model was created by shuffling the two groups over 1,000 times, for further statistical testing

to interregional pathways). The connectivity structure of a graph is represented by its adjacency matrix; here, an asymmetric binary matrix representing unweighted edges (van den Heuvel & Sporns, 2013). To construct the brain connectivity network for each subject, we followed the approach suggested by Mansour et al. (2016). As shown in Figure 1a, the brain was divided in 256 spherical ROIs, as described by Power et al. (2011), (original parcellation scheme with 264 regions, cerebellum was excluded from the analysis), with 5-mm radius, located at coordinates showing reliable activity across a set of tasks and displaying a plausible functional structure, spanning the cerebral cortex and subcortical structures. Blood oxygenation level-dependent (BOLD) signal of each ROI was extracted and linear Pearson's correlations were performed on time courses averaged within each ROI, generating a 256 × 256 correlation matrix for each subject. To avoid arbitrary thresholding, network analysis was conducted on fully connected graphs, with both positive and negative values. These matrices were then thresholded to generate binary undirected graphs with connection density (number of edges proportional to the maximum possible number of edges ($(N \times N - 1)/2$)) in the range 2–10%.

Following, several topological graph properties were computed using the brain connectivity toolbox (Rubinov & Sporns, 2010), as shown in Figure 1b. Under each link density, distinct topological properties were estimated at each node of each individual graph (local properties): degree (D), captures the number of connections that a node has to other nodes of the graph, and high degree nodes can be considered as centers for information integration; efficiency (E), measures how the information is propagated in the network, with high nodal efficiency reflecting higher information propagation ability; clustering coefficient (CC): represents the fraction of edges (out of all possible) that connect the neighbors of a given node, a measure of segregation; betweenness centrality (BC): represents the number of short paths between all nodes of the network that pass through a given node, a measure of influence. For each subject, at each link density, these metrics were estimated for all 256 nodes—local properties; correspondent global properties are calculated as the average across all nodes (Rubinov & Sporns, 2010).

Two other properties were estimated at a global level—modularity (Q, measure of the decomposability of a graph into several sparsely interconnected structures) and small-worldness (evaluates the network organization compared to a matched random graph). Modularity was calculated using the Louvain community detection algorithm averaged over 100 repetitions (Rubinov & Sporns, 2010). Small-worldness, based on the tradeoff between clustering and global efficiency (Humphries & Gurney, 2008), is calculated as: $((\text{clustering}_J/\text{clustering}_{\text{random}})/(\text{efficiency}_{\text{random}}/\text{efficiency}_J))$, where a network is deemed a "small-world" if the ratio >2.

Differences in global graph properties between groups (KOA and HC) were computed using repeated measures ANCOVA (densities 2–10%), controlling for the effects of age and gender.

2.7 | Graph topological hub disruption indices

We estimated the hub disruption index, *K*, for the different graph properties computed before: disruption index for degree (K_D), efficiency (K_E), clustering coefficient (K_{CC}), and betweenness centrality (K_{BC}), following methods described by Achard et al. (2012). This measure allows us to summarize the abnormal profile of nodal connectivity and topological metrics of an individual subject in relation to the normative topology of the HC group. Figure 1c depicts the computation process. For each subject, we first subtract the HC group mean nodal degree from the degree of the corresponding node in a given individual; next, we plot this individual difference against the HC group mean. The hub disruption index, *K*, is then defined as the gradient of a straight line fitted to the scatter plot following the linear regression ($y = K \times x + b$), where *y* = nodal degree of the subject—mean nodal degree of HC; *x* = mean nodal degree of HC; *b* = residual or intercept of the regression. After computing the individual disruption indices, significant differences between groups in K_D, K_E, K_{CC}, and K_{BC} were calculated at 5% link density using an ANCOVA with age and sex as covariates of no-interest. We additionally performed a repeated measure ANCOVA accounting for all link densities (2–10%), while controlling for age and sex. Relationships between *K* measures and clinical parameters were estimated using linear partial correlations, controlling for the effect of age and sex. Given the multiplicity of measures (4 hub disruption indices; 12 clinical parameters), FDR correction for multiple comparisons was applied at $\alpha = .05$.

In order to investigate the contributions of regional perturbations to *K* measures, we recomputed individual *K* indices after random removal of 80% of nodes. Pearson's correlation with the original *K* measures was then examined.

2.8 | Characterization of hub disruption—Nodal statistical analysis

Nodal degree properties were further studied in an effort to better characterize the particular patterns underlying these global changes (K_D), and better examine their relationship with clinical properties of the disease. We applied two distinct strategies:

1. We identified nodes that showed a difference in mean degree (*y*, nodal degree of OA group—nodal degree of HC) greater than ±2 *SD* from the mean difference value; we used permutation-based testing to estimate statistical significance of the between group differences for identified ROIs by randomly assigning subjects to two groups, arbitrarily defining one as the reference and estimating the nodal differences between groups. We repeated this process 10,000 times to sample the null distribution of the nodal group mean difference. After identifying topmost disrupted cortical nodes, we studied their association with clinical parameters of the disease. We then linearly modeled each clinical variable of interest with the identified nodes, applying a stepwise forward

and backward selection method, with α-to-enter set at .05 and α-to-remove at .10. For all regression models, assumptions of linearity, independence of observations, homoscedasticity, and absence of multicollinearity were met, and residuals were approximately normally distributed.

2. In a more exploratory form, and given that *K* permeates the whole-brain network, implicating that the disruption is not merely driven by functional changes to specific regions or pathways, we studied the relationship of whole-brain nodal degree and pain intensity in OA using a L1/L2 regularized linear regression (i.e., elastic net) (Zou & Hastie, 2005). This method allows us to remove predictors with low influence on the outcome while regularizing for enhanced generalization. The coefficients of the nonrelevant features are shrunk toward zero, simplifying the model and reducing overfitting. Using the KOA discovery group, we applied a linear regression with a regularization penalty α = .5, to predict pain intensity (NRS), based on the nodal degree properties of all 256 ROIs. Ten-fold cross-validation was used to choose the hyperparameter, λ (shrinkage parameter), that minimized mean squared error (MSE) over a default grid size of 100; the hyperparameter λ that generated the smallest MSE was selected for the final model (Friedman, Hastie, & Tibshirani, 2010). Performance of the model was assessed in the discovery and validation cohorts. All degree nodal properties were adjusted for age and sex prior to these analyses, by linearly regression and adding the adjusted fitted values and residuals for each observation.

2.9 | Modular reorganization analysis

We studied brain networks at an intermediate scale of organization—community structure or modularity—following methods described by Mano et al. (2018)); this approach is based on community detection in multislice networks (Mucha, Richardson, Macon, Porter, & Onnela, 2010) and focuses on detecting differences in brain network modularity between groups (OA, HC) by calculating a measure of consensus modularity pattern – modularity agreement matrix (AM). Analytical steps are depicted in Figure 1d. First, for each group separately (OA discovery, HC), we use a *categorical* multislice modularity algorithm (Jeub, Bazzi, Jutla, & Mucha, 2011), where the same node is coupled among all subjects (slices), with 10% link density matrices. Coupling strength (ω = 0.1) and modularity resolution (γ = 1.5) are free parameters that were a priori defined based on previous research (Mano et al., 2018; Mucha et al., 2010). This allows us to create a single symmetric AM representing each group, where each entry has a value within [0,1], representing the agreement between pairs of nodes. As the number of subjects in each group was different (OA = 46; HC = 35), and the modularity estimation is a probabilistic procedure, we calculated the AMs 1,000 times, selecting randomly 34 patients for each group, and computed the average across repetitions. Next, having one mean AM per group, we computed the agreement difference matrix: <OA AM> – <HC AM>. Here, values range from [−1,1]; large negative values correspond to nodes that are recurrently part of the same modules in controls but not in the OA group, large positive values represent the opposite. Values close to 0 represent nodes with the same behavior, either with high agreement or low agreement in both groups. In order to attain an overall metric of reorganization per region, the absolute sum of positive and negative contributions was computed per node—nodal modular reorganization.

Finally, following Mano et al. (2018), in order to evaluate the statistical significance, we performed a permutational analysis, were we randomly resampled pain and control subjects into two groups and repeated the full analysis—also 1,000 times. Based on the proportion of times the resampled nodal modular reorganization exceeded the correct value we calculated one-sided *p*-values and used a threshold of $p < .01$ to consider significant nodal modular reorganization values.

2.10 | Analysis validation

We aimed to validate the principal findings from the discovery cohort, specifically determining the hub disruption index significance, determining the hub status of disturbed regions and relationship with clinical properties; we also validated the machine learning algorithm applied for pain intensity prediction and modular reorganization in the KOA and HOA validation groups. Connectivity matrices for the validation groups were created and thresholded using identical procedures as described above. Contrasts requiring HCs were assessed with the same 35 HC participants from the discovery data set.

2.11 | Software/code

Analysis was performed using MATLAB 2019.b (MATLAB and Brain Connectivity Toolbox release 2019a, The MathWorks, Inc., Natick, MA) and tools from the brain connectivity toolbox (Rubinov & Sporns, 2010). Code for modularity reorganization analysis was adapted from Mano et al (http://doi.org/10.5281/zenodo.1183399) (Mano et al., 2018). Brain figures of ROI and functional connectivity networks were visualized on a surface rendering of a human brain atlas with BrainNet Viewer (http://www.nitrc.org/projects/bnv/).

3 | RESULTS

3.1 | Demographic and clinical characteristics

No significant differences for gender, BMI, or smoking habit were seen between the KOA and HC groups (Table 1). However, the HC group had a significantly lower mean age ($t = -9.27$; $p < .001$), supporting the importance of controlling for this variable in further analyses. Social-cultural variables (educational level; habitation; marriage status) did not show significant differences between groups ($p > .05$ for all). Comparing the validation samples (KOA and HOA) with the KOA discovery sample (demographic, pain related, and

TABLE 1 Demographic and clinical characteristics of osteoarthritis patients (discovery group) and controls. To identify demographic difference between groups ANOVA and *t* tests were performed for continuous data. Chi-square tests were performed for categorical data

	Controls (*n* = 35)	Knee OA (discovery group; *n* = 46)	*p*-Value
Age (years), mean, *SD*	59.5 ± 7.91	65.3 ± 7.41	.001**
Sex (female), *n*, %	20; 57.1%	30; 65.2%	.49
BMI (kg/m^2), mean, *SD*	28.2 ± 4.57	30 ± 4.3	.07
Smoking, *n*, %	7; 20%	4; 8.7%	.19
Education, *n*, %			.09
Primary education	20; 57.1%	34; 73.9%	
Secondary education	8; 22.9%	8; 17.4%	
Postsecondary education	7; 20%	4; 8.7%	
Habitation, *n*, %			.78
Alone	6; 17.4%	10; 21.7%	
Cohabitation	29; 82.8%	36; 78.3%	
Marital status, *n*, %			.28
Married	26; 74.3%	30; 65.2%	
Never married	3; 8.6%	3; 6.5%	
Divorced	2; 5.7%	4; 8.7%	
Widowed	4; 11.4%	9; 19.6%	

Note: $p < .01$.
Abbreviations: ANOVA, analysis of variable; BMI, body mass index; OA, osteoarthritis.

behavioral data presented in Table 2), both KOA groups were balanced regarding demographic and clinical outcomes; HOA patients presented shorter pain duration, worse radiographic severity and a lower neuropathic pain score; this group had a younger mean age and a significantly higher number of male subjects.

3.2 | Global connectivity and network topology properties are not altered in KOA

There were no statistically significant differences between groups (KOA vs. HC) on global measures of network topology as depicted in Figure S1. At every density of functional connections tested (1–10%), functional networks had similar clustering coefficient, global efficiency, betweenness centrality, and modularity, measures reflecting distinct network properties (segregation, integration, centrality, community structure). Both groups' networks exhibited characteristic small-world organization (high clustering combined with high global efficiency). Hence, despite the clinical differences, global network topological measures were conserved in KOA patients when contrasting to HC.

3.3 | Disruption of hub organization in OA patients

As previous research in diverse clinical conditions has demonstrated that even though global properties of a network may be preserved, nodal properties are reorganize (Achard et al., 2012), we queried if local level disruptions were present in OA patients. We calculated hub disruption indices, a metric that allows to summarize and visualize the pattern of nodal abnormalities. Figure 2a illustrates the results of this metric at group level for degree; rank order for nodal degree is disrupted, with some nodes showing abnormal decrease and others abnormal increase in degree properties. This disruption pattern is summarized by the gradient of a straight line fitted to the data (K_D = −0.18; $p < .001$). Other topological measures exhibited similar results for group-averaged maps (Figure S2). Next, we assessed hub disruption at an individual level, for all our subjects; Figure 2b shows between-group differences (HC; OA) of the individually estimated indices; these were statistically significant ($p < .001$) at 5% link density networks, and this result was further validated across other graph connection densities (Figure S3). The four hub disruption indices were significantly correlated with each other, and the strength of correlation was higher overall in HCs than in KOA patients (Figure 2c).

We then assessed the influence of regional perturbations to the magnitude of the disruption indices. At 5% link density networks, individual *K* values were recomputed after random removal of 80% of the nodes (K''), and this process repeated 100 times. Mean K'' was significantly correlated with K across all topology measures ($p < .002$; *r* values: .58–.81) (Figure S4). These results imply rank order disruption permeates the whole brain network and is not exclusively a product of specific regional perturbations.

3.4 | Hub disruption indices do not strongly associate with clinical properties of OA

Following previous research, where key clinical properties of a disease were reflected in the hub disruption indices (De Pauw et al., 2020; Itahashi et al., 2014), we studied the relationship

TABLE 2 Demographic and clinical characteristics of osteoarthritis patients: discovery and testing groups

	Knee OA (discovery group; *n* = 46)	Knee OA (testing group; *n* = 45)	*p*-Value	Hip OA (testing group; *n* = 23)	*p*-Value
Age (years), mean, *SD*	65.3 ± 7.41	65.78 ± 5.6	.75	59.5 ± 7.41	.007*
Sex (female), *n*, %	30; 65.2%	38; 84%	.035*	8; 40%	.008*
BMI (kg/m^2), mean, *SD*	30 ± 4.3	30.87 ± 5.54	.41	28.8 ± 3.36	.08
Education, *n*, %			.15		.76
Primary education	34; 73.9%	38; 84.4%		14; 70%	
Secondary education	8; 17.4%	6; 13.3%		4; 20%	
Postsecondary education	4; 8.7%	1; 2.2%		2; 10%	
Smoking, *n*, %	4; 8.7%	3; 6.7%	.71	2; 8.7%	1.0
Habitation, *n*, %			.59		.52
Alone	10; 21.7%	7; 15.6%		3; 13%	
Cohabitation	36; 78.3%	38; 84.4%		20; 90%	
Marital status, *n*, %			.19		.57
Married	30; 65.2%	35; 77.8%		16; 70%	
Never married	3; 6.5%	2; 4.4%		2; 8.7%	
Divorced	4; 8.7%	3; 6.7%		2; 8.7%	
Widowed	9; 19.6%	5; 11.1%		3; 13%	
NRS, mean, *SD*	6.48 ± 1.42	6.8 ± 1.93	.37	6.2 ± 1.59	.21
DN4, mean, *SD*	2.7 ± 2.26	2.9 ± 2.15	.55	1.82 ± 1.49	.025*
HADS_D, mean, *SD*	7.9 ± 3.93	6.7 ± 4.33	.15	5.8 ± 4.45	.46
HADS_A, mean, *SD*	8.6 ± 4.07	9 ± 5.71	.71	6.5 ± 4.19	.07
HOOS_S, mean, *SD*	60.5 ± 19.31	61.9 ± 21.8	.74	50 ± 16.02	.023*
HOOS_P, mean, *SD*	63.6 ± 16.52	64.2 ± 16.43	.87	55 ± 17.75	.063
HOOS_ADL, mean, *SD*	61.4 ± 15.84	64.4 ± 17.54	.38	57.9 ± 18.3	.15
HOOS_SR, mean, *SD*	91.5 ± 17.63	91.6 ± 15.75	.97	83.15 ± 19	.054
HOOS_QL, mean, *SD*	78.6 ± 16.37	80 ± 17.46	.68	70.6 ± 20.4	.051
PCS, mean, *SD*	19.1 ± 12.33	23.3 ± 15.75	.15	18.1 ± 11.01	.16
Pain duration (years), mean, *SD*	6.8 ± 5.45	8.5 ± 6.44	.61	5.03 ± 4.2	.021*
Radiographic KLS, *n*, %			.33		<.001*
Grade 1	1; 2.2%	—		—	
Grade 2	12; 26.1%	9; 20%		—	
Grade 3	21; 45.7%	22; 48.9%		5; 21.7%	
Grade 4	12; 26.1%	14; 31.1%		18; 72.2%	
STUG, mean, *SD*	13.12 ± 3.93	13.9 ± 4.8	.41	14.26 ± 4.46	.77
6MWT, mean, *SD*	257.8 ± 75.5	272.4 ± 68.93	.33	271.7 ± 99	.9

*p<.05.

Abbreviations: 6MWT, 6-min walking test; ADL, activities of daily living; ANOVA, analysis of variable; BMI, body mass index; DN4, Douleur Neuropathique en 4 questions; HADS, Hospital anxiety and Depression Scale; HOA, hip OA; HOOS, Hip Injury and Osteoarthritis Outcome Score; KL, Kellgren–Lawrence scale; KOA, knee OA; KOOS, Knee injury and Osteoarthritis Outcome Score; NRS, numeric pain rating; OA, osteoarthritis; PCS, Pain Catastrophizing Scale; QoL, quality of life; SR, sports and recreation; STUG, stand up and go test.

Note: p-Values represent statistical tests between KOA discovery groups and the holdout testing samples; KOA testing sample showed a significantly higher number of females, no other differences were captured; HOA group was significantly different regarding age, gender, DN4 scale, pain duration, and radiographic severity (KLS). ANOVA and *t* tests were performed for continuous data. Chi-square tests were performed for categorical data.

between *K* indices and numerous clinical properties of the disease: pain intensity and quality, anxiety and depression, pain catastrophizing, disability, and motor skill tests. We calculated Pearson's partial correlations, controlling for age and sex. As shown in Figure S5, only K_{CC} presented a significant association with pain catastrophizing (r = .3, p = .043) and KOOS symptoms subscale (r = .33, p = .025); however, these did not survive FDR correction for multiple comparisons (at p = .05).

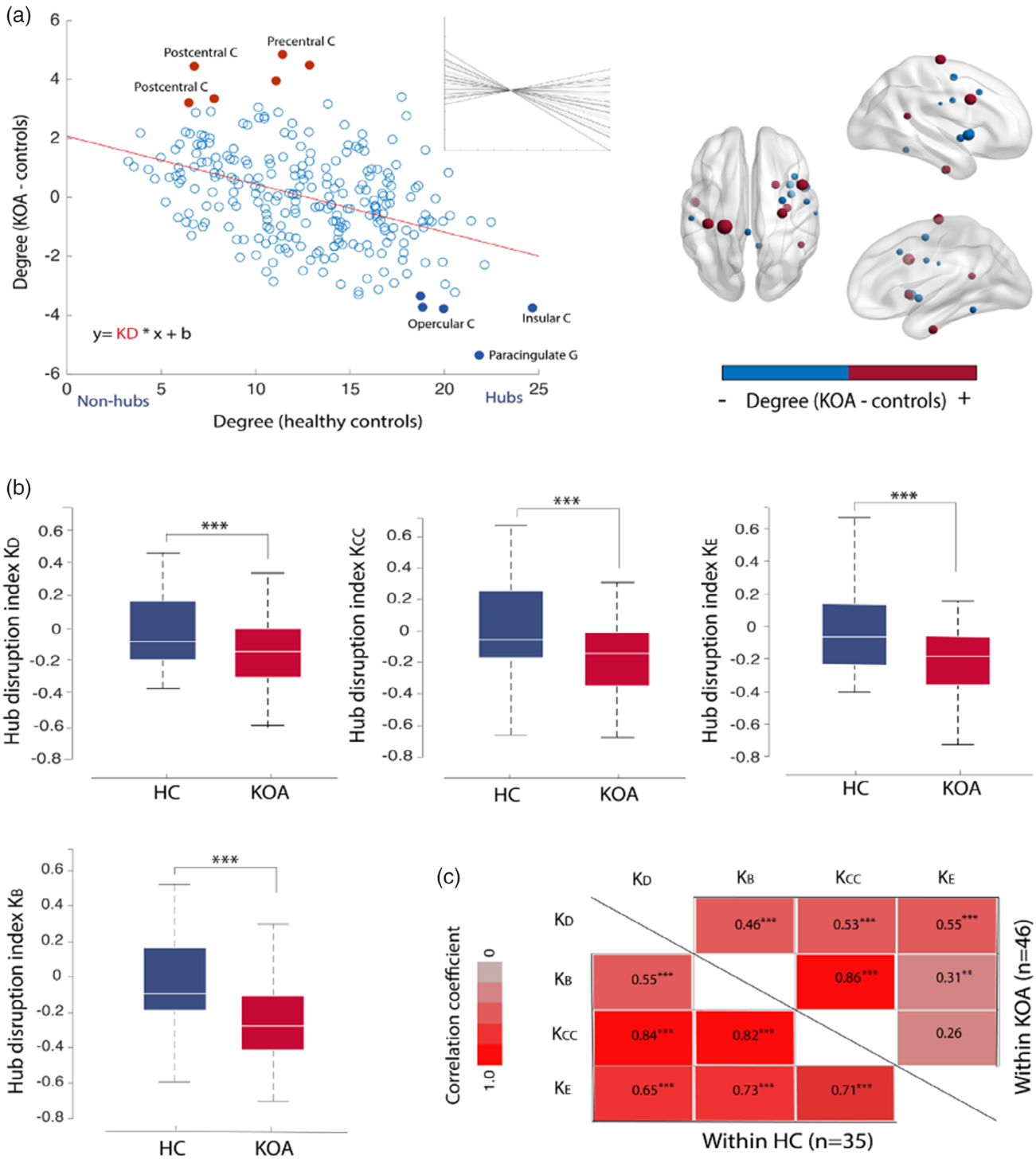

FIGURE 2 Disruption of functional network hub organization in osteoarthritis (OA) patients. (a) Group hub disruption index calculation for degree (K_D) at 5% link density: for each node (256 regions), the mean degree in the control group (x-axis) is plotted against the mean nodal difference between groups (KOA—control) (y-axis). Red dots represent nodes that are non-hubs in controls but show an abnormal increase in degree in KOA patients: precentral and postcentral gyrus; filled blue dots represent nodes that are typically hubs in healthy controls and show a reduction in degree for KOA: insula; paracingulate gyrus; opercular cortex. The hub disruption index corresponds to the slope of the line fitted to the data (red line), $K_D = -0.18$, $p < .001$. Insert shows individual K_D values. On the right, brain graphical representation of the difference in mean degree between KOA and controls, top 10% most different regions of interest (ROIs) are depicted, red denotes abnormally increased degree and blue abnormally decreased degree in KOA compared to healthy controls. (c) Boxplots of the subject-wise estimated hub disruption indices for the control group (blue) and KOA (red) at 5% link density. Between-group differences in K_D, K_{BC}, K_E, and K_{CC} were deemed significant by an ANCOVA ($p < .001$), while controlling for age and gender. Corresponding results for the same measures different graph connection densities are shown in Figure S2. (d) The four hub disruption indices here significantly correlated with each other (Person's r), and the strength of correlation was overall higher in healthy controls than in KOA patients. ***$p < .001$; **$p < .01$; HC, healthy control; KOA, knee osteoarthritis

3.5 | Localized hub topology alterations in OA and its relationship with clinical endpoints

To better characterize the particular patterns underlying global changes rendered in the *K* metrics, we explored changes at a nodal level by selecting degree, which is the simplest and most commonly used means of identifying hubs (Power, Schlaggar, Lessov-Schlaggar, & Petersen, 2013) and upon which many other graph properties are based. We started by identifying nodes displaying between group degree differences greater than ±2 *SD* (Figure 3a; Table 3), hereby categorized as top disrupted nodes. Statistical significance of the differences was analyzed with permutational testing. Moreover, significant differences were validated in a subset if nodes in the knee and hip holdout samples (Figure 3b; Table 3): two nodes localized in the insular cortex and one node located in the postcentral gyrus showed consistent loss of hubness in KOA patients; abnormally increased hubness was reliably observed in the precentral gyrus and postcentral gyrus (both nodes assigned to the sensorimotor [SM] network) in KOA/ HOA and temporal fusiform/ parahippocampal gyrus in KOA patients compared to HC. Hence, there was a gain in degree in primary motor and sensory nodes that was accompanied by a loss of degree in characteristic associative regions in KOA.

Given the consistent disruption of nodal topology, we examined if hubness changes in these regions reflected clinical properties of KOA. Hierarchical multiple regression models were built for each clinical variable of interest (i.e., pain duration; pain intensity; HADS anxiety; HADS depression; PCS; KLS; 6MWT; TUG; DN4; and KOOS subscales). Two models yielded statistical significance: worse ratings in KOOS/Sports and recreation subscale was related to loss of hubness in the postcentral gyrus ($F(46,44) = 6.98$, Adj $R^2 = .11$, $p = .001$; $s\beta = -.65$); worse scores in TUG were related also to loss of hubness in these regions ($F(46,45) = 6.42$, Adj $R^2 = .1$, $p = .014$; $s\beta = -.2$). These associations were not validated in the KOA hold out sample (linear regression for selected nodes: KOOS/SR: $F(45,43) = 0.2$, $p = .65$; TUG: $F(45,43) = 0.4$, $p = .56$), and were not tested in the HOA sample (as the identified regions were not validated in the KOA sample).

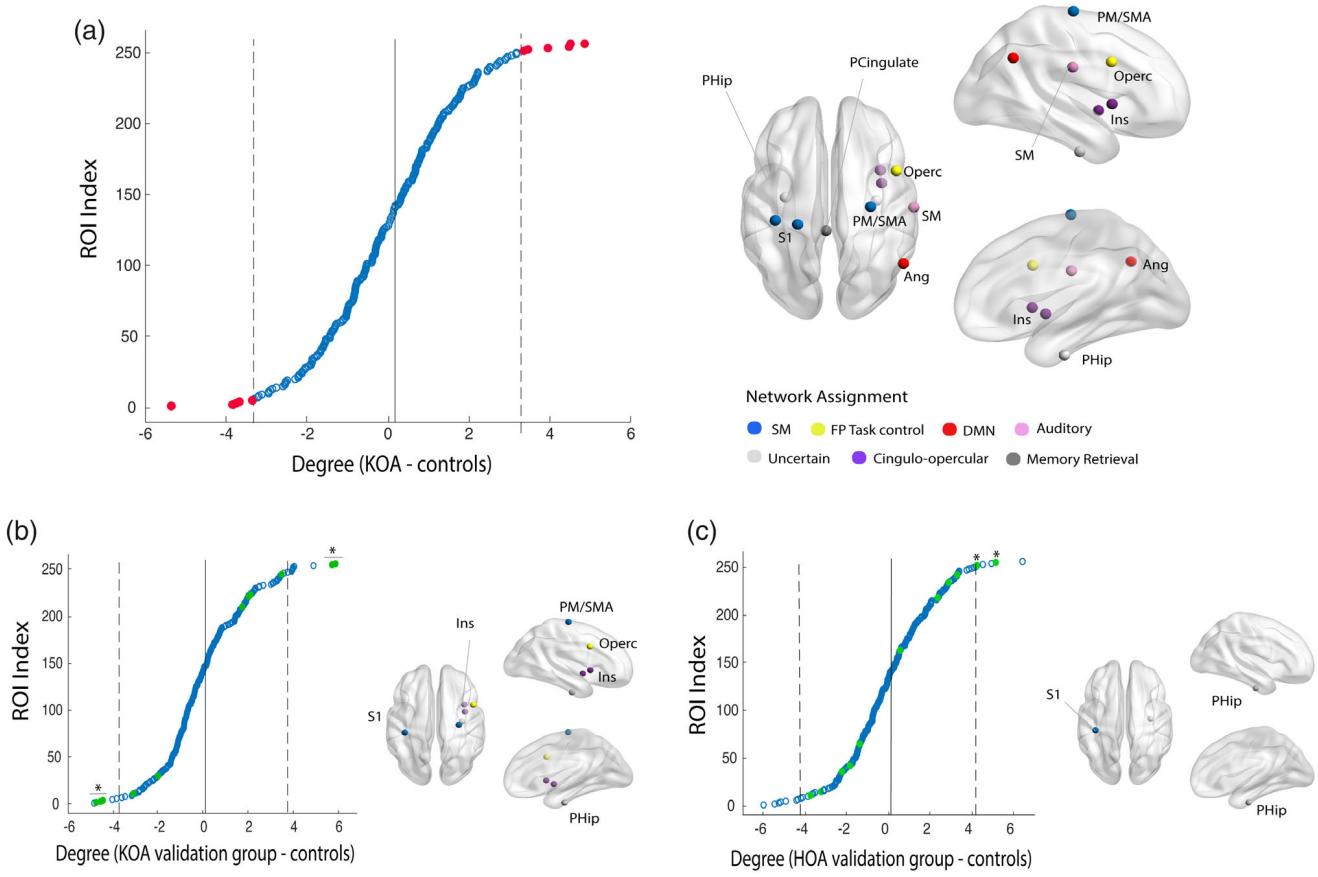

FIGURE 3 Hub topology is altered in knee OA (KOA): differences in hub status between osteoarthritis (OA) patients and healthy controls. (a) Mean nodal difference between groups (KOA—control), organized by score and thresholded at ±2 *SD* (gray lines) from the mean difference (red dots) and graphic representation of selected nodes. (b) Validation of nodal disruption in KOA hold out sample: 6 out of 11 regions were validated: sensory-motor regions and parahippocampal gyrus present a significant degree gain and insula/operculum, normal hub nodes, show an abnormal reduction of degree in KOA patients. (c) Hip OA group, validates uniquely the increase in degree for S1 and parahippocampal gyrus. FP, frontoparietal cortex; DMN, default mode network; ROI, region of interest; S1, primary somatosensory cortex; SM, sensory-motor cortex. *$p < .05$, permutational test

TABLE 3 Differences in hub status between OA patients and healthy controls

Difference in mean degree	Coordinate in MNI space	Harvard-Oxford cortical and subcortical structural atlas	Network assignment[a]	*p*-Value[b] 10,000 permutations
(Patient < control)				
5.36	(−2, 35, 31)	Paracingulate cortex, L (68%)	Memory retrieval	< .001
3.77	(52, −59, 36)	Lateral occipital cortex, R (51%)	DMN	.027
3.75	(36, 10, 1)	Insular cortex, R (47%)	CO task control	.04[c]
3.72	(59, −17, 29)	Postcentral gyrus, R (45%)	Auditory	.071
3.35	(37, 1, −4)	Insular cortex, R (53%)	CO task control	.025[c]
(Patient > control)				
4.84	(29, −17, 71)	Precentral gyrus, R (35%)	SM	.006[c]
4.49	(−38, −27, 69)	Postcentral gyrus, L (51%)	SM	.009[c,d]
4.45	(−31, −10, −36)	Temporal fusiform gyrus, L (32%); parahippocampal gyrus, L (29%)	Uncertain	.01
3.95	(47, 10, 33)	Precentral gyrus, R (37%)	FP task control	.022
3.41	(−23, −30, 72)	Postcentral gyrus, L (36%)	Uncertain	.044
3.35	(33, −12, −34)	Temporal fusiform gyrus, R (40%), parahippocampal gyrus R (23%)	Uncertain	.026[c,d]

Abbreviations: CO, cingulo-opercular; DMN, default mode network; FP, frontoparietal; MNI, Montreal Neurological Institute; OA, osteoarthritis; SM, sensory-motor.

Note: Regions identified in Figure 3. Peak coordinates (x,y,z) are displayed according to MNI atlas, labels accordingly to the Oxford-Harvard Structural Cortical Atlas (http://fsl.fmrib.ox.ac.uk/fsl/fslwiki/Atlases).

[a]Network assignment in accordance with Figure 3.

[b]Statistical significance of difference was tested under 10,000 permutational tests.

[c]Nodal differences were further validated in the KOA holdout sample at p<0.05.

[d]HOA group at $p < .05$ (Figure 3).

3.6 | Whole brain distributed changes in degree predict pain intensity in KOA

Given that the top disrupted nodes partially explained only two clinical properties of the disease, that the association was weak and did not generalize and, moreover, given that K_D permeates the whole brain network, we hypothesized that smaller, distributed changes in nodal reorganization could explain clinical properties of OA. We limited the analysis only to clinical pain intensity (NRS scale); we applied a linear regression using all 256 nodal degree properties as predictors; to remove predictors with low impact to the outcome while improving generalization, we used an elastic net regularized regression. As shown in Figure 4a,b, the combination of 12 brain nodal degree properties, both with increased (i.e., inferior temporal gyrus; paracingulate cortex; insula; lateral occipital cortex) and decreased degree (i.e., putamen; operculum; middle frontal gyrus; parahippocampus) were strong predictors of pain intensity in KOA (Figure 4c predicted/real NRS Pearson's $R = .83$); this result was validated in the KOA hold out sample (predicted/real NRS Pearson's $R = .57$), as shown in Figure 4d. and replicated in HOA (predicted/real NRS Pearson's $R = .93$), Figure 4e. Thus, we show that small, distributed changes in network information-sharing map pain intensity in KOA, and this result is valid and generalizes to HOA.

3.7 | Modular reorganization affects mainly regions classified in the frontoparietal and cingulo-opercular networks

To study brain network reorganization at an intermediate level, we evaluated modularity. Modularity assesses how well a network can be divided into a set of sparsely interconnected subnetworks or modules. We hypothesized that despite the fact that global modularity (Q) is not different between groups (Figure S1); the modular structure could be perturbed in OA, with regard to the identity of nodes making up the different modules.

Closely following methods recently described (Mano et al., 2018), we estimated a modularity consensus or AM for each group (OA, HC), and computed the difference between group matrices, generating the agreement difference matrix (Figure 5a). Here, each entry takes a value from 1 (red), to −1 (blue). Large positive values identify nodes that appear more commonly in the same network in pain patients than in controls and large negative values relate to pairs of nodes that are less likely to be part of the same network in those patients. Entries close to zero identify regions that have the same behavior in both groups. By creating an index per node, the absolute sum of values per row, defines its overall modular reorganization. Figure 5b represents the following steps, where statistical significance for modular reorganization indices was tested against a null model. Figure 5c illustrates

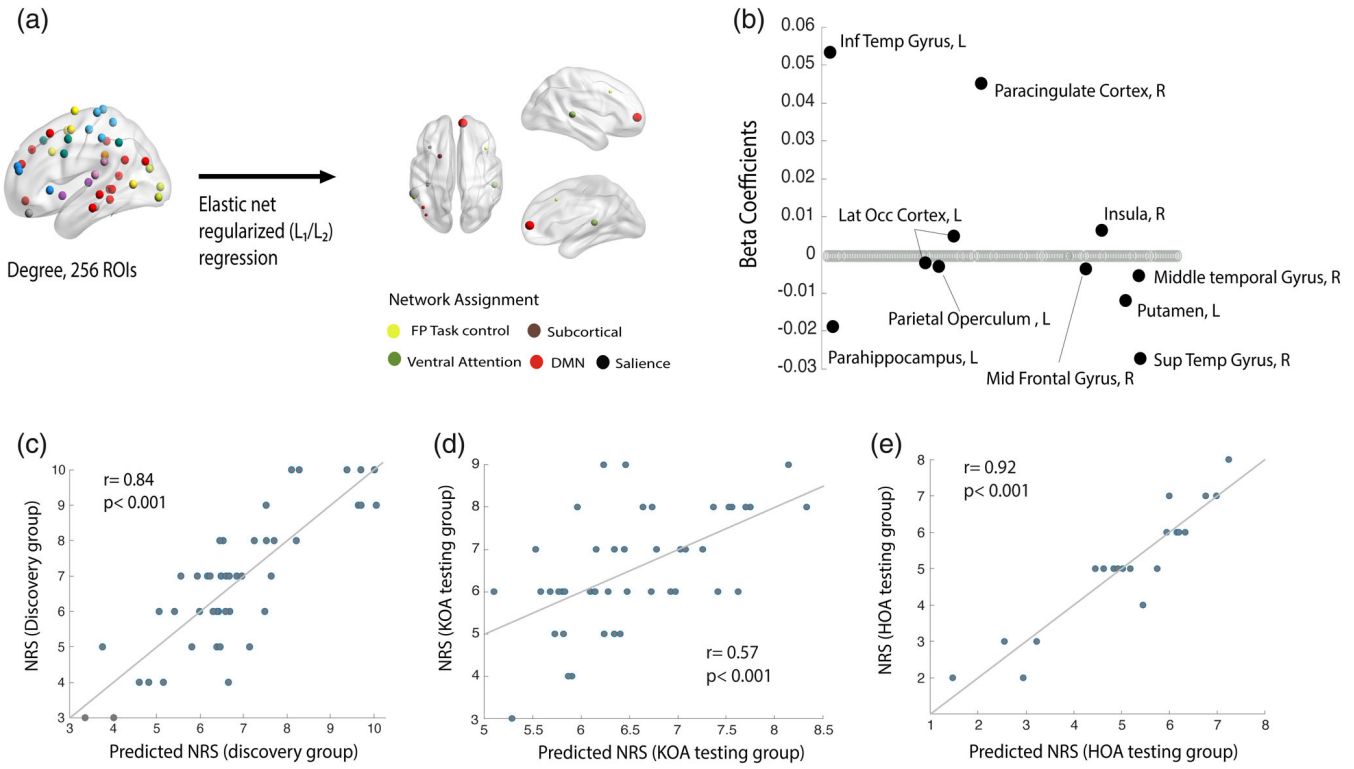

FIGURE 4 Multinodal distributed degree properties predict pain intensity numeric pain rating (NRS) in osteoarthritis (OA) patients. (a) Graphical representation of the linear regression model using Elastic net regularization and variable selection with penalty weight (α) of .5 and regularization parameter (λ) choice via a 10-fold cross validation. Brain nodes depicted correspond to regions predicting pain intensity; node size reflects the weight (B-coefficients) in the regression model. This is also illustrated in (b) the majority of nodes has regression coefficients set to zero, indicating that the corresponding variables are not contributing to the model. Nonzero regression coefficients identify the predictive features and indicate the weight and direction of degree change in relation to the response variable: that is, higher levels of pain (NRS) relate with lower degree in parahipoccampal gyrus, putamen, and superior temporal gyrus and higher degree in paracingulate cortex and inferior temporal gyrus. (c) Features selected in the elastic net regression predicted the magnitude of response and (d) validate in the hold out knee OA (KOA) and (e) hip OA samples: high correlation value between predicted and actual NRS scores in the KOA discovery group (Pearson's r = .84, p < .001) KOA holdout testing group (r = .57, p < .001) and HOA holdout testing group (r = .92, p < .001)

the regions after thresholding at p-value of .01. Nodes showing larger modular reorganization were located mainly in the middle frontal gyrus, part of the frontal–parietal task control network. Supramarginal gyrus, angular gyrus and regions located at the cingulate cortex, insula and operculum were also identified. When validating our findings in the KOA and HOA holdout groups, regions located in the frontoparietal and cingulo-opercular network were validated (Table 4).

4 | DISCUSSION

Using a large sample of OA patients, together with a robust methodology, we sought to study brain functional network properties and their relation to the clinical properties of the disease. We demonstrate for the first time that (a) OA patients have a global reorganization of nodal centrality properties while preserving network global topology, as captured by the hub disruption indices; (b) at a finer scale, we could identify a shift in the hierarchy of hub nodes. Primary sensory, motor, and parahippocampal regions become hubs; there is a large difference in connectivity between healthy subjects and OA patients, where these regions show high connectivity in KOA. On the other hand, the insula, a multimodal association area loses its centrality properties in KOA. (c) At a subnetwork, or community level, we showed that while brain networks can be equally well decomposed, the modular identity of multiple regions is rearranged in OA, in particular middle frontal gyrus, insula, and cingulate cortex. Finally, (d) we found that the defining feature of OA, pain intensity, is related to the interrelationship of the nodal degree of multiple brain regions in KOA and this result generalized to HOA.

4.1 | Global topological properties

Global topological network properties were conserved in OA patients, as observed in earlier studies of chronic pain (De Pauw et al., 2020; Mansour et al., 2016). As Achard et al. (2012) expound, given that human brain networks have qualitatively similar global properties to those of other small world networks (Eguíluz, Chialvo, Cecchi, Baliki, & Apkarian, 2005), the preservation of these properties even in disease is expected. As long as the general architecture of the network is

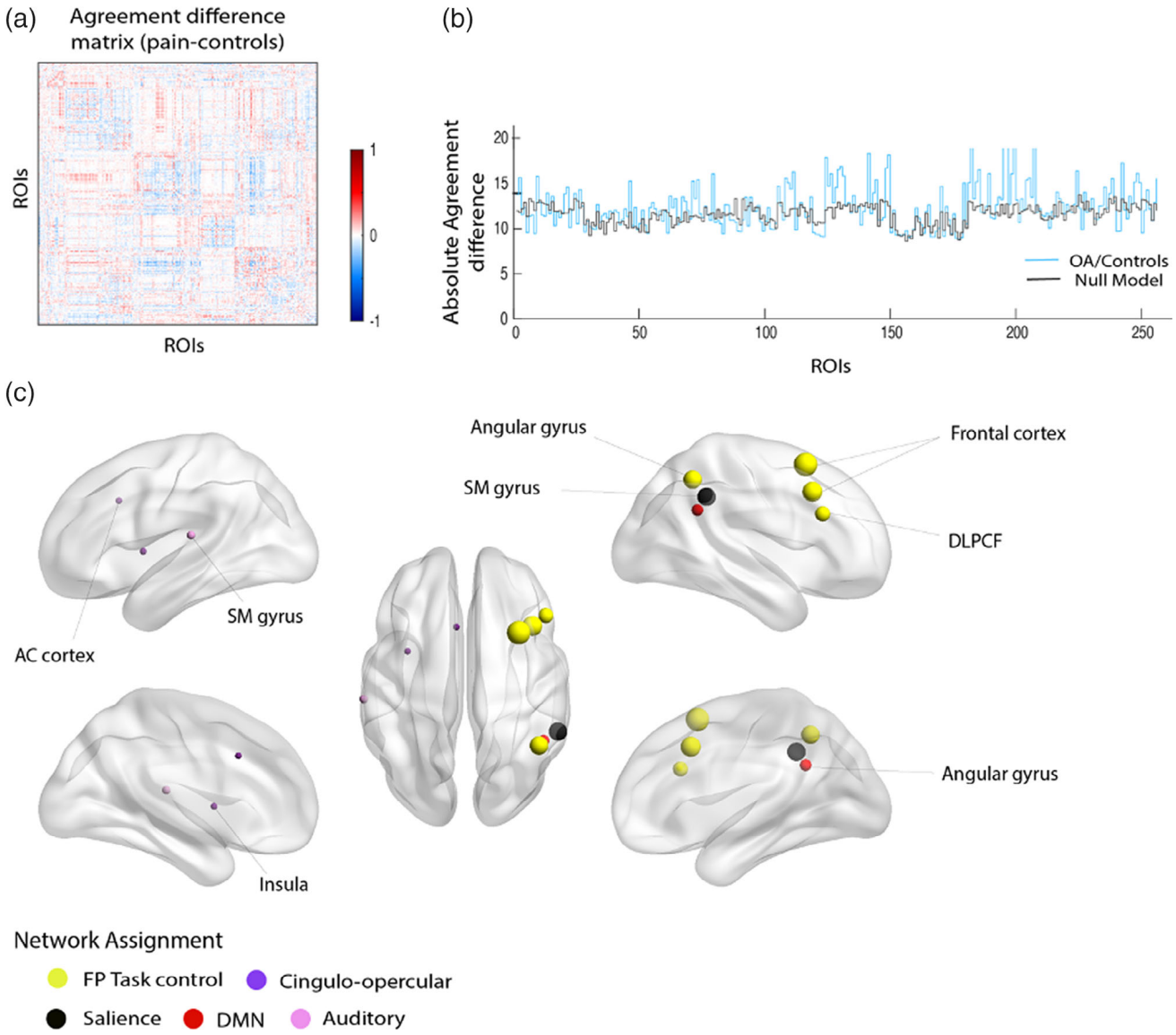

FIGURE 5 Modular reorganization in osteoarthritis (OA) involves predominantly nodes assigned the frontoparietal and cingulo-opercular task control networks. (a) Agreement difference matrix obtained from the difference between the modular agreement matrix from OA and control groups. Positive (red) values reflect pairs of nodes that are estimated to appear more commonly in the same module in OA patients, and negative (blue) values represent pairs of nodes that are estimated to appear less commonly in the same module in OA. White value represents regions of interest (ROIs) that has the same behavior in both groups. (b) Blue line shows overall modular reorganization for each node as the sum of both positive and negative values for each node (sum of absolute value per row in (a)), meaning the largest value, the greater reorganization. To statistically evaluate these values, we performed a permutation test of sum reorganization estimation (null model, gray color), yielding one-side *p*-values across all ROIs. (c) Representation of statistically significant nodes showing modular reorganization at a threshold of $p < .01$; size reflects magnitude of the absolute agreement difference

preserved, its global topological properties can be conserved, even when the system undergoes large changes.

4.2 | Hub disruption indices

Consistent with the latter concept, we found local disruption in the order of importance of cortical nodes, calculated globally as hub disruption indices (*K*), both at the group and individual level. The local nodal connectivity properties counterbalances the increases and decreases throughout the brain resulting in an overall shift (*K*), while the overall mean property remains invariant (Achard et al., 2012). Interestingly, the magnitude of this disruption, about 20% when compared to the normative state, is similar to that seen in other chronic pain conditions (Mansour et al., 2016). In comatose patients, this shift is much larger (80%) (Achard et al., 2012) reflecting a more dramatic rebalancing of local connectivity.

TABLE 4 Brain regions showing modular reorganization after permutational-based analysis against a random model, at a cut-off threshold of $p < .01$

Absolute agreement difference (+/−)	Coordinate in MNI space	Harvard-Oxford cortical and subcortical structural atlas	Network assignment[a]	*p*-Value[b] 1,000 permutations
23.28 (10.27, −13.01)	(44, −53, 47)	Angular gyrus, R (40%)	FP task control	<.001
26.25 (12.84, −13.39)	(32, 14, 56)	Middle frontal gyrus, R (42%)	FP task control	<.001[c,d]
23.35 (10.14, −13.21)	(55, −44, 37)	Supramarginal gyrus, R (43%)	Salience	<.001
21.45 (10.59, −10.87)	(48, 25, 27)	Middle frontal gyrus, R (39%)	FP task control	.002
24.31 (10.56, −13.76)	(39, 18, 39)	Middle frontal gyrus, R (50%)	FP task control	.004[b]
17.15 (8.14, −9.01)	(−60, −25, 14)	Parietal operculum cortex, L (35%)	Auditory	.004
16.46 (6.97, −9.48)	(−5, −18, 34)	Cingulate gyrus, L (29%)	CO task control	.006[c]
16.35 (7.10, −9.25)	(−34, 3, 4)	Insular cortex, L (4%)	CO task control	.007[b]
19.42 (8.28, −11.15)	(47, −50, 29)	Angular gyrus, R (56%)	Default mode	.009

Note: Absolute agreement difference (average of absolute value per node) and its decomposition into positive and negative contributory factors are listed on the first column. Nodes are labeled with the probabilistic Harvard-Oxford cortical and subcortical structural atlas, using peak coordinate for each ROI. Abbreviations: CO, cingulo-opercular; DMN, default mode network; FP, frontoparietal; HOA, hip OA; KOA, knee OA; MNI, Montreal Neurological Institute; OA, osteoarthritis.

[a]Network assignment in accordance with Figure 5.

[b]*p*-Values are one-sided and calculated after randomly permutating participants over 1,000 iterations and generating a null model for reorganization estimates (agreement difference matrix).

[c]Nodal differences were further validated in the KOA holdout sample.

[d]HOA group at $p < .05$ (Table S1).

4.3 | Localized hub topology alterations

Although *K* indices were statistically significant in our discovery group, when testing across multiple link densities in our hold out sample (KOA and HOA), only centrality properties validated. Previous data showed regions which express aspects of node centrality (e.g., degree, larger number of edges), defined as hubs, tend to be more vulnerable to local perturbations (Stam, 2014). Remarkably, when we studied the nodal disruption profile at a finer-grained level, we observed that the reduction in functional connectivity happened at the insula, a high-order associative area. On the other hand, there was an increased centrality at the somatosensory cortex (M1/S1) and right fusiform gyrus/parahippocampal gyrus, the latter an area previously identified to predict drug analgesia in OA (Tétreault et al., 2016). This phenomenon, a selective loss of connectivity in highly central hub nodes accompanied with gain in degree in peripheral nodes seems to be a consistent finding in network studies of multiple neurological disorders (Crossley et al., 2014; Stam, 2014). An explanatory theory is provided by Stam (2014): in an initial phase of disease there is a rerouting of traffic from failing nodes to higher hierarchical nodes, which in time become overloaded. Eventually, in the chronic phase, peripheral (minimally connected) nodes become hubs, thus compensating for the overload of the failing hubs. It is not clear the extent to which our current results support this concept. All nodes that shifted their hubness are brain regions most likely involved in the OA pain state. It is possible that observed response is maladaptive, according to the *Stam* theory, where insula connectivity changes secondarily control rerouting of information and outgrowth of new connections to S1/M1. Alternatively, the decreased connectivity of the insula together with increased connectivity of S1/M1 and parahippocampus can reflect a coping process, diminishing the influence of the pain in the cortex, and increasing attention to SM control. At this point, we do not know the specific mechanisms or direction of influence regarding the observed shifts hub properties.

Although we were able to reliably isolate specific patterns underlying network disruption, there was an important finding that deserves further discussion: as also seen before (Mansour et al., 2016), by recalculating the *K* indices using only 20% of the nodes (randomly over multiple trials), we showed that nodal rank order disruption reflects altered connectivity that permeates the whole brain and is not merely driven by changes to specific regions. Most likely this is a reflection of the extent of stress that living with OA imposes on information processing throughout the brain (an overall decrease in high connectivity compensated by increase in low connectivity regions, diminishing the ability of information sharing, and thus the efficiency of cognitive processing).

4.4 | Modular reorganization

Modular reorganization of brain networks allows us to evaluate network architecture at an intermediate level of organization, between global and local properties. In the past our group evaluated module allegiance (probability of a given node to be located in the same functional community of HC) in different chronic pain conditions, identifying the insular cortex and lateral parietal cortex (part of the SM network and DMN) as showing the largest variability in community membership. Mano et al., applying the same analytical approach in chronic back pain patients as we do here, identified mainly nodes located in the SM cortex (Mano et al., 2018). In our dataset, changes

in modular identity were seen in the middle frontal gyrus, insula, and cingulate cortex, part of frontoparietal and cingulo-opercular networks (validated in KOA and/or HOA) (Power et al., 2011). Why these regions are inconsistent between studies is not obvious. The rerouting of nodal information should affect the hierarchical modular organization of a network; thus, it is not surprising that the insular cortex shows modular reorganization. Middle frontal gyrus, part of the frontoparietal network, is highly related to task-control, serving to initiate new task states by flexibly interacting with other control and processing networks (Marek & Dosenbach, 2018). Still, the across study variability of this outcome raises issues as to behavioral and physiological parameters that control modular reorganization, and future studies are needed to better clarify underling mechanisms.

4.5 | Relationship between graph indices and OA clinical properties

In our study there was no strong association between *K* indices and clinical variables, in contrast to previous reports, where the hub disruption indices in chronic pain were related to pain intensity (Crossley et al., 2014; Mansour et al., 2016) or to other clinical key properties of disease (De Pauw et al., 2020). In another study, we also showed that for low back pain associated with disk herniation, K_D association with pain intensity was limited to males with high education (Huang et al., 2019). Thus, there are across study variations in the extent to which *K* indices relate to clinical parameters. Given that OA is a heterogeneous pathology with multiple clinical phenotypes (Deveza et al., 2019), it is likely that subgrouping patients with more in-depth phenotyping could shed light into the relationship between *K* indices and clinical parameters.

When examining brain nodal degree properties, we could identify a set of nodes and their interrelationships reflecting OA pain intensity. This result was validated in our KOA holdout sample and generalized to the HOA sample. Regions in this model were located both in cortical and subcortical areas, across multiple functional networks. These results are consistent with our recent observation regarding brain structural properties and their relationship with clinical pain in OA, where we observed distributed regional changes, related in the latter case to the neuropathic pain in OA (Barroso et al., 2020). The causality of this relationship remains unclear, yet we showed that the distributed set of nodes and their information sharing with the rest of the brain relates to OA pain. If the OA pain is presumed to be dominantly reflecting nociceptive signals from the injured joint, then one would expect to observe a more circumscribed set of nodes reflecting related pain perception, and perhaps primarily the insula and S1 regions, according to prevailing concepts in the field (Malfait & Schnitzer, 2013). Our results instead suggest that distributed circuits throughout the brain contribute to OA pain and corroborate previous research showing OA pain may be better associated with brain regions involved in emotional and cognitive processing (Kulkarni et al., 2007; Parks et al., 2011).

4.6 | Limitations

Some important limitations of the present study should be acknowledged. First, we use a single parcellation scheme to study nodal functional connectivity (Power et al., 2011). The hub disruption indices are known to be resilient to different parcellation schemes (Achard et al., 2012; Mansour et al., 2016); however, nodal graph properties are sensitive to distinct parcellations schemes, which could account for differences across studies (Fornito, Zalesky, & Bullmore, 2010). Another important technical limitation is the network link thresholding, a necessary step to use binary graphs. There is no current consensus on what threshold to use. Although global properties and graph disruption indices were stable across several correlation thresholds, caution should be used when interpreting results from binary graph models (Garrison, Scheinost, Finn, Shen, & Constable, 2015). In the modularity analysis, the choice of parameters for coupling strength and resolution $\{\omega, \gamma\}$ is nontrivial, and there is no current consensus (Sporns & Betzel, 2016). Finally, it is important to restate that since the control group was not large enough to be divided, it was used both in the discovery and validation analysis, therefore introducing some uncontrolled bias. Finally, the HOA group was small relative to our KOA group; thus, all HOA analyses were limited for validating/generalizing results obtained in KOA.

5 | CONCLUSIONS

We demonstrated that OA pain is associated both with the disruption of whole-brain and local functional connectivity. Although major nodal connectivity changes were identified in the S1/M1 regions, parahippocampal gyrus and the insula, the functional reorganization seemed to have propagated and eventually percolated throughout the whole brain, possibly reflecting the cost of the disease on information sharing across the brain. Pain intensity, a primary clinical concern in OA, was localized to distributed nodal functional connectivity changes in KOA, and this result strongly generalized for pain intensity in HOA. Therefore, our results dissociate the major hub disruptions from network connectivity related to OA pain, challenging the extent of dependence of OA pain on nociceptive signaling.

ACKNOWLEDGMENTS

The authors thank to Dr Paulo Oliveira, for the clinical support and supervision of patients enrolled in the study and all the members of the Orthopedic Department of Centro Hospitalar Universitário de São João, Porto, for their support with data collection. The authors thank to Unilabs Boavista and Dr Nuno Martins for all the support in imaging data acquisition. The authors are thankful to all Apkarian lab and Galhardo lab members that contributed to this study with their time and resources. J. B. was funded through CCDRN (Norte-08-5369-FSE-000026), OARSI Collaborative Scholarship 2018, and Luso-American Development Foundation R&D@PhD scholarship grant. Neuroimage data acquisition was provided by Unilabs Boavista and the Grünenthal Young Pain Researcher 2017 Grant.

CONFLICT OF INTEREST

The authors declare no conflict of interest.

DATA AVAILABILITY STATEMENT

The data that support the findings of this study are available from the corresponding author upon reasonable request.

ETHICS STATEMENT

All procedures performed in studies involving human participants were in accordance with the ethical standards of the institutional research committee and with the 1964 Helsinki Declaration and its later amendments. Informed consent was obtained from all individual participants involved in the study.

ORCID

Apkar Vania Apkarian https://orcid.org/0000-0002-9788-7458

REFERENCES

Achard, S., Delon-Martin, C., Vertes, P. E., Renard, F., Schenck, M., Schneider, F., … Bullmore, E. T. (2012). Hubs of brain functional networks are radically reorganized in comatose patients. *Proceedings of the National Academy of Sciences*, *109*, 20608–20613.

Azevedo, L. (2007). Tradução, adaptação cultural e estudo multicêntrico de validação de instrumentos para rastreio e avaliação do impacto da dor crónica (Translation, cultural adaptation and multicentric validation study of chronic pain screening and impact assessment instruments). *Dor*, *15*, 6–65.

Balke, B. (1963). A simple field test for the assessment of physical fitness. Rep 63-6. Report Civil Aeromedical Research Institute (U.S.) 1–8.

Barroso, J., Vigotsky, A.D., Branco, P., Reis, A.M., Schnitzer, T.J., Galhardo, V., & Apkarian, A.V. (2020). Brain gray matter abnormalities in osteoarthritis pain: a cross-sectional evaluation. *Pain,*. *161*, 2167–2178.

Bouhassira, D., Attal, N., Alchaar, H., Boureau, F., Brochet, B., Bruxelle, J., … Vicaut, E. (2005). Comparison of pain syndromes associated with nervous or somatic lesions and development of a new neuropathic pain diagnostic questionnaire (DN4). *Pain*, *114*, 29–36.

Centers for Disease Control and Prevention (CDC). (2009). Prevalence and most common causes of disability among adults—United States, 2005. *MMWR. Morbidity and Mortality Weekly Report*, *58*, 421–426.

Cottam, W. J., Iwabuchi, S. J., Drabek, M. M., Reckziegel, D., & Auer, D. P. (2018). Altered connectivity of the right anterior insula drives the pain connectome changes in chronic knee osteoarthritis. *Pain*, *159*, 929–938.

Crossley, N. A., Mechelli, A., Scott, J., Carletti, F., Fox, P. T., McGuire, P., & Bullmore, E. T. (2014). The hubs of the human connectome are generally implicated in the anatomy of brain disorders. *Brain*, *137*, 2382–2395.

De Pauw, R., Aerts, H., Siugzdaite, R., Meeus, M., Coppieters, I., Caeyenberghs, K., Cagnie, B. (2020). Hub disruption in patients with chronic neck pain: A graph analytical approach. *Pain*, *161*, 729–741.

Deveza, L. A., Nelson, A. E., & Loeser, R. F. (2019). Phenotypes of osteoarthritis: Current state and future implications. *Clinical and Experimental Rheumatology*, *37*(Suppl 120), 64–72.

Eguíluz, V. M., Chialvo, D. R., Cecchi, G. A., Baliki, M., & Apkarian, A. V. (2005). Scale-free brain functional networks. *Physical Review Letters*, *94*, 018102.

Fornito, A., Zalesky, A., & Bullmore, E. T. (2010). Network scaling effects in graph analytic studies of human resting-state FMRI data. *Frontiers in Systems Neuroscience*, *4*(22).

Friedman, J., Hastie, T., & Tibshirani, R. (2010). Regularization paths for generalized linear models via coordinate descent. *Journal of Statistical Software*, *33*, 1–22.

Garrison, K. A., Scheinost, D., Finn, E. S., Shen, X., & Constable, R. T. (2015). The (in)stability of functional brain network measures across thresholds. *NeuroImage*, *118*, 651–661.

Gonçalves, R. S., Cabri, J., Pinheiro, J. P., & Ferreira, P. L. (2009). Cross-cultural adaptation and validation of the Portuguese version of the Knee injury and Osteoarthritis Outcome Score (KOOS). *Osteoarthritis and Cartilage*, *17*, 1156–1162.

Hawker, G. A. (2009). Experiencing painful osteoarthritis: What have we learned from listening? *Current Opinion in Rheumatology*, *21*, 507–512.

Huang, S., Wakaizumi, K., Wu, B., Shen, B., Wu, B., Fan, L., … Huang, L. (2019). Whole-brain functional network disruption in chronic pain with disk herniation. *Pain*, *160*, 2829–2840.

Humphries, M. D., & Gurney, K. (2008). Network 'small-world-ness': A quantitative method for determining canonical network equivalence. *PLoS One*, *3*, e0002051.

Itahashi, T., Yamada, T., Watanabe, H., Nakamura, M., Jimbo, D., Shioda, S., … Hashimoto, R. (2014). Altered network topologies and hub organization in adults with autism: A resting-state fMRI study. *PLoS One*, *9*, e94115.

Jeub, L., Bazzi, M., Jutla, I. & Mucha, P (2011–2019). A generalized Louvain method for community detection implemented in MATLAB. Retrieved from http://netwiki.amath.unc.edu/GenLouvain

Kaplan, C. M., Schrepf, A., Vatansever, D., Larkin, T. E., Mawla, I., Ichesco, E., … Harris, R. E. (2019). Functional and neurochemical disruptions of brain hub topology in chronic pain. *Pain*, *160*, 973–983.

Kellgren, J. H., & Lawrence, J. S. (1957). Radiological assessment of osteo-arthrosis. *Annals of the Rheumatic Diseases*, *16*, 494–502.

Kulkarni, B., Bentley, D. E., Elliott, R., Julyan, P. J., Boger, E., Watson, A., … Jones, A. K. P. (2007). Arthritic pain is processed in brain areas concerned with emotions and fear. *Arthritis and Rheumatism*, *56*, 1345–1354.

Malfait, A.-M., & Schnitzer, T. J. (2013). Towards a mechanism-based approach to pain management in osteoarthritis. *Nature Reviews Rheumatology*, *9*, 654–664.

Mano, H., Kotecha, G., Leibnitz, K., Matsubara, T., Sprenger, C., Nakae, A., … Seymour, B. (2018). Classification and characterisation of brain network changes in chronic back pain: A multicenter study. *Wellcome Open Research*, *3*, 19.

Mansour, A., Baria, A. T., Tetreault, P., Vachon-Presseau, E., Chang, P. C., Huang, L., … Baliki, M. N. (2016). Global disruption of degree rank order: A hallmark of chronic pain. *Scientific Reports*, *6*, 34853.

Marek, S., & Dosenbach, N. U. F. (2018). The frontoparietal network: Function, electrophysiology, and importance of individual precision mapping. *Dialogues in Clinical Neuroscience*, *20*, 133–140.

Miller, R. E., Block, J. A., & Malfait, A.-M. (2017). Nerve growth factor blockade for the management of osteoarthritis pain: What can we learn from clinical trials and preclinical models? *Current Opinion in Rheumatology*, *29*, 110–118.

Miller, R. E., Tran, P. B., Obeidat, A. M., Raghu, P., Ishihara, S., Miller, R. J., & Malfait, A. M. (2015). The role of peripheral nociceptive neurons in the pathophysiology of osteoarthritis pain. *Current Osteoporosis Reports*, *13*, 318–326.

Mucha, P. J., Richardson, T., Macon, K., Porter, M. A., & Onnela, J.-P. (2010). Community structure in time-dependent, multiscale, and multiplex networks. *Science*, *328*, 876–878.

Murray, C. J., Vos, T., Lozano, R., Naghavi, M., Flaxman, A. D., Michaud, C., … Memish, Z. A. (2012). Disability-adjusted life years (DALYs) for 291 diseases and injuries in 21 regions, 1990–2010: A systematic analysis for the Global Burden of Disease Study 2010. *The Lancet*, *380*, 2197–2223.

Neogi, T. (2013). The epidemiology and impact of pain in osteoarthritis. *Osteoarthritis and Cartilage*, *21*, 1145–1153.

Pais-Ribeiro, J., Silva, I., Ferreira, T., Martins, A., Meneses, R., Baltar, M. (2007). Validation study of a Portuguese version of the Hospital Anxiety and Depression Scale. *Psychology, Health & Medicine*, *12*, 225–235.

Parks, E. L., Geha, P. Y., Baliki, M. N., Katz, J., Schnitzer, T. J., Apkarian, A. V. (2011). Brain activity for chronic knee osteoarthritis: Dissociating evoked pain from spontaneous pain. *European journal of pain (London, England)*, *15*(843), e1–e14.

Podsiadlo, D., & Richardson, S. (1991). The timed "up & go": A test of basic functional mobility for frail elderly persons. *Journal of the American Geriatrics Society*, *39*, 142–148.

Power, J. D., Barnes, K. A., Snyder, A. Z., Schlaggar, B. L., & Petersen, S. E. (2012). Spurious but systematic correlations in functional connectivity MRI networks arise from subject motion. *NeuroImage*, *59*, 2142–2154.

Power, J. D., Cohen, A. L., Nelson, S. M., Wig, G. S., Barnes, K. A., Church, J. A., … Petersen, S. E. (2011). Functional network organization of the human brain. *Neuron*, *72*, 665–678.

Power, J. D., Mitra, A., Laumann, T. O., Snyder, A. Z., Schlaggar, B. L., & Petersen, S. E. (2014). Methods to detect, characterize, and remove motion artifact in resting state fMRI. *NeuroImage*, *84*, 320–341.

Power, J. D., Schlaggar, B. L., Lessov-Schlaggar, C. N., & Petersen, S. E. (2013). Evidence for hubs in human functional brain networks. *Neuron*, *79*, 798–813.

Rejeski, W. J., Ettinger, W. H., Jr., Schumaker, S., James, P., Burns, R., & Elam, J. T. (1995). Assessing performance-related disability in patients with knee osteoarthritis. *Osteoarthritis and Cartilage*, *3*, 157–167.

Roos, E. M., & Toksvig-Larsen, S. (2003). Knee injury and Osteoarthritis Outcome Score (KOOS)—Validation and comparison to the WOMAC in total knee replacement. *Health and Quality of Life Outcomes*, *1*, 17.

Rubinov, M., & Sporns, O. (2010). Complex network measures of brain connectivity: Uses and interpretations. *NeuroImage*, *52*, 1059–1069.

Smith, S. M., Jenkinson, M., Woolrich, M. W., Beckmann, C. F., Behrens, T. E. J., Johansen-Berg, H., … Matthews, P. M. (2004). Advances in functional and structural MR image analysis and implementation as FSL. *NeuroImage*, *23*, S208–S219.

Sporns, O., & Betzel, R. F. (2016). Modular brain networks. *Annual Review of Psychology*, *67*, 613–640.

Stam, C. J. (2014). Modern network science of neurological disorders. *Nature Reviews. Neuroscience*, *15*, 683–695.

Sullivan, M. J. L., Bishop, S. R., & Pivik, J. (1995). The pain catastrophizing scale: Development and validation. *Psychological Assessment*, *7*, 524–532.

Tétreault, P., Mansour, A., Vachon-Presseau, E., Schnitzer, T. J., Apkarian, A. V., & Baliki, M. N. (2016). Brain connectivity predicts placebo response across chronic pain clinical trials. *PLoS Biology*, *14*, e1002570.

van den Heuvel, M. P., & Sporns, O. (2013). Network hubs in the human brain. *Trends in Cognitive Sciences*, *17*, 683–696.

Zigmond, A. S., & Snaith, R. P. (1983). The hospital anxiety and depression scale. *Acta Psychiatrica Scandinavica*, *67*, 361–370.

Zou, H., & Hastie, T. (2005). Regularization and variable selection via the elastic net. *Journal of the Royal Statistical Society, Series B (Statistical Methodology)*, *67*, 301–320.

SUPPORTING INFORMATION

Additional supporting information may be found online in the Supporting Information section at the end of this article.

How to cite this article: Barroso J, Wakaizumi K, Reis AM, et al. Reorganization of functional brain network architecture in chronic osteoarthritis pain. *Hum Brain Mapp*. 2020;1–17. https://doi.org/10.1002/hbm.25287

2.4 Manuscript in preparation

Barroso J, Branco P, Baliki M, Reis AM, Schnitzer TJ, Galhardo V, Apkarian AV. *Limbic brain structural and functional properties predict pain after joint replacement surgery in knee osteoarthritis*.

Limbic brain structural and functional properties predict chronic pain after joint replacement surgery in knee osteoarthritis

Joana Barroso MD MSc [1,2,3], Paulo Branco PhD[3], Ana Mafalda Reis MD PhD [5], Thomas J. Schnitzer MD PhD[2,6,7], Vasco Galhardo PhD[1], A. Vania Apkarian PhD[2,3,7]

Affiliations:

[1] Departamento de Biomedicina, Faculdade de Medicina, Universidade do Porto, Porto, Portugal. Instituto de Investigação e Inovação em Saúde - i3S, Universidade do Porto, Porto, Portugal.

[2] Department of Physical Medicine and Rehabilitation, Northwestern University, Feinberg School of Medicine, Chicago, IL, USA.

[3] Department of Physiology, Northwestern University, Feinberg School of Medicine, Chicago, IL, USA.

[4] Departments of Biomedical Engineering and Statistics, Northwestern University, Evanston, IL, USA.

[5] Unilabs Boavista, Porto, Portugal.

[6] Department of Rheumatology, Northwestern University, Feinberg School of Medicine, Chicago, IL, USA.

[7]Department of Anesthesia, Northwestern University, Feinberg School of Medicine, Chicago, IL, USA.

Abstract:

Mechanisms of osteoarthritis (OA) pain after total knee replacement (TKR) remain poorly understood. Functional and anatomical properties of limbic structures have been both implicated in the transition from acute to chronic pain and proposed as à priori risk factors for pain chronification in low back pain. Here, bridging these concepts, we studied a population of knee OA patients before and after TKR, hypothesizing that brain limbic structures relate to maintenance of OA pain after surgery. We included a total of 81 patients and tracked their pain before and after surgery as they either recovered (OAr) or transitioned to chronic pain (OAp). We show volumetric properties of limbic structures (thalamus, hippocampus and amygdala) are predictive of pain persistence after surgery. Moreover, by contrasting the shape of the hippocampus, a more granular anatomical measure we reveal the anterior hippocampus, a region previously associated with the transition from acute to chronic pain in low back pain patients is inward displaced in the OAp group. Additionally, we show the functional and white matter connectivity between limbic brain structures is related to the pain outcome. Our results imply that persistence of OA chronic pain after TKR may be associated with limbic brain properties. These results support the importance of limbic neuroanatomical factors in OA pain pathophysiology and open new avenues for future clinical care and management of OA pain patients.

1.Introduction:

Osteoarthritis is the most common type of arthritis worldwide and one of the most prevalent causes of chronic musculoskeletal pain[1]. Total knee replacement (TKR) is commonly performed to treat the disorder, when pharmacological and conservative treatments cannot provide adequate pain relief and level of functionality. Although TKR is seen as a highly successful surgery offering substantial improvement in functional status and quality of life, an important proportion of patients still report moderate to severe pain post-TKR that is not explained by prosthetics-related outcomes[23].

Multiple clinical, demographic and psychologic factors have been proposed as risk factors for persistent pain in patients undergoing TKR[4], e.g., anxiety and depressive symptoms, pain catastrophizing[24], coping strategies, higher levels of pre-surgical pain[5] and neuropathic quality of pain[6]. While psychosocial factors and quantitative sensory testing (e.g., temporal summation, pressure pain thresholds) are interpreted as clinical manifestations of altered central pain modulation in OA, they are at most indirect manifestations. At the same time, while the concept of altered pain central sensitization has been associated with pain persistence after TKR, mechanistically, it has mostly been studied at the spinal cord and anti-nociceptive descending modulation levels.

Though direct evidence of the brain as a precursor of OA pain persistence is still lacking, brain structural and functional changes in OA have been described. Brain anatomy is distorted in knee and hip OA[7,8] and there is evidence of global whole-brain reorganization of resting-state functional connectivity[9]; locally, major changes in information sharing were previously identified in sensory-motor regions and the insular cortex[10]. Additionally, brain

activity associated with spontaneous ongoing OA pain is known to engage prefrontal-limbic brain circuitry[11]. At the same time, brain functional and anatomical properties have been implicated in the progression from acute to chronic pain in low back pain. Corticolimbic white matter connectivity, volumetric properties of limbic structures and functional connectivity between corticolimbic regions prospectively relate to pain chronification[12,13]. This data suggests that pain in OA may not only be contingent on the peripheral nociceptive signaling but also in brain circuitry, particularly limbic brain properties. If so, such properties may have a critical role in the development of pain, and also in explaining its persistence after a technically successful TKR.

In this longitudinal assessment we followed a large sample of advanced knee OA patients scheduled for TKR. In order to investigate the brain's influence in knee OA pain persistence, we collected brain scans using Magnetic Resonance Imaging (MRI) before surgery, together with a multiplicity of clinical outcomes and questionnaires. We studied limbic brain structural and functional properties as predictors of chronic pain 6-months after surgery. Our main hypothesis was that distinct structural properties of subcortical brain nuclei were associated with the unfavorable pain outcome. Additionally, we hypothesized that distorted anatomic regions may exhibited functional and white matter anatomical connectivity properties associated with the outcome, and that this information may shed light on brain dynamics of persistent OA pain.

2. Methods

2.1 Study design

The present work is part of a longitudinal observational project in which osteoarthritis patients were evaluated before joint replacement surgery and followed over a period of 6 months after surgery [14]. The protocol involved a total of 4 visits: 1-3 months before surgery (visit 1); a second pre-surgical visit, 2-6 weeks before surgery (visit 2); two post-surgical visits at 3 and 6 months (visit 3 and 4). Visits 1, 3 and 4 included a clinical evaluation and multiple pain, mood and general health questionnaires; brain magnetic resonance imaging (MRI) scans were performed at visits 2 and 4. Only patients who completed the 4 visits were included in this report (n=82).

2.2 Participants (study population)

Participants included in this study were knee OA patients with clinical indication for total knee replacement (TKR) surgery. Hip OA subjects and healthy controls were part of this project, however not included in the present report.

Recruitment took place at the Orthopedic Surgery Department, *Centro Hospitalar e Universitário de São João*, Porto, Portugal. The study protocol was approved by the local Ethics Committee – *Comissão de Ética para a saúde, Centro Hospitalar de São João*, and all participants provided informed written consent before initiating the study.

Patients that met the following criteria were considered eligible: age between 45 and 75 years; knee OA diagnosis according to the clinical classification criteria of the American College of Rheumatology[15]; clinical indication for TKR surgery by a certified orthopedic surgeon in our center. Exclusion criteria were evidence of secondary osteoarthritis due to congenital or development disease, inflammatory or auto-immune disorders; clinical indication for bilateral arthroplasty or bilateral knee pain with less than or equal to 4 points difference (NRS, numeric rating scale) between the two joints; other chronic pain conditions (e.g. fibromyalgia, chronic pelvic pain, chronic headache); chronic neurological or psychiatric disease (e.g. dementia, Parkinson's disease, demyelinating diseases, major depressive disorder, obsessive compulsive disorders); previous history of stroke or traumatic brain injury.

2.3 Clinical Outcomes

The main clinical outcome of the study was the numeric rating scale (NRS) for pain over the previous week. All patients completed a battery of questionnaires assessing multiple domains: Knee and Hip Injury and Osteoarthritis Score (KOOS)[16]; Hospital Anxiety and Depression Scale (HADS) [,18]; Pain Catastrophizing Scale (PCS)[19,20]; *Doleur Neuropathique en 4 questions* - Neuropathic pain scale (DN4)[21,20]. Questionnaires were applied in their Portuguese validated versions. Physical performance was assessed with two distinct tasks: timed up and go test (TUG) [22] and six-minute walking test (6MWT)[23,24]. Knee x-rays were reviewed by two clinical radiologists and classified using the Kellgren-Lawrence scale[25].

2.4 Magnetic Resonance Imaging acquisition

MPRAGE type T1-anatomical brain images were acquired with a 3.0 T Siemen Magnetom Spectra scanner (Siemens Medical, Erlagen, Germany). Acquisition parameters: time of repetition (TR) = 2500 ms, echo time (TE) = 3.31 ms, flip angle = 9º, field-of-view (FOV) = 256 x 256 mm^2, voxel-size = 1 x 1 x 1 mm, number of slices = 160. Resting state fMRI (rs-fMRI) images were acquired with the following parameters: Multi-slice T2*-weighted echo-planar images with TR = 2500 ms, TE = 30 ms, flip angle = 90 º, voxel size = 3.4 x 3.4 x 3.0, in-plane resolution = 64 x 64, number of volumes 300, number of slices = 40 (slices covered the whole brain from the cerebellum to the vertex), with interleaved ordering. The time of acquisition lasted 12 minutes and 30 seconds, and patients were instructed to keep their eyes open and to remain still during the acquisition. Diffusion weighted images were likewise acquired at the same session and scanner, with the following parameters: TR = 11300 ms, TE = 99 ms, in-plane matrix resolution, 128 x 128, field of view [FOV] = 256 x 256 mm^2, slice thickness = 2.0 mm, number of axial slices = 72. Images had an isotropic distribution along 64 directions, with a b-value of 1000 s/ mm^2. 1 volume with no diffusion weighting (b-value = 0 s/ mm^2) was acquired in the start of the protocol. Two repetitions of the same protocol were acquired to average out noise.

2.5 MRI data pre-processing

2.5.1 Functional MRI preprocessing

Pre-processing of each subject's time series of rs-fMRI volumes was done following previous published methods[10], using the FMRIB Software Library (FSL) (www.fmrib.ox.ac.uk/fsl). [26] and in-house software. Briefly, it included the ensuing steps: the first four volumes (10 seconds) were discarded to exclude T1 saturation effects; non-brain tissue was extracted using BET [27]; slice-time correction; motion correction using MCFLIRT [28]; special smoothing with a full width at half maximum (FWHM) Gaussian kernel of 5 mm; high-pass temporal filtering (0.1 Hz). Additional sources of noise were removed from the data by regressing out: (1) the six parameters obtained by rigid body correction of head motion, (2) global signal averaged over all grey matter voxels, (3) white matter signal averaged over all voxels of eroded white matter and (4) ventricular signal averaged over all voxels of eroded ventricle regions. Following, to further reduce the effect of residual motion artifacts, we applied motion-volume censoring: a composite motion score was calculated based on normative thresholds (volumes with frame-wise displacement larger than 0.5 mm, derivative variance root mean square after Z-normalization larger than 2.3 and deviation of volume intensity within the predefined gray matter mask larger then 2.3); we then scrubbed the detected volume (volume = i) and adjacent 4 volumes (i-2 ,i-1 , i , i+1 , i+2) [29,30]. Finally, a Butterworth band-pass filter (0.008-0.1 Hz) was applied to the scrubbed time-series. Functional data were normalized to standard MNI space using a two-step process: first, functional images were co-registered to the high-resolution T1 image using a 6 DOF linear transformation. Then, T1 images were normalized to MNI space using a 12 DOF linear transformation (FLIRT) followed by a non-linear transformation (FNIRT) (ref: https://www.fmrib.ox.ac.uk/datasets/techrep/tr07ja1/tr07ja1.pdf); which was then

applied to the functional images. Registered images were further visually inspected to ensure optimal registration.

2.5.2 Diffusion tensor imaging preprocessing

Preprocessing of diffusion weighted images was performed using tools from the FDT package from FSL. DTI data were manually checked for obvious artefacts and distortions and corrected for eddy currents and head motion using EDDY 6.0.3 [31]. Images were affinely registered to the first no-diffusion weighted (b = 0 s/mm^2) image of each subject. Data were then skull extracted (BET) and a diffusion tensor model was fit at each voxel, and principal directions were calculated using DTIFIT. To account for possible crossing-fibers, a Bayesian Estimation of Diffusion Parameters Obtained using Sampling Techniques (BEDPOSTX)[32], modelling up to three main directions.

2.6 MRI data quality control (QC)

Individual T1-weighted structural images were visually inspected for technical artifacts as radiofrequency noise, head coverage and radiofrequency noise and for motion artifacts. Contrast to noise ratio (CNR) for grey matter was calculated for each subject and group outliers tested at 2 SDs below the average CNR. No subjects were excluded given these criteria.

For functional data, a two-step QC procedure was performed, following the same criteria as in our previous protocol[10]. First, the number of censored motion values was

evaluated: a subject reached the criterion for exclusion if having less then 200 volumes after censoring (8 minutes of rs-fMRI scanning). Mean and standard deviation (SD) of volume censoring was 28 ± 8.1, maximal volume censoring was 49. No subjects were excluded given this criterion.

Secondly, a functional connectivity outlier detection was implemented: for each subject the resting-state functional connectivity (RSFC) was calculated across 256 regions of interest (ROIs)[33]. A group ROI x ROI correlation matrix was built, and the average of each column was calculated, representing the mean correlation coefficient across subjects of the correlation coefficient between the 256 ROIs[33]. Subjects with low average within-group correlation (<2 SDs from the average in each group) were identified as outliers and excluded from the analysis. No subjects were excluded given this criterion.

Finally, tools that automatically perform QC were applied for DTI data quality control: Quality Assessment for DMRI (QUAD) and Study-wise Quality Assessment for DMRI (SQUAD)[34]. QC was performed at a group level using SQUAD, which main input is a list of single-subject QC folders, generated by QUAD. Subjects flagged as outliers in relative displacement, and/or signal to noise ratio were excluded (n = 4).

2.7 Statistical analysis

In order to classify pain surgery outcome – OA recovering (OAr) and OA persisting (OAp) - we evaluated pain scores after and before surgery. Firstly, we visually inspected the distribution of absolute pain scores after surgery for 3 different scales, NRS, KOOS pain and SF-36 pain. Here, to maintain the direction of the scale, KOOS and SF-36 were

reversed; also, all scales were converted to a grading of 0-10. Then, using the same cut-off for classification for the 3 scales, we evaluated the accuracy of classification among them (probability threshold for group classification at 0.5), computed with 95% confidence intervals under 1000 bootstraps for each model. Finally, we assessed the agreement between absolute NRS score and % change from baseline using the same methodology as described above.

For demographic and clinical data, comparisons between OA groups were made with ANOVA and independent sample t-tests or Chi-square(X^2) tests for continuous parametrical variables and categorical data respectively. Correlation between all clinical variables at baseline was computed. Finally, univariate statistics were performed for all clinical variables at baseline: analyses of covariance, controlling for initial pain levels, with OA group as between-subjects factor. Bonferroni correction for multiple comparisons was applied.

2.8 MRI data analysis

2.8.1 Morphometric analysis of subcortical structures

Subcortical volume and shape data were analyzed with the standard automated processing stream from the FMRIB's Integrated Registration and Segmentation Tool (FIRST)[35]. In this routine, the image is skull striped (BET)[27], registered to the MNI 1mm T1 MRI brain template, and segmented into the different subcortical ROIs. Visual inspection if

the subcortical segmentation was ensued for all subjects. No gross mismatches between underlying anatomy and FIRST outcome were identified.

The volumes of right and left amygdala, caudate, hippocampus, nucleus accumbens, putamen, pallidum and thalamus were calculated for each subject. Group comparisons (OA surgery outcome) were performed using repeated analysis of covariance with subcortical volume (SCv) as the dependent factor, brain hemisphere as within-subject factor, the group as a between-subject factor, and age, sex, baseline pain level and total intracranial volume (estimated using FSL SIENAX[36]) as covariates of no interest. Post-hoc analyses for significant interactions were conducted with analysis of covariance controlling for the same variables of no-interest as stated above. Afterwards, group classification performance using significant different subcortical structures was evaluated by constructing receiver operating characteristic (ROC) curves and computing areas under the curve (AUC).

Then, we queried if localized specific deformations underlined volumetric dissimilarities uncover in the previous analysis. Using FSL's FIRST, we generated a vertex representation of these structures[37]. This model used a Bayesian approach representing the structure in 3D from meshes fitting the form of the subcortical structure to a dataset that was manually segmented. The shapes of the subcortical structures were represented from meshes parametrized by the coordinates of their vertices. A multivariate permutation test on the 3D coordinates of corresponding vertices provided the F-values representing differences between groups (OAr/OAp). Significant clusters were determined through threshold free cluster enhancement (TFCE), with FWE correction to control for multiple comparisons.

2.8.2 Subcortical functional connectivity analysis

In order to study subcortical functional connectivity, we started by building group-specific subcortical masks. For each subject, all subcortical regions segmentations obtained with FIRST were non-linearly aligned to a standard MNI152 T1 brain. Appropriate transformation parameters were determined by registration of the whole brain to standard space using FNIRT (ref: https://www.fmrib.ox.ac.uk/datasets/techrep/tr07ja1/tr07ja1.pdf). Following, for each subcortical structure we identified voxels present in at least 25% of all study participants creating sample-specific subcortical masks. Next, we extracted the mean timeseries for each ROI, per subject. A correlation matrix was then built, between subcortical regions displaying structural changes in the volumetric analysis and all subcortical regions (right and left amygdala, caudate, hippocampus, nucleus accumbens, putamen, pallidum and thalamus). Then, we used permutation-based testing to estimate statistical significance of between group differences (OAr/OAp) for each connection (correlation ROIxROI). We randomly assigned subjects to two groups, arbitrarily defining one as the reference and estimating the correlation differences between groups. We repeated this process 10,000 times to sample the null distribution of the connectivity mean difference to which we statistically contrast the corrected labeled data using unpaired t-tests with significance level threshold of $p<0.05$.

2.8.3 Subcortical white mater connectivity analysis

For structural connectivity analyses, the same subcortical masks generated for functional connectivity analysis were used. Afterwards, we selected regions that were statistical significant in our volumetric analysis (thalamus, hippocampus and amygdala, left and right) and applied FSL's tool PROBTRACKX2[38] to estimate the connectivity probability between ROIs'. Briefly, for each voxel within each selected ROI (seeds), 5000 streamlines are seeded, and the number of connections reaching each other ROI (target, here considering all subcortical structures) is counted. To normalize for the size of the ROI, we divided the number of connections by the number of streamlines seeded from each structure, essentially converting the raw connectivity estimate to a probability of connectivity measure, ranging from 0 (none of the streamlines reached the target) to 1 (all streamlines reached the target). Since distance between ROIs can influence connectivity results, and introduce a head-size bias, connectivity count was further corrected for distance by multiplying the number of streamlines by the Euclidian distance between the two ROIs. Finally, since the connectivity matrix is not symmetrical, we averaged the upper and lower triangles of the matrix, to get a single ROI-to-ROI value reflecting connectivity probability. Since we collected two DTI scans for each subject, the resulting matrices were averaged across the two runs (6 subjects failed quality-control for only one of the DTI scans; in such case, only the adequate DTI protocol was used). Statistical analysis of between-group (OAr/OAp) connectivity differences was carried using the same analytical procedure as previously detailed for functional connectivity.

2.9 Software/code

Data was preprocessed and analyzed using MATLAB 2019.b (MATLAB 2019a, The Mathworks, Inc., Natick, Massachusetts, US) and tools from the Oxford Center for Functional Magnetic Resonance Imaging of the Brain Software Library (FMRIB, Oxford, UK; FSL version 5.0.10, https://fsl.fmrib.ox.ac.uk/fsl/). Brain regions were visualized on a surface rendering of a human brain template with BrainNet Viewer (http://www.nitrc.org/projects/bnv/).

3. Results

3.1 Pain outcomes after surgery

Given that the selection of a cut-off for persisting vs recovering OA pain can be subjective, we examined the distribution of absolute pain scores after surgery with 3 different scales (NRS; KOOS pain; SF-36 pain). A clear pattern emerged, with two subgroups separating at a pain cutoff of 3 for the 2 first scales**, Figure 1.a**. We explored the robustness of this cutoff point by contrasting different scales: using KOOS to classify the outcome (same cut-off >=3) in classifying NRS outcomes, we achieved a mean accuracy of 0.81 (bootstrapped CI [0.54,0.82]); for SF-36 a mean accuracy of 0.48 [0.35,0.57] was reached. We also looked at the impact of presurgical pain in the outcome, by computing the pain % change from baseline. We applied the same analysis as before, using a cut-off classification of 50% of change for recovering/persisting pain; our mean accuracy in classifying NRS outcome was 0.91, [0.86,0.96]. Overlap of absolute NRS and % change is illustrated in **Figure 1. (b)**.

Taken together, these findings suggest that an absolute score of NRS >= 3 after surgery is appropriate to classify pain outcomes into persisting (OAp) and recovering (OAr) groups. It is noteworthy that this cut-off is commonly used in the literature to define pain outcomes after surgery, lending confidence to our outcome classification[39,40].

3.2 Demographic and socio-economic characteristics of OAp and OAr patients

No significant differences for age, gender, BMI or smoking habit were seen between the OAr and OAp groups **(Table 1).** Also, social-cultural variables (educational level; habitation; marriage status) did not show significant differences ($p>0.05$). Regarding the clinical presentation of the disease, pain intensity previous to surgery and severity of radiographic damage were not distinctive between groups; however, OAp patients showed greater pain duration before surgery (mean ± sd: 9.8±6.4) when compared recovering patients (mean ± sd: 7.0 ± 5.8 yr, $t=2.06$, $p=0.04$).

3.3 Neuropathic pain profile and HADS anxiety scale before surgery associate with pain persistence after surgery

Next, we studied clinical differences between outcome groups prior to surgery. Firstly, we computed the correlation matrix between questionnaire metrics and physical performance tasks (**Figure 2(c)**). Univariate statistics showed that initial neuropathic pain measured with DN4 scale ($F(2,81) = 13.61$, $p<0.001$), and anxiety, measured with HADS-Anxiety subscale ($F(2,81)$, $p=9.44$, $p=0.002$), were distinctive between pain recovering and persisting patients **(Figure 1. (d))**. The OAp group presented significantly higher levels of pre-surgery anxiety, and higher scores in the DN4 scale. Finally, in order to better understand the predictive value of these variables for the outcome, we applied linear regression to model to the absolute pain after surgery with each predictor: DN4 ($F(78,81) = 13.4$, $p<0.001$, adj. $R^2 = 0.236$); HADS-A ($F(78,81) = 16.1$, $p<0.001$, adj. $R^2 = 0.282$). Though predictive, the percent of variance on post-operative pain explained by these variables is inferior to 30%.

3.4 Limbic anatomic structural properties predisposing to pain persistence after TKR

In order to study brain limbic circuitry as a predictor of pain after surgery in OA, we first examined grey matter morphometric properties. Subcortical volumes (SCv) were predictive of pain persistence after surgery, as shown in **Table 2**. A significant group by subcortical volumes (SCv) interaction was observed, together with a significant main effect of Group**.** This interaction was further studied, showing the group differences were located in the thalamus, amygdala and hippocampus, as total volumes (right + left), **Table 3**. These structures showed statistically significant larger volumes in the OAp group, while controlling for age, gender, TICV and baseline pain levels **(Figure 2(a))**. The classification performance of the outcome by each structure resulted in AUC values between 0.64 and 0.73. Moreover, adding these features together improved the classifier's accuracy (AUC of 0.75) **(Figure 2(c))**.

Given that thalamus, hippocampus and amygdala exhibited significant group differences, we queried whether these volumetric changes could be attributed to localized structural deformations. For each singular structure, a vertex-wise shape analysis was conducted. As shown in **Figure 2(d)**, the anterior hippocampus displayed a significant shape displacement (TFCE $p < .05$, FWE-corrected for multiple comparisons). The OAp group presented an inward displacement of this circumscribed region, indicating anterior hippocampal shape distortion was significantly related to OA pain persistence. Other regions tested did not show statistically significant shape deformations.

3.5 Limbic functional and anatomic connectivity predisposing to chronic pain after TKR

After recognizing that structural limbic properties conferred greater risk for chronic pain post TKR, we interrogated the anatomical intrinsic and functional organization of the subcortical limbic circuitry. Anatomical and functional connectivity matrices were built from connections of the 6 regions deemed structurally distinct to all SC regions (total of 14). Connections between these regions were contrasted between the two OA groups, and statistical significance of the differences was analyzed with permutation testing, as depicted in **Figure 3**.

A stronger functional connectivity between the right amygdala and right thalamus and nucleus accumbens was present in the OAp group ($p<0.05$); on the other hand, this group presented with a weaker connectivity between right hippocampus and putamen/pallidum and left amygdala-right pallidum, as displayed in the connectome, **Figure 3.b**.

For the anatomic connectivity, links (here drawn from DTI-based probabilistic white matter tractography), exhibited significant larger connectivity for the OAr group. The larger probabilistic connectivity of the left NAc with bilateral thalamus and left hippocampus was related to a better outcome after surgery, **Figure 3.c and 3.d.**

These results support the concept that the functional connectivity within the limbic circuitry is related to pain persistence after TKR. Increased white matter connections observed between limbic subcortical structures were more likely to predispose individuals to pain recovery after surgery.

4. Discussion

This is the first large longitudinal study specifically designed to study predictive brain biomarkers of osteoarthritis pain after knee replacement surgery. We have shown that limbic brain anatomic properties predicted chronic pain after surgery, namely the volume of bilateral thalamus, amygdala and hippocampus. Taken together, the volumetric properties of these structures predicted the unfavorable surgical outcome at a high level of accuracy. Additionally, we localized a specific surface deformation in the anterior left hippocampus related to the TKR outcome. Finally, by studying the functional and anatomic connectivity profile of limbic brain structures, we showed that this circuitry is implicated in OA chronic pain and the identified connectivity changes implicate subcortical brain regions known to be involved in chronic pain maintenance, or in the transition to chronic pain. Additionally, we have demonstrated that pain neuropathic characteristics, together with pre-surgery anxiety (HADS-A) are also associated with pain persistence after surgery.

Chronic pain after TKR affects a significant proportion of patients; the unfavorable long-term pain outcomes range from 10-34% of the patients[3]. In our sample, the proportion of subjects experiencing pain 6 months after surgery was 32% which is in general agreement with other published series[3]. An important subject of debate is how to define/classify pain outcomes after an intervention. We have previously argued that post-surgical outcomes are highly dependent on the outcome definition, and that different pain scales relate to distinct dimensions of the pain experience[14]. Here, we applied a robust methodology to categorize pain outcomes. We choose as our primary outcome variable the NRS scales,

one of the most utilized of clinical pain scales; the cut-off agreement with KOOS pain was high, as it was with % pain change from baseline, thus supporting the robustness of the classification. Moreover, the cut-off at NRS or VAS (visual analogue scale) of => 3/4 points is commonly used for post-surgical pain classification in the literature[39,40,41], strengthening our confidence in the classification.

We have formerly argued that presurgical clinical and biopsychosocial variables may not be robust predictors of post-surgery pain in OA[14]. In this analysis we studied group differences for each clinical/questionnaire outcome as an individual predictor, and we showed that before surgery the DN4 scale and HADS-anxiety have higher scores in the persisting group. It has been shown before that such traits may be associated with worse outcomes after an intervention, both for OA and other pain conditions [6,42,43]. Even though these isolated variables are distinctive between the groups, their predictive value is still limited, supporting our previous thesis that clinical and psychometric variables are in important, they can only account for a small effect on the outcome.

We showed that the volumetric properties of thalamus, amygdala and hippocampus were predictive of chronic pain after TKR. Importantly, persistent pain patients presented with larger volumes for all identified structures. Volumetric properties of the amygdala and hippocampus have been identified as important risk factors for the transition from acute to chronic pain, in which case smaller volumes were related to pain chronification[12]. Amygdala and hippocampus volumes are also commonly associated with affective disorders[44]. These structures are implicated in different cognitive tasks, as emotional learning[45], fear acquisition[46], and stress regulation[47]. Limbic-volume related properties differentiating the

TKR outcomes further support our proposed thesis that pain and negative emotions are a continuum of processes[48]. However, the directionality of the effect should be discussed. Given that OA patients, contrary to acute pain patients, live with pain for several months/years, central adaptations secondary to the persistent nociceptive stimuli may occur as a consequence of long-lasting pain, and be a result of adaptive plasticity[9]. On the other hand, the evolution of pain after surgery is complex: how much of the pain after TKR reflects the pre-surgical pain? How much of the pain is induced by the surgical aggression? Given the clinical differences between models: acute to chronic pain (acute to chronic back pain) and chronic pain to relief (OA and TKR), it is not surprising that the results are not overlapping; it is important to reiterate that the same limbic structures are involved in both cases.

The cross-sectional study of OA brain biomarkers impedes us to disentangle, between diagnostic biomarkers (those that arise with and as a consequence of the disorder), and prognostic biomarkers (*à priori* traits that condition the outcome of the disease). *Gwilym et at*[49], showed that in the presence of OA (hip) pain, thalamus volume is smaller than in healthy, and that these thalamic volume changes reverse after hip arthroplasty with decreased pain. The thalamus has a central role in pain processing; it's a relay of ascending nociceptive information, associated with both sensory discriminative and affective motivational components of pain, with distinct regional functions. Though we do not know at this point if the volumetric changes are reversible in our sample, given previous data we can speculate that structural changes may happen as a response to the ongoing nociceptive stimuli. Future longitudinal assessment of brain biomarkers after surgery is essential to clarify these questions.

Volume is the integral of many properties; conversely, shape is a more granular measure. We uncovered that patients progressing to a worse outcome after surgery presented with an inward displacement in the anterior hippocampus, indicating that the structure is thinner in this region than in the recovering group, consistent with local atrophy. The anterior hippocampus functions are still not completely understood; however the region seems to be important not only in consolidating memories and recalling autobiographic memories[50] but also in regulating emotional and motivating behaviors[51]. *Mutso et al*[52], studied the functional profile of the hippocampus and showed that chronic and subacute pain are associated with larger anterior hippocampal connectivity when compared with pain-free controls. Their data suggests an important role for this region in the transition from acute to chronic pain as well as in the pathophysiology of chronic pain, possibly reflecting the learning and emotional deficits seen in these patients. In our study, patients lived with pain for a medium time of 9 years; however, individuals more prone to progress to chronic pain after TKR showed specific atrophy of the anterior hippocampus. Our data suggests that the shape of the hippocampus, a perhaps more stable biological property, underlies the persistence of OA pain after TKR.

In an effort to better understand the interaction between limbic regions showing structural changes between groups, we studied its functional and anatomical connectivity to all subcortical limbic structures. It is known that during the transition to chronic pain, brain regions that undergo structural changes also exhibit concomitant functional connectivity changes. Importantly, our group has shown that anatomic and structural

changes in the cortico-limbic circuity match the transition from acute to chronic pain[12,13]. The patterns of connectivity in our sample showed a larger anatomic connectivity for patients recovering from surgery, specially from the thalamus and hippocampus to other subcortical structures. Functionally, the amygdala showed larger connectivity to NAc and thalamus in patients who progressed to persistent pain. The relationship between functional connectivity and anatomical reorganization and the extent to which each other or both, can explain surgical pain outcome after TKR remains unknown. Longitudinal assessment of this complex interplay may help disentangle between a priori stable traits that predispose to a positive/negative outcome from and consequences of ongoing pain in the limbic circuitry.

The present work has limitations that should be acknowledged. In our functional and anatomical connectivity analysis values were not corrected for multiple comparisons; however, this was a post-hoc analysis in which we choose to only study regions that showed structural properties differences. Also, it is important to reinstate that in this report we only studied subcortical brain circuitry; it can be that neocortical properties, both independently and in association with subcortical regions, may help shed light onto central mechanisms of chronic pain in OA. Finally, the follow-up time after surgery was limited to 6 months, which can also be seen as a limitation – longer follow-up times should be studied in the future.

Current notions of persistent pain after a successfully technical TKR surgery have focused on peripheral and spinal cord sensitization and abnormal descending pain modulation, or clinical/psychological dimensions, without a clear mechanistic link to pain

physiology. We have shown that structural and functional properties of the brain's limbic circuitry, particularly the amygdala, hippocampus and thalamus, are accurate predictors of pain maintenance after TKR surgery. These results support the importance of limbic neuroanatomical factors in the persistence of chronic pain and open a new avenue not only for studying post-surgery pain mechanisms but also for future clinical care and management of OA pain patients.

References:

1. Neogi, T. The epidemiology and impact of pain in osteoarthritis. *Osteoarthritis Cartilage* **21**, 1145–1153 (2013).
2. Kim, D. H., Pearson-Chauhan, K. M., McCarthy, R. J. & Buvanendran, A. Predictive Factors for Developing Chronic Pain After Total Knee Arthroplasty. *J. Arthroplasty* **33**, 3372–3378 (2018).
3. Beswick, A. D., Wylde, V., Gooberman-Hill, R., Blom, A. & Dieppe, P. What proportion of patients report long-term pain after total hip or knee replacement for osteoarthritis? A systematic review of prospective studies in unselected patients. *BMJ Open* **2**, e000435 (2012).
4. Lewis, G. N., Rice, D. A., McNair, P. J. & Kluger, M. Predictors of persistent pain after total knee arthroplasty: a systematic review and meta-analysis. *Br. J. Anaesth.* **114**, 551–561 (2015).
5. Singh, J. A., Gabriel, S. & Lewallen, D. The impact of gender, age, and preoperative pain severity on pain after TKA. *Clin. Orthop.* **466**, 2717–2723 (2008).
6. Hochman, J. R., Gagliese, L., Davis, A. M. & Hawker, G. A. Neuropathic pain symptoms in a community knee OA cohort. *Osteoarthritis Cartilage* **19**, 647–654 (2011).
7. Barroso, J. *et al.* Brain gray matter abnormalities in osteoarthritis pain: a cross-sectional evaluation. *Pain* **Publish Ahead of Print**, (2020).
8. Baliki, M. N., Schnitzer, T. J., Bauer, W. R. & Apkarian, A. V. Brain Morphological Signatures for Chronic Pain. *PLoS ONE* **6**, e26010 (2011).

9. Mansour, A. *et al.* Global disruption of degree rank order: a hallmark of chronic pain. *Sci. Rep.* **6**, 34853 (2016).
10. Barroso, J. *et al.* Reorganization of functional brain network architecture in chronic osteoarthritis pain. *Hum. Brain Mapp.* hbm.25287 (2020) doi:10.1002/hbm.25287.
11. Parks, E. L. *et al.* Brain activity for chronic knee osteoarthritis: dissociating evoked pain from spontaneous pain. *Eur. J. Pain Lond. Engl.* **15**, 843.e1–14 (2011).
12. Vachon-Presseau, E. *et al.* Corticolimbic anatomical characteristics predetermine risk for chronic pain. *Brain* **139**, 1958–1970 (2016).
13. Baliki, M. N. *et al.* Corticostriatal functional connectivity predicts transition to chronic back pain. *Nat. Neurosci.* **15**, 1117–1119 (2012).
14. Barroso, J. *et al.* Prognostics for pain in osteoarthritis: Do clinical measures predict pain after total joint replacement? *PLOS ONE* **15**, e0222370 (2020).
15. Altman, R. *et al.* Development of criteria for the classification and reporting of osteoarthritis: Classification of osteoarthritis of the knee. *Arthritis Rheum.* **29**, 1039–1049 (1986).
16. Gonçalves, R. S., Cabri, J., Pinheiro, J. P. & Ferreira, P. L. Cross-cultural adaptation and validation of the Portuguese version of the Knee injury and Osteoarthritis Outcome Score (KOOS). *Osteoarthritis Cartilage* **17**, 1156–1162 (2009).
17. Zigmond, A. S. & Snaith, R. P. The Hospital Anxiety and Depression Scale. *Acta Psychiatr. Scand.* **67**, 361–370 (1983).
18. Pais-Ribeiro, J. *et al.* Validation study of a Portuguese version of the Hospital Anxiety and Depression Scale. *Psychol. Health Med.* **12**, 225–235; quiz 235–237 (2007).

19. Sullivan, M. J. L., Bishop, S. R. & Pivik, J. The Pain Catastrophizing Scale: Development and validation. *Psychol. Assess.* **7**, 524–532 (1995).
20. Azevedo, L. Tradução, adaptação cultural e estudo multicêntrico de validação de instrumentos para rastreio e avaliação do impacto da dor crónica (Translation, cultural adaptation and multicentric validation study of chronic pain screening and impact assessment instruments). Dor 2007;15:6–65.
21. Bouhassira, D. *et al.* Comparison of pain syndromes associated with nervous or somatic lesions and development of a new neuropathic pain diagnostic questionnaire (DN4): *Pain* **114**, 29–36 (2005).
22. Podsiadlo, D. & Richardson, S. The Timed “Up & Go”: A Test of Basic Functional Mobility for Frail Elderly Persons. *J. Am. Geriatr. Soc.* **39**, 142–148 (1991).
23. Balke, B. A SIMPLE FIELD TEST FOR THE ASSESSMENT OF PHYSICAL FITNESS. REP 63-6. *Rep. Civ. Aeromed. Res. Inst. US* 1–8 (1963).
24. Rejeski, W. J. *et al.* Assessing performance-related disability in patients with knee osteoarthritis. *Osteoarthritis Cartilage* **3**, 157–167 (1995).
25. Kellgren, J. H. & Lawrence, J. S. Radiological assessment of osteo-arthrosis. *Ann. Rheum. Dis.* **16**, 494–502 (1957).
26. Smith, S. M. *et al.* Advances in functional and structural MR image analysis and implementation as FSL. *NeuroImage* **23**, S208–S219 (2004).
27. Smith, S. M. Fast robust automated brain extraction. *Hum. Brain Mapp.* **17**, 143–155 (2002).

28. Jenkinson, M., Bannister, P., Brady, M. & Smith, S. Improved Optimization for the Robust and Accurate Linear Registration and Motion Correction of Brain Images. *NeuroImage* **17**, 825–841 (2002).
29. Power, J. D., Barnes, K. A., Snyder, A. Z., Schlaggar, B. L. & Petersen, S. E. Spurious but systematic correlations in functional connectivity MRI networks arise from subject motion. *NeuroImage* **59**, 2142–2154 (2012).
30. Power, J. D. *et al.* Methods to detect, characterize, and remove motion artifact in resting state fMRI. *NeuroImage* **84**, 320–341 (2014).
31. Andersson, J. L. R. & Sotiropoulos, S. N. An integrated approach to correction for off-resonance effects and subject movement in diffusion MR imaging. *NeuroImage* **125**, 1063–1078 (2016).
32. Jbabdi, S., Sotiropoulos, S. N., Savio, A. M., Graña, M. & Behrens, T. E. J. Model-based analysis of multishell diffusion MR data for tractography: How to get over fitting problems. *Magn. Reson. Med.* **68**, 1846–1855 (2012).
33. Power, J. D. *et al.* Functional Network Organization of the Human Brain. *Neuron* **72**, 665–678 (2011).
34. Bastiani, M. *et al.* Automated quality control for within and between studies diffusion MRI data using a non-parametric framework for movement and distortion correction. *NeuroImage* **184**, 801–812 (2019).
35. Nugent, A. C. *et al.* Automated subcortical segmentation using FIRST: Test-retest reliability, interscanner reliability, and comparison to manual segmentation: Reliability of Automated Segmentation Using FIRST. *Hum. Brain Mapp.* **34**, 2313–2329 (2013).

36. Smith, S. M. *et al.* Accurate, Robust, and Automated Longitudinal and Cross-Sectional Brain Change Analysis. *NeuroImage* **17**, 479–489 (2002).
37. Patenaude, B., Smith, S. M., Kennedy, D. N. & Jenkinson, M. A Bayesian model of shape and appearance for subcortical brain segmentation. *NeuroImage* **56**, 907–922 (2011).
38. Behrens, T. E. J., Berg, H. J., Jbabdi, S., Rushworth, M. F. S. & Woolrich, M. W. Probabilistic diffusion tractography with multiple fibre orientations: What can we gain? *NeuroImage* **34**, 144–155 (2007).
39. Andersen, L. Ø. *et al.* Subacute pain and function after fast-track hip and knee arthroplasty. *Anaesthesia* **64**, 508–513 (2009).
40. Lahtinen, P., Kokki, H. & Hynynen, M. Pain after Cardiac Surgery. *Anesthesiology* **105**, 794–800 (2006).
41. Gerbershagen, H. J., Rothaug, J., Kalkman, C. J. & Meissner, W. Determination of moderate-to-severe postoperative pain on the numeric rating scale: a cut-off point analysis applying four different methods. *Br. J. Anaesth.* **107**, 619–626 (2011).
42. Fletcher, D. *et al.* Chronic postsurgical pain in Europe: An observational study. *Eur. J. Anaesthesiol.* **32**, 725–734 (2015).
43. Alattas, S. A., Smith, T., Bhatti, M., Wilson-Nunn, D. & Donell, S. Greater pre-operative anxiety, pain and poorer function predict a worse outcome of a total knee arthroplasty. *Knee Surg. Sports Traumatol. Arthrosc.* **25**, 3403–3410 (2017).
44. Nolan, M. *et al.* Hippocampal and Amygdalar Volume Changes in Major Depressive Disorder: A Targeted Review and Focus on Stress. *Chronic Stress* **4**, 247054702094455 (2020).

45. Richter-Levin, G. The Amygdala, the Hippocampus, and Emotional Modulation of Memory. *The Neuroscientist* **10**, 31–39 (2004).
46. Kim, W. B. & Cho, J.-H. Encoding of contextual fear memory in hippocampal–amygdala circuit. *Nat. Commun.* **11**, 1382 (2020).
47. Ressler, K. J. Amygdala Activity, Fear, and Anxiety: Modulation by Stress. *Biol. Psychiatry* **67**, 1117–1119 (2010).
48. Baliki, M. N. & Apkarian, A. V. Nociception, Pain, Negative Moods, and Behavior Selection. *Neuron* **87**, 474–491 (2015).
49. Gwilym, S. E., Filippini, N., Douaud, G., Carr, A. J. & Tracey, I. Thalamic atrophy associated with painful osteoarthritis of the hip is reversible after arthroplasty: A longitudinal voxel-based morphometric study. *Arthritis Rheum.* **62**, 2930–2940 (2010).
50. Viard, A. *et al.* Hippocampal activation for autobiographical memories over the entire lifetime in healthy aged subjects: an fMRI study. *Cereb. Cortex N. Y. N 1991* **17**, 2453–2467 (2007).
51. Sahay, A. & Hen, R. Adult hippocampal neurogenesis in depression. *Nat. Neurosci.* **10**, 1110–1115 (2007).
52. Mutso, A. A. *et al.* Abnormalities in Hippocampal Functioning with Persistent Pain. *J. Neurosci.* **32**, 5747–5756 (2012).

Tables:

	OAPp (26)		OAPr (55)		*p* value
Subjects, n, %	26	32.1	55	67.9	
Age (years), mean, SD	65.7	5.9	65.7	6.8	0.99
Female, n, %	22	84.6	43	78.2	0.56
BMI (kg/m^2), mean, SD	32.1	5.1	30.0	4.7	0.08
Education, n, %					0.28
Primary Education	19	73	44	80	
Secondary Education	4	15.4	9	16.4	
Post- secondary Education	3	11.5	2	3.4	
Smoking, n, %	3	11.5	3	5.5	0.40
Habitation, n, %					0.27
Alone	8	16.7	9	18.7	
Co-habitation	18	83.3	46	81.3	
Marital Status, n, %					0.17
Married	15	57.7	44	80	
Never married	3	11.5	3	5.5	
Divorced	5	19.2	0	0	
Widowed	3	11.5	8	14.5	
Pain Duration (years), mean, SD	9.8	6.4	7.0	5.8	**0.04***
Pain Intensity (NRS), mean, SD	6.9	1.8	6.4	1.6	0.24
Radiographic KL, n, %					0.53
Grade 1	1	3.8	0	0	
Grade 2	6	23.1	14	25.5	
Grade 3	13	50	25	45.5	
Grade 4	6	23.1	16	19.1	

Table 1. Demographic and socio-economic characteristics of OAr and OAp patients. T-tests and ANOVA were used to test differences in continuous outcomes. Chi-square (X^2) tests were applied for categorical data. *p<0.05.

ANOVA, analysis of variance; BMI, body mass index; KL, Kellgren-Lawrence scale; NRS, numeric rating scale; SD, standard deviation.

Variable	Sumsq	*df*	*F* value	*p* value
Within-Subject				
Intercept (SCv)	931955.78	1	5.015	0.026
SCv x Group	**1273298.48**	**1**	**6.851**	**0.009 ****
SCv x Hemisphere	23590.12	1	0.126	0.722
SCv x Group x Hemisphere	108472.44	1	0.583	0.446
Error (SCv)	28618264.10	154		
Between-Subject				
Intercept (SCv)	3317344.98	1	9.631	0.002**
Group	2704401.70	1	7.852	0.005**
Hemisphere	44948.05	1	0.131	0.718
Age	124178.97	1	0.361	0.549
Gender	6284514.79	1	18.248	0.001**
Baseline pain	695590.33	1	0.019	0.157
TICV	6082067.03	1	17.66	0.001**
Error (SCv)	53037085.75	154		

Table 2. Repeated measures ANCOVA for the main and interaction effects of group (OAr/OAp), and cerebral hemisphere on subcortical volumes, while controlling for age, gender, TICV and baseline pain. *p<0.01; ** p<0.001.

df, degrees of freedom; SCv, subcortical volumes; TICV, total intracranial volume.

Variable	Sumsq	*df*	*F* value	*p* value
SCv x Group				
Thalamus	**3630664.64**	**1**	**15.68**	**0.0001****
Caudate	80111.51	1	0.58	0.448
Putamen	189677.07	1	0.93	0.336
Pallidum	342982.46	1	3.32	0.070
Hippocampus	**914882.17**	**1**	**5.63**	**0.018***
Amygdala	**304404.41**	**1**	**5.53**	**0.019***
N. Accumbens	9972.81	1	1.01	0.317

Table 3. Main effect of group (OAr/OAp) on each level of the dependent factor (SCv). p<0.01; ** p<0.001. *df*, defrees of freedom. SCv, subcortical volumes; Sumsq, sum of squares.

Figures:

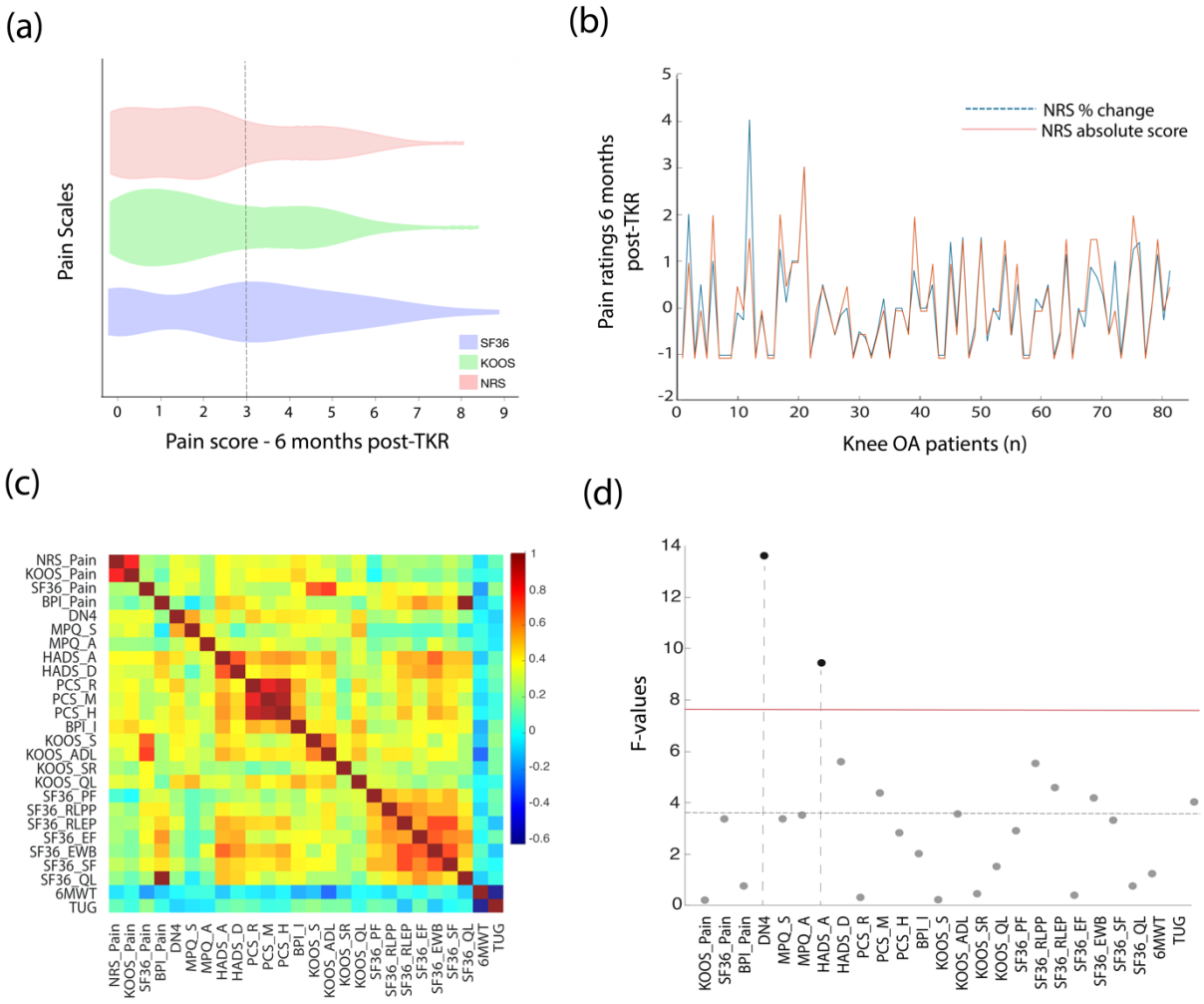

Figure 1. Classification of post-operative pain outcomes and baseline clinical data. **(a)** Distribution of pain scores after surgery for 3 distinct scales. Dotted line corresponds to threshold used to classify outcomes into 2 distinct groups: OA recovering (OAr)/OA persisting (OAp). **(b)** Overlap between absolute pain score and pain change from baseline for each individual subject. **(c)** Correlation matrix shows the relationship between each subscale in the questionnaire data and physical performance tasks collected before

surgery. **(d)** Univariate statistics shows pre-surgery DN4 scale and HADS Anxiety subscale were able to separate the two outcome groups (OAPr/OAPp); pre-surgical pain levels were introduced as covariates of no interest; these survived Bonferroni correction for 26 comparisons ($p<0.0019$, shown in black; red line corresponds to significant t-value after multiple comparison correction; dotted line corresponds to uncorrected significance at $p>0.05$).

6MWT, 6 Minute Walking Test; BMI, Body mass index; DN4, Douleur Neuropathique en 4 questions; HADS, Hospital anxiety and Depression Scale; KOOS, Knee injury and Osteoarthritis Outcome Score, (ADL, Activities of Daily Living; SR, Sports and Recreation; QoL, Quality of Life); PCS, Pain Catastrophizing Scale (R – Rumination subscale, M – Magnification subscale, H – Helplessness subscale); KL, Kellgren-Lawrence scale; SF36, Short-form (36) Health Survey, (PF – Physical Functioning), (PH, physical role functioning; (EP, emotional role functioning), (EF, energy/fatigue), (E, emotional well-being), (SF, social functioning), (GH, general health); TUG, Test stand-up and go.

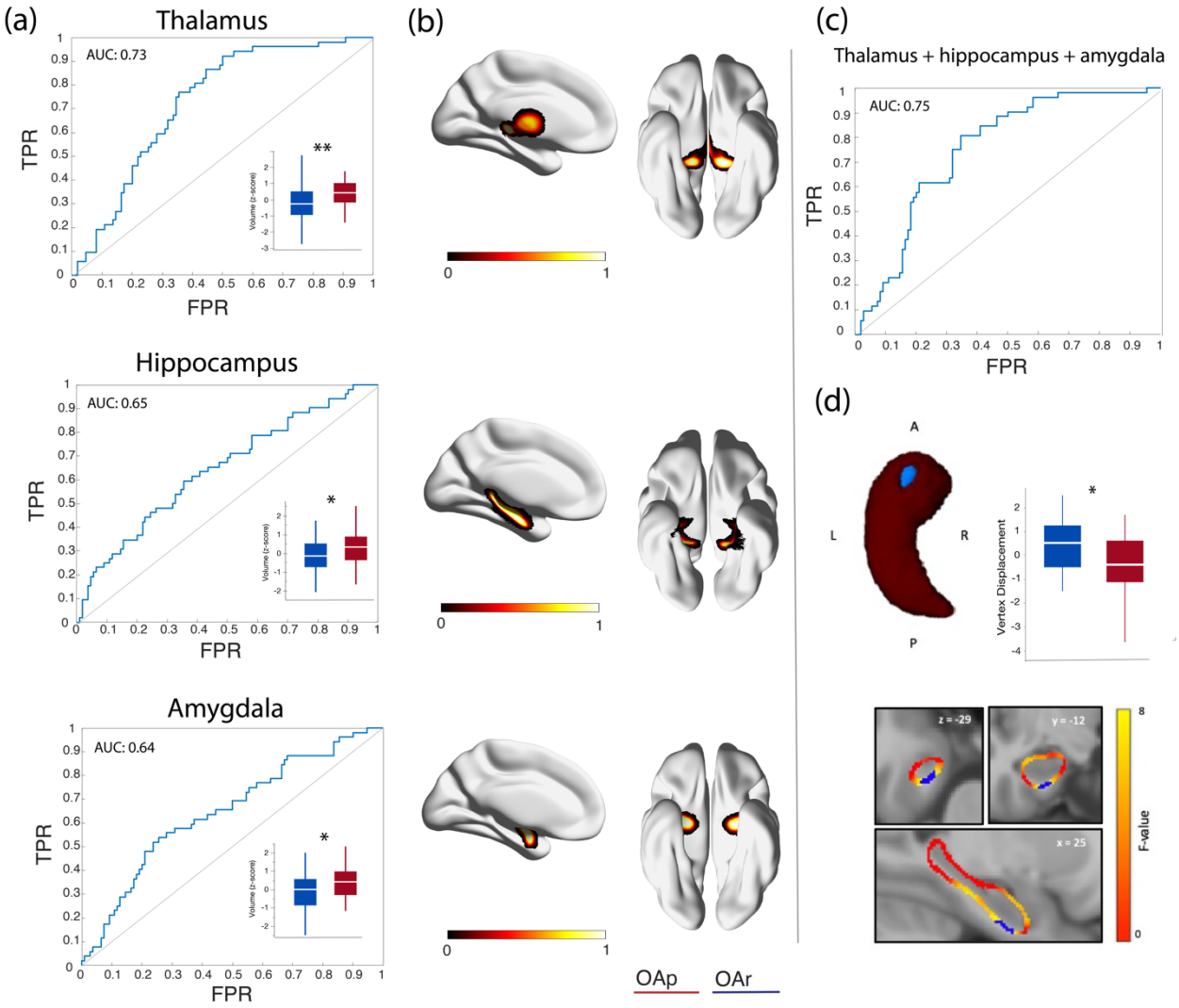

Figure 2. Subcortical brain limbic anatomic properties classify OA pain outcome after surgery. (a) ROC curves show specificity and sensitivity of each region modelling the outcome; inserts show boxplot for subcortical volumes per OA group. (b) Brain diagrams show heat-maps of overlap (from 0 to 1) in the segmentation of subcortical regions across OAr and OAp groups. Subcortical volumes are projected into cortical surface for illustration. (c) Collective volumetric properties of thalamus, hippocampus and amygdala improves OA outcome prediction, as shown in the ROC and AUC value. (d) Left hippocampal shape displacement was associated with OA outcome. Statistics were corrected for multiple

comparisons using threshold free cluster enhancement (TFCE); the blue mask displayed on the surface of the left hippocampus indicates the area with p-values <0.05 after correction. Boxplot shows vertex displacement difference for the displayed cluster between OA groups. *p<0.05.

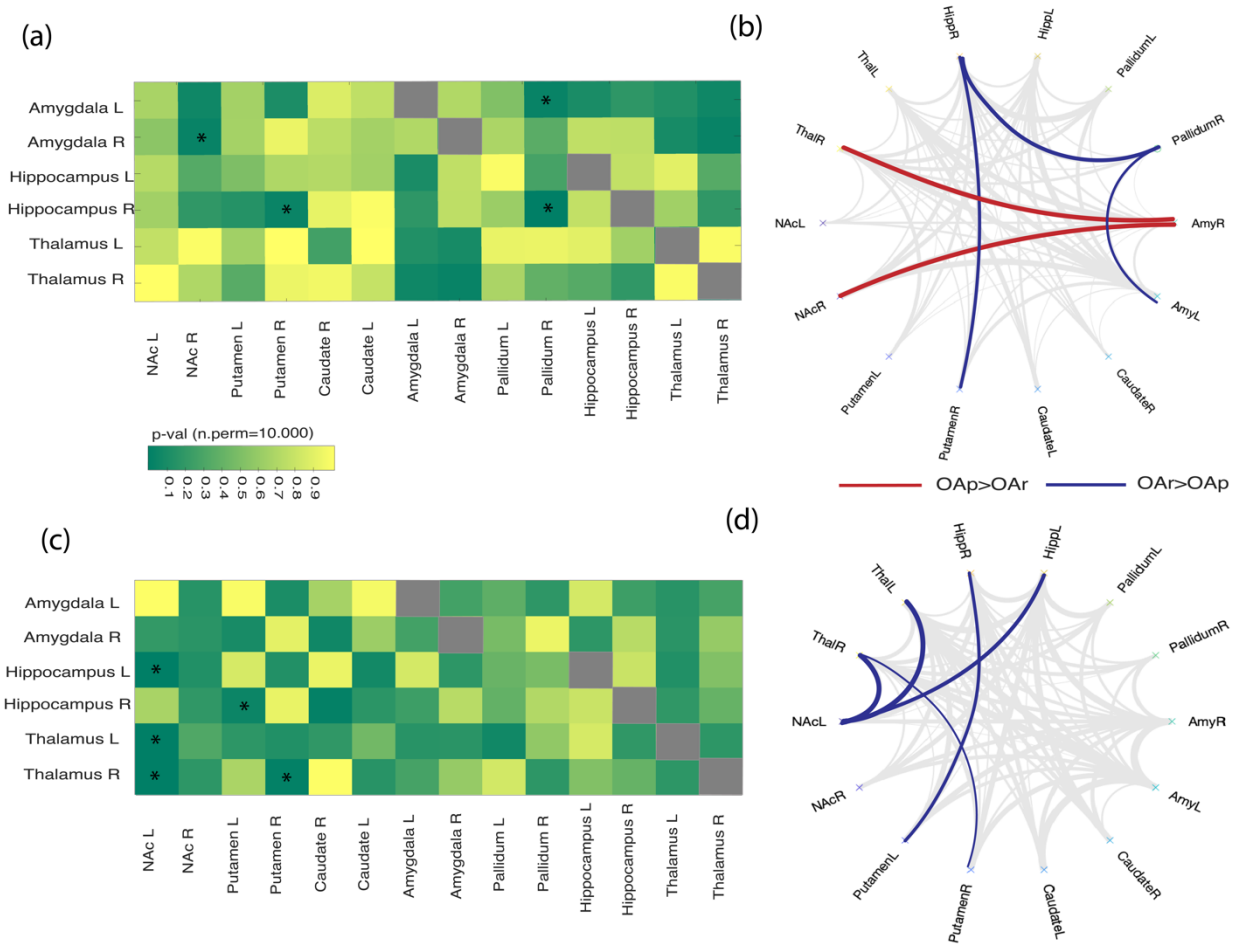

Figure 3. Functional and anatomic limbic properties associated with pain persistence after TKR surgery. **(a)** and **(b)** show the p-values on correlation differences (t-tests) in functional and anatomic connectivity (respectively) for the 6 brain regions previously identified and all 14 subcortical structures. Independent sample t-tests were carried using a permutation-based analysis (100.000 permutations); p-values <0.05 were redeemed significant. **(c)** and **(d)** show circular graphs illustrating t-statistics, corresponding to the significant p values showed in (a) and (b) in color. Red color was used to illustrate positive t-values (OAp>OAr) and blue color was used to illustrate negative contrast (OAr>OAp). *p<0.05. OAr, recovering; OAp, persisting.

3. General discussion and conclusions

In the present thesis we sought to understand brain mechanisms of OA pain by cross-sectionally evaluating brain structural and functional properties of OA patients, and longitudinally studying clinical, psychological and brain biomarkers of pain persistence in OA after TJR.

In **publication I** we showed that distinct pain scales related to different aspects of the pain experience in OA, and post-surgical pain intensity was mostly independent from pre-surgical pain levels across different scales. Moreover, we showed that though clinical and psychological variables are not reliable predictors of pain after TJR in our sample, these characteristics change/reorganize with surgery, mostly for hip OA, where pain relief with surgery is also larger. In **publication II**, we defined brain grey matter structural changes in OA. While univariate voxel-based morphometry analysis showed decreased grey matter in areas associated with pain processing (e.g., ACC, prefrontal cortex), these did not relate to clinical outcomes. Using multivariable analysis, we defined with high accuracy brain morphological distortions that associated with the neuropathic pain characteristics in knee OA and related to pain and motor control terms in the brain imaging literature. In **publication III**, using properties of rsfMRI and applying a network analysis, we demonstrated that there is a disruption in neural information sharing in OA that can be captured at a whole-brain level. At a local level, the insula/operculum lost its chief placement in information sharing and sensorimotor regions become hubs, or areas with larger information flow. Lastly, pain intensity was reliably predicted by a distributed set of regions in the brain, that dissociated from the major local disruptions described. Finally, in **Manuscript in preparation**, we studied the brain as a possible predictor of pain

maintenance after TJR and presumed cessation/lessening of nociceptive drive in OA. We show that structural anatomical properties, together with functional and anatomic white matter connectivity properties of the limbic system, particularly the amygdala, hippocampus and thalamus, are predictors of pain maintenance after TKR for knee OA, thus presenting a strong mechanistic link between the limbic brain and OA pain physiology. Altogether, the studies included in the present thesis provide original data on brain anatomical and functional changes underlying OA pain, evaluate predictors of pain after TKR surgery and propose limbic brain circuitry as a predictor for pain persistence after surgery.

3.1 The brain adapting with OA pain

Brain structural and functional changes that relate to the ongoing chronic pain have been reported in the past, in multiple chronic pain conditions. Here we studied brain morphologic (**Publication II**) and functional adaptations (**Publication III**) in a large population of knee and hip OA patients. Structural grey matter and network reorganization, have been proposed in the literature as biomarkers underlying the chronic pain state in the brain [1,2], and the cross-sectional study of these properties allows us to probe into the mechanics of chronic OA pain.

We show grey matter distortions, and the disruption of information share are both largescale processes, involving multiple regions of the brain. Grey matter changes in OA were previously exposed in the literature as more circumscribed regional changes [3,4], however, when we account for the interrelationship between regions, we show that these

distortions reflect a more pervasive restructuring process of the neocortical anatomy **(Publication II)**. Though the relationship between functional connectivity and anatomical reorganization and the extent on which they are interdependent is not known, we have shown in **Publication III** that the hub disruption indices reflect altered connectivity that permeates the whole brain and is not merely driven by specific regional connectivity changes. Together, anatomic and functional changes show a widespread reorganization in OA. Importantly, we show that these distortions are related to clinical outcomes of OA. Structural grey matter adaptations in OA were associated with the neuropathic pain profile (for knee OA) (**Publication II**); and pain intensity (NRS) was related to distributed changes in functional connectivity (**Publication III**). This favors the theory that these metrics are reflective of the ongoing chronic pain syndrome [1,2].

Notably, though structural grey matter changes were largely distributed, when we accounted for their relative importance (their weight in our regularized multivariable model), the decoding terms were pain and motor-related in the general fMRI literature (**Publication II**). This suggests that although distortions are widespread, the influence of regions associated with pain perception, sensory and motor tasks is larger. In parallel, local patterns of reorganization of functional connectivity emerged (**Publication III)**. There was a loss of information share from insula/operculum and a gain in sensory regions. We interpret that this may reflect maladaptive plasticity, where the overload of information to the insula leads to its failure, and information is rerouted to lower levels of processing; or an adaptive process where the brains information sharing adapts to the stress of continuous nociceptive signaling by diminish the influence of pain in the insular cortex and increasing attention to SM control. In accordance with previous data in other CHRONIC

PAINconditions[5,6], our data suggests that the global scale reorganization is associated with local scale changes that may reflect specific coping and learning characteristics that are unique to the OA syndrome.

We conclude that presented structural and functional changes may reflect adaptive or maladaptive plasticity, as a response to living with chronic pain in OA. The brain in chronic pain is a far more complex state than a simple persistence of nociceptive encoding, that is associated with a global and local scale structural and functional reorganization.

3.2 Brain properties imparting risk for pain chronification in OA

The limbic system has been related with higher risk for pain chronification in CPB as discussed in the introduction of this thesis. Our results show that regions of the limbic structures are associated with OA pain persistence after surgery, **Manuscript in preparation.** Our anatomical result is quite striking – subcortical limbic volumes are decreased in patients that recover versus persisting pain patients. It has been proposed that brain gray matter decrease in chronic pain is the consequence and not the cause of pain[7]; previous studies in the field have shown that grey matter decreases (thalamus; amygdala, insular cortex, ACC, DLPFC) reverse after successful treatment in hip OA[7,3,8]. The successful treatment of CBP is also associated with reversal of brain grey matter decrease (DLPFC)[9]. In our sample, patients who progressed to recover after TKR had decreased thalamus, amygdala and hippocampal volumes when contrasted with patients who maintain chronic pain. One can envision that patients who recover will follow the same path as in the studies aforementioned, with reversion of volumetric changes – thus

contributing for the theory that brain structural changes are a consequence of the painful state. The larger volume in persistent pain patients remains obscure so far – one can theorize that the decreased volumes are a result of maladaptive plasticity to the long-lasting nociceptive stimuli, and the lack of such adaptation is a) indirect result of predisposing influence from other brain regions; b) the result of primary predisposing features from limbic brain or c) a combination of both. As proposed in the transition from acute to chronic pain, thalamocortical circuits may be modulated by abnormal dopaminergic signaling secondary to the enhanced functional connectivity between mPFC-NAc, thus amplifying the value of nociceptive input[10]. A larger volume of the thalamus could reflect such process in OAp versus OAr patients.

As for the amygdala and the hippocampus, they are central to the consolidation of emotional memories, such as those relating to painful or stressful events[10]. It is known that amygdala inputs to the mPFC change the inhibitory drive to this region in animal models of pain,[11,12] and in humans with chronic pain the subjective perception of pain leads to amygdala activation[13]. Functional connectivity of the anterior hippocampus (the same region found to have a shape difference in OAp patients), has been associated with transition of acute to back pain and the chronic pain state in humans[14]. Hence, subtle anatomic differences may relate to distinct functional states that underlie pain persistence in OA after TJR.

So far, given our data, we can hypothesize that the amygdala, hippocampus and thalamic structural properties reflect a limbic readaptation or/and predisposition, that may control or amplify the persistent pain state in OA. The better characterization of the limbic brain in OA is of great interest, given the possibility to unravel mechanistic insights of pain

in the brain, and predict future transition to chronic pain or remission, opening avenues for new treatment options.

3.3 Diagnostic and prognostic biomarkers of OA pain

We can discuss our findings again from the aspect of their diagnostic/prognostic value. Tough clinical and psychological features have long been proposed as predictors of pain persistence after surgery, their value is still conflicting [15]. In **Publication I** we show that though these characteristics are not reliable predictors of pain after surgery, they change with surgery – larger change for hip OA where pain relief is also greater than in knee OA. Also, when significant (though low), the predictive value of these outcomes is dependent on the scale used to measure pain, showing us that distinct facets of the pain experience are partially explained by different variables; no predictor is transversal to multiple pain measurements. These suggest that these variables may be diagnostic properties reflecting a state of pain, more than pre-existing traits that predispose patients to chronic pain after surgery.

We believe our data supports the fact that grey matter changes and disruption of information sharing (*K* indices) are diagnostic biomarkers of OA pain. Given they may reflect an ongoing chronic pain process and are possibly emergent in time, they should also be reversible with successful pain treatment and thus useful in assessing efficacy of therapies for chronic OA pain.

Finally, we believe that more nuanced grey matter changes of limbic structures may be reflective of possible traits, or the result of the influence of other functional/anatomical

risk factors for pain persistence after surgery. If pre-existing risk factors, they should remain constant, and not change with treatment. This concept remains to be tested.

3.4 Limitations and future directions

The most important limitation of the present work is that we could not entirely disentangle the prospective/diagnostic value of brain biomarkers in OA pain. This comes as a limitation of the cross-sectional evaluation of the brain – in our last paper we evaluate the brain as a predictor of pain persistence, hinting new and important findings, however, evaluating brain properties as they change with pain/recovery is essential to accurately distinguish between the cause and consequence of persistent pain. This is an ongoing work. Brain MRI data was collected at 6 months after surgery and currently being studied.

Other limitations of the present thesis may be detailed. (1) Corticolimbic dynamics where not evaluated in **Manuscript in preparation**. Given the neocortical influence in the limbic circuit in transition to chronic pain in CBP and its reorganization in OA, studying the limbic-cortical interaction is vital in the future. (2) Hip OA brain properties were not studied as predictors of pain persistence as most of our patients recovered from their pain after THR (**Publication I**). We believe this population can be studied in the future, namely by validating the structural and functional results of the OAr group, and thus assessing the generalizability of our findings in a different type of OA. Finally, though clinical properties differentiated the the OAr and OAp groups at baseline in **Manuscript in preparation**, they were not studied in relation to brain properties so far, which should also be explored.

3.5 Conclusions

In the present work we advance the scientific knowledge on brain mechanisms of OA pain. Given the brain structural and functional reorganization in OA, we state that OA pain reflects the interplay between brain properties and injury-related sensory input. At the same time, we suggest that brain limbic properties may impart risk for pain persistence after the peripheral injury is resolved.

In conclusion, we believe OA pain may depend on multiple phenomena: tissue damage and nociceptive drive, sensitization of peripheral nociceptors, spinal cord circuitry, descending modulation and brain neocortical and limbic properties. The extent to which each one of these mechanisms contributes to pain may be different from patient to patient and may also be contingent on the progression of the disorder. Moreover, the influence of each one of these factors in the OA pain experience may underly the heterogenous response to distinct types of treatment in OA. A better understanding of individual profiles in OA pain, only achieved by the mechanistic insight on its pathophysiology will lead to novel and better treatment strategies.

3.6 References

1. Reckziegel, D. *et al.* Deconstructing biomarkers for chronic pain: context- and hypothesis-dependent biomarker types in relation to chronic pain. *PAIN* **160**, S37–S48 (2019).
2. Baliki, M. N. & Apkarian, A. V. Nociception, Pain, Negative Moods, and Behavior Selection. *Neuron* **87**, 474–491 (2015).
3. Gwilym, S. E., Filippini, N., Douaud, G., Carr, A. J. & Tracey, I. Thalamic atrophy associated with painful osteoarthritis of the hip is reversible after arthroplasty: A longitudinal voxel-based morphometric study. *Arthritis Rheum.* **62**, 2930–2940 (2010).
4. Liao, X. *et al.* Brain gray matter alterations in Chinese patients with chronic knee osteoarthritis pain based on voxel-based morphometry. *Medicine (Baltimore)* **97**, e0145 (2018).
5. Mansour, A. *et al.* Global disruption of degree rank order: a hallmark of chronic pain. *Sci. Rep.* **6**, 34853 (2016).
6. Baliki, M. N., Mansour, A. R., Baria, A. T. & Apkarian, A. V. Functional Reorganization of the Default Mode Network across Chronic Pain Conditions. *PLoS ONE* **9**, e106133 (2014).
7. Rodriguez-Raecke, R., Niemeier, A., Ihle, K., Ruether, W. & May, A. Brain Gray Matter Decrease in Chronic Pain Is the Consequence and Not the Cause of Pain. *J. Neurosci.* **29**, 13746–13750 (2009).
8. Rodriguez-Raecke, R., Niemeier, A., Ihle, K., Ruether, W. & May, A. Structural Brain Changes in Chronic Pain Reflect Probably Neither Damage Nor Atrophy. *PLoS ONE* **8**, e54475 (2013).

9. Seminowicz, D. A. *et al.* Effective Treatment of Chronic Low Back Pain in Humans Reverses Abnormal Brain Anatomy and Function. *J. Neurosci.* **31**, 7540–7550 (2011).
10. Vachon-Presseau, E. *et al.* The Emotional Brain as a Predictor and Amplifier of Chronic Pain. *J. Dent. Res.* **95**, 605–612 (2016).
11. Neugebauer, V., Li, W., Bird, G. C. & Han, J. S. The Amygdala and Persistent Pain. *The Neuroscientist* **10**, 221–234 (2004).
12. Ji, G. & Neugebauer, V. Pain-related deactivation of medial prefrontal cortical neurons involves mGluR1 and GABA $_A$ receptors. *J. Neurophysiol.* **106**, 2642–2652 (2011).
13. Baliki, M. N. *et al.* Chronic Pain and the Emotional Brain: Specific Brain Activity Associated with Spontaneous Fluctuations of Intensity of Chronic Back Pain. *J. Neurosci.* **26**, 12165–12173 (2006).
14. Mutso, A. A. *et al.* Abnormalities in Hippocampal Functioning with Persistent Pain. *J. Neurosci.* **32**, 5747–5756 (2012).
15. Harmelink, K. E. M. *et al.* Are There Prognostic Factors for One-Year Outcome After Total Knee Arthroplasty? A Systematic Review. *J. Arthroplasty* **32**, 3840-3853.e1 (2017).